REAL-TIME MONITORING OF PROBE-TISSUE PRESSURE EFFECTS ON IN VIVO SKIN OPTICAL SPECTROSCOPY USING A PRESSURE SENSITIVE FIBEROPTIC PROBE

ARNOLD JULIAN VINOJ BENJAMIN

NATIONAL UNIVERSITY OF SINGAPORE

2014

REAL-TIME MONITORING OF PROBE-TISSUE PRESSURE EFFECTS ON IN VIVO SKIN OPTICAL SPECTROSCOPY USING A PRESSURE SENSITIVE FIBEROPTIC PROBE

ARNOLD JULIAN VINOJ BENJAMIN **2014**

REAL-TIME MONITORING OF PROBE-TISSUE PRESSURE EFFECTS ON IN VIVO SKIN OPTICAL SPECTROSCOPY USING A PRESSURE SENSITIVE FIBEROPTIC PROBE

ARNOLD JULIAN VINOJ BENJAMIN

A THESIS SUBMITTED

FOR THE DEGREE OF MASTER OF ENGINEERING

DEPARTMENT OF BIOMEDICAL ENGINEERING

NATIONAL UNIVERSITY OF SINGAPORE

2014

DECLARATION

I hereby declare that the thesis is my original work and it has been written by me in its entirety. I have accordingly acknowledged all the sources of information, which have been used in the thesis.

This thesis has not been submitted for any degree in any university previously

_____

Arnold Julian Vinoj Benjamin

14 August 2014

Dedicated to my family and friends

Acknowledgements

The research work presented in this thesis was conducted in the Optical Bioimaging Laboratory in the department of Biomedical Engineering, National University of Singapore (NUS) from August 2012 to April 2014. It would not have possible to submit my thesis had it not been for the support and guidance of many people during the course of my Master's degree.

First and foremost, I would like to show my sincere gratitude to my supervisor, Professor Huang Zhiwei for giving me the opportunity to work in his prestigious laboratory which is at the forefront of biomedical cancer research. I would like to thank him for his great support, expert guidance and immense patience throughout my study. I strongly believe that Dr. Huang's insight and the high standard of research would surely be a tremendous advantage for my future research career.

I would also like to acknowledge my colleagues and lab members in the Optical Bioimaging Laboratory: Dr. Zheng Wei, Dr. Lin Jian, Dr. Shiyamala Duraipandian, Dr. Lin Kan, Mads Sylvest Bergholt, Wang Zi and Wang Jianfeng for their valuable suggestions and feedback about my research work.

I would like to thank the funding agencies: Ministry of Education (Singapore), National Medical Research Council and Biomedical Research Council for their financial support to carry out my experiments.

Last but not the least; I would like to thank my parents, family members, relatives and friends for their unwavering support and emotional guidance during my difficult moments.

Table of Contents

Abstract

Optical Spectroscopic techniques like Diffuse Reflectance (DR), autofluorescence (AF) and Raman Spectroscopy have been utilized for the diagnosis of various diseases and disorders. Cancer, diabetes, Alzheimer's disease, asthma and brain disorders are some of the diseases which can be diagnosed by fiber-based optical spectroscopic techniques. These spectroscopic techniques are highly sensitive to subtle changes in tissue biochemical composition and this forms the basis for disease diagnosis. However, a number of challenges have to be addressed in order to further improve the clinical utility and diagnostic efficacy of optical spectroscopy.

The confounding effect of the exerted probe-tissue contact pressure is one of the potential factors that might have a significant influence on the acquired spectral data. Till date, the existing studies on probe pressure have been limited to analyzing the static changes in probe pressure using pre-calibrated spring loaded devices or arbitrary operator-dependent pressure measurements. The real-time dynamic changes in exerted probe pressure have not been analyzed adequately. Therefore, it is necessary to comprehensively characterize the dynamic probe pressure induced effects on in vivo optical spectroscopy. The major objective of this dissertation is to develop a miniaturized, pressure sensitive fiber-optic probe for real-time, quantitative monitoring of the dynamic effects of probe-tissue contact pressure and to utilize the developed pressure sensitive probe to evaluate the pressure-induced distortions on *in vivo* skin optical spectroscopy (i.e. DR, AF and Raman).

Firstly, the pressure sensitive probe was developed by coupling a piezo-resistive thin-film pressure sensor (high sensitivity of 20.6 mV/kPa and short response time of <

5μs) to the probe tip. The in-house developed pressure sensor coupled probe was then utilized to acquire *in vivo* AF spectra (λ_{ex}=405nm) from two sites on the skin tissue (finger and volar forearm) at three different reference pressure levels (low pressure (LP) ~10 kPa, moderate pressure (MP) ~50 kPa and high pressure (HP) ~130 kPa). The acquired spectra were then analyzed using powerful chemometric methods which showed that the exerted probe-tissue contact pressure had a significant site-specific effect on the AF signal. Partial least squares-discriminant analysis (PLS-DA) models were developed to classify the spectra according to the exerted probe pressure and they showed that there is a distinct differentiation between spectra acquired at LP vs. MP+HP; thereby demonstrating the influence of pressure induced distortions on AF spectra.

Encouraged by these results, we utilized the developed pressure-sensitive spectroscopic platform to evaluate the probe pressure induced distortions on *in vivo* skin tissue NIR AF spectroscopy. Three skin sites (finger, palm and forearm) were chosen for measurement and spectra were acquired at the aforementioned reference pressure levels (L.P, M.P and H.P). PLS-DA analysis of the NIR AF spectra showed that higher pressures (i.e., MP and HP) affect the NIR AF spectral profiles to a certain extent; indicating that there is a great necessity to monitor the applied probe pressure in real-time.

Till date, the probe pressure induced effects on *in vivo* Raman Spectroscopy have not been studied in detail. Therefore, the developed pressure sensitive spectroscopic platform was used to investigate the probe pressure induced spectral variations on *in vivo* Raman Spectroscopy. Finger, palm and volar forearm were chosen as measurement sites on the skin to characterize the Raman spectral distortions that arise due to the exerted probe pressure. Subtle changes in the Raman spectra were introduced if MP (50 kPa) or

HP (130 kPa) were applied on the target tissue. The results show that the probe pressure variations affect the Raman spectral profiles and causes subtle spectral changes; demonstrating the inevitability of real-time monitoring of probe-tissue contact pressure during Raman spectroscopic procedures.

Finally, the developed pressure sensitive optical spectroscopy platform was tested on *in vivo* skin tissue DR spectroscopy for the real-time quantitative assessment of probe-tissue contact pressure effects on DR. Major chromophores that contributed to the probe pressure induced spectral distortions were identified from the spectral data. Further analysis of the spectra using PLS-DA showed the enormous influence of probe pressure on DR spectra and validate the need for real-time quantitative monitoring of probe-tissue contact pressure during spectroscopic measurements.

This work demonstrates for the first time the successful development and utilization of a pressure sensitive fiber-optic probe for real-time quantitative monitoring of probe-tissue contact pressure on in vivo optical spectroscopy. The developed pressure sensitive fiber-optic probe has the potential to mitigate the probe pressure induced tissue spectral alterations in real-time by providing instantaneous feedback of probe-tissue contact pressure to operators during *in vivo* spectroscopic measurements.

List of Figures

List of Tables

List of Abbreviations

DR	diffuse reflectance
DRS	diffuse reflectance spectroscopy
AF	autofluorescence
FS	fluorescence spectroscopy
LP	low pressure
MP	medium pressure
HP	high pressure
PLS-DA	partial least squares - discriminant analysis
PCA	principal component analysis
LDA	linear discriminant analysis
ANOVA	analysis of variance
SD	standard deviation
SE	standard error
LV	latent variables
CV	cross validation
CCD	charge coupled device
UV	ultraviolet
NIR	near infrared
SNR	signal to noise ratio
GRIN	graded-index
GUI	graphical user interface
GI	gastro-intestinal
NADH	nicotinamide adenine dinucleotide
FAD	flavin adenine dinucleotide

Chapter 1. Introduction

1.1 Motivation

Optical Spectroscopy techniques have been effective in characterizing the properties of physical objects by measuring how an object interacts with light. These methods have been used for a long time to identify and test the composition and purity of various materials by efficiently tracking the changes in the chemical composition and providing valuable information about the quality of materials. Characteristic spectral response of substances can be utilized to identify their presence in the material. These techniques have been extensively employed in recent years to characterize the biochemical composition of various tissues in the human body and rely on light-tissue interactions to identify the various biochemicals present in the body.

Some of the most common fiber-based optical spectroscopic techniques that have been comprehensively investigated for the diagnosis of diseases and disorders in various organs are diffuse reflectance, fluorescence and Raman spectroscopy.[1-8] Diagnostic information for diseases like cancer[9-11], diabetes[12, 13], asthma[14, 15], Alzheimer's disease[16-18] and brain disorders[19-21] can be extracted by the use of the aforementioned fiber-based optical spectroscopic techniques. Clinical trials for disease diagnosis have been carried out extensively especially for the diagnosis of cancer.[22-28] Efforts that have been taken to further improve the diagnostic efficacy of these spectroscopic techniques has posed a number of challenges.

One of the potential challenges that needs to be addressed lies in understanding the operator-dependent spectral distortions introduced by probe-tissue contact pressure in

order to enhance the diagnostic capability of optical spectroscopy. Existing studies on probe pressure induced spectral variations have shown that the exerted probe pressure is a confounding variable and therefore, it is important to characterize the probe pressure effects definitively to mitigate its effects on the acquired spectral data. Probe-tissue contact pressure is an important parameter in conventional spectroscopic instruments because a fiber-optic probe is required to be in contact with the tissue site during spectral data acquisition. The probe is placed against the target tissue during laser radiation, and remains unchanged during *in vivo* spectroscopy measurements. This ensures probe-tissue contact, avoids inconsistent illumination-detection geometry, reduces refractive index mismatch, and increases light penetration to enhance the diagnostic capability of spectroscopy instruments.[29] However, the high probe contact pressure generally produces the following effects on tissue under compression: decreased thickness, reduced blood volume and oxygen saturation, vasodilation, microcirculation impairment, densely packed scatterers and occlusion under the probe tip,[30] altering the optical properties of underlying tissue.[31, 32] Moreover, the applied probe pressure is especially hard to control in case of clinical scenario such as *in vivo* diagnosis in internal organs (e.g., endoscopy) due to difficulty in accessibility. Thereby, the utilization of hand-held fiber-optic probe in tissue optical spectroscopy may introduce operator-induced variations in the magnitude of pressure exerted onto the tissue.[31, 33] This leads to potential concerns such as changes in tissue spectral profiles, disparities in data collection and calibration[34] and potential inaccuracies in diagnosis. Although it has been reported that the applied probe pressure might induce changes in the optical properties of tissues[29, 33, 35, 36], the conventional spectroscopic techniques do not monitor the applied probe pressure in real-time during

spectral data acquisition. This is based on the assumption that the applied probe pressure induces negligible variations in the spectral profiles which is extremely contentious based on existing literature.[29, 30, 32, 37] Studies that have previously investigated the effect of exerted probe pressure have been limited to static pressure measurements utilizing a pre-calibrated spring loaded device, or making use of the extent of tissue compression (in mm) as a criterion for applying a particular pressure or operator-dependent arbitrary probe pressures. The dynamic changes in applied probe pressure that occur due to differences in deformability of various measurement sites on skin tissue, inter-subject variations in the extent of tissue compression and orientation of the probe are important sources of variation in the exerted probe pressure that have not been analyzed sufficiently. Hence, in this study, we highlight the significance of real-time, quantitative monitoring of dynamic changes in the applied probe pressure that can serve the purpose of minimizing the pressure induced distortions introduced in the spectral profiles by providing instantaneous, quantitative probe pressure feedback to operators in real-time. Moreover, the integration of the instant probe pressure feedback with the developed on-line real-time spectroscopic diagnostic framework[38] serves to further improve the diagnostic accuracy by mitigating the probe pressure induced spectral distortions in the acquired spectral data.

1.2 Specific aims and organization

The major objective of this dissertation is to develop a miniaturized, pressure sensitive fiber-optic probe for real-time, quantitative monitoring of the dynamic effects of probe-tissue contact pressure and to utilize the developed pressure sensitive probe to evaluate the pressure-induced distortions on *in vivo* skin optical spectroscopy (i.e. DR,

AF and Raman). The motivation of this study along with its specific objectives is presented in chapter 1. Chapter 2 focuses on the background information that is necessary to understand and solve the research challenge. The various aims of this study are as follows:

1. To develop a pressure sensitive fiber-optic robe for real-time quantitative monitoring of probe-tissue contact pressure and to integrate the instantaneous probe pressure feedback with the developed real-time online spectroscopic diagnostic framework (chapter 3).
2. To utilize the developed pressure sensitive probe to evaluate the probe pressure induced distortions on *in vivo* skin AF (both UV/visible and NIR) spectroscopy (chapter 3).
3. To study in detail the consequences of probe pressure induced distortions on in vivo skin tissue Raman spectroscopy (chapter 4).
4. To analyze the implications of probe-tissue contact pressure on *in vivo* skin diffuse reflectance spectroscopy using the developed pressure sensitive spectroscopic platform (chapter 5).

The final chapter (chapter 6) summarizes the entire work in this thesis and provides information about future improvements that can be made to the developed pressure sensitive spectroscopic platform and its use in other applications.

Chapter 2. Background

2.1 Skin Optics (human skin)

Skin optics, i.e. the manner in which skin reflects and transmits light of different colors, or wavelengths, is determined by the inherent optical properties of the skin layers. Each of these layers has different inherent optical properties, primarily due to differences in the concentration of endogenous components of the human skin.

2.1.1 Anatomy of human skin

The skin is the largest organ of the body, with a total area of about 1.8 square metres (20 square feet) and covers eighteen square feet in an average adult. It protects the body from microbes, helps regulate body temperature and permits the sensations of touch, heat and cold. The skin is composed of three layers, i.e., epidermis, dermis and hypodermis as shown in Figure 2.1

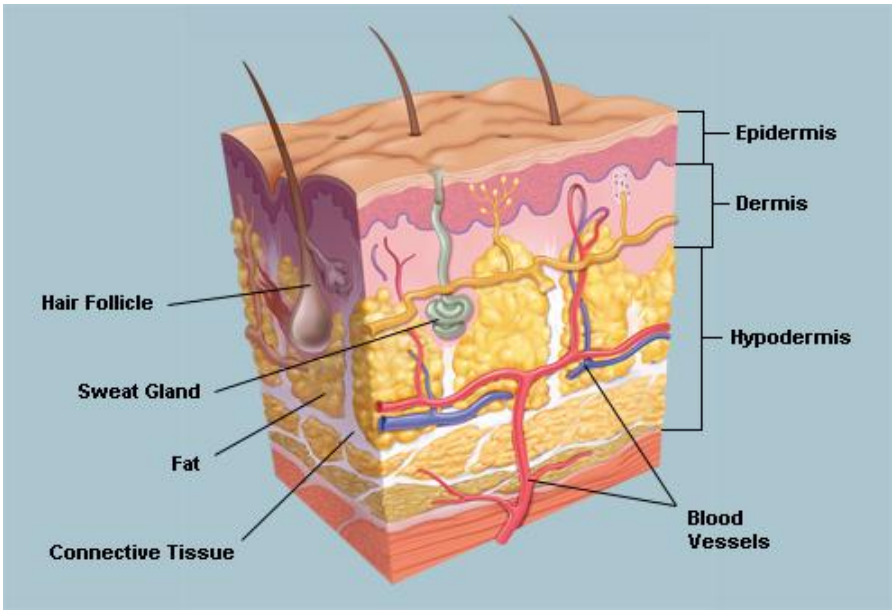

Figure 2.1 Anatomy of the human skin

The outermost (top) layer of the skin is called epidermis. The epidermis is a 0.027-0.15mm thick structure[39-41] composed of four layers (stratum basale, stratum spinosum, stratum granulosum and stratum lucidum). It acts as a waterproof barrier, strengthens the skin and protects it from the outside environment. The cells in the skin are capable of synthesizing keratin which is responsible for the waterproof nature of the skin. The epidermis also contains melanin, a dark pigment that gives color to the skin and controls the skin tone of an individual. The epidermis provides immunity to the body by preventing foreign invaders like germs or bacteria from entering the body.

The dermis is the middle layer of the skin. The dermis is a 0.6-3mm thick structure[39-41] which can be divided into two layers: the papillary dermis and the reticular dermis. It contains tough connective tissue, hair follicles and sweat glands. Blood vessels are located in the dermis and provide the skin with nutrients and also helps in removal of waste products. The dermis also contains sensory receptors which helps the body to feel the various sensations like pressure, pain and temperature.

The very bottom layer of the skin is the hypodermis. The hypodermis is a subcutaneous adipose tissue characterized by a negligible absorption of light in the visible region of the spectrum[42]. Its size varies considerably throughout the body, i.e. it can be up to 3cm thick in the abdomen and absent in the eye lids. It contains fat cells, or adipose tissue, that insulate the body and help it conserve heat.

2.1.2 Components of human skin

2.1.2.1 Blood vessels

The blood vessels make up an integral part of the skin. They help in the transport of oxygenated blood throughout the body and provide the required nutrients to the skin

cells. The blood vessels also help in the removal of waste from the body.

2.1.2.2 Sebaceous glands

The sebaceous glands secrete sebum, an oily substance that helps keep skin from drying out. Most of the glands are located in the base of hair follicles. Acne starts when the tiny hair follicles become plugged with these oily secretions.

2.1.2.3 Sweat glands

When the body gets hot or is under stress, these glands produce sweat, which evaporates to cool you. Sweat glands are located all over the body but are especially abundant in your palms, soles, forehead, and underarms.

2.1.2.4 Hair follicle

Every hair on the body grows from a live follicle with roots in the fatty layer of the dermis called subcutaneous tissue.

2.1.2.5 Collagen

Collagen is the most abundant protein in the skin, making up 75% of the skin. Over time, environmental factors and ageing diminish the body's ability to produce collagen.

2.1.2.6 Elastin

This protein is found with collagen in the dermis and is responsible for giving structure to the skin and organs. Diminished levels of this protein cause the skin to wrinkle and sag.

2.1.2.7 Keratin

Keratin is the strongest protein in the skin. It is also dominant in the hair and nails. Keratin is responsible for the rigidity of the skin.

2.1.2.8 Color

The color of the skin is created by special cells called melanocytes, which produce the pigment melanin. Melanocytes are located in the epidermis.

2.1.3 Optical properties of skin

The optical properties of the skin are governed by two important phenomenon, i.e. absorption and scattering. Absorption and scattering are caused by the various absorbers and scatterrers in the skin. The extent of absorption and scattering varies for different skin tissue types due to the differences in concentration of melanin, blood and keratin between them.

2.1.3.1 Absorbers in skin

When a photon is absorbed, its energy is invested in the chromophore molecule, and the photon ceases to exist.[43] Absorption in skin occurs primarily due to the presence of absorbers like blood, melanin and keratin. The absorption of light is dependent on the wavelength of incident light and each chromophore has characteristic absorption peaks at which absorption is maximum. The absorption coefficient (μ_a) is used to determine how far light can penetrate into the tissue before it is absorbed. The absorption coefficient depends on the concentrations of the absorbers in the skin and therefore, it varies for different skin tissue types (palm, nails, forearm, etc.) and also for different skin color profiles (asian, Caucasian, African, etc.) due to difference in skin melanin concentration.

2.1.3.2 Scatterrers in skin

Most scattering is an elastic interaction between optical radiation and matter in which only the direction of photon propagation is altered. Some types of scattering are inelastic and result in a change of wavelength as well (fluorescence, phosphorescence and

Raman scattering).[43] If the change in direction of the incident photon is less than 90º, it is called forward scattering. If the change in direction is greater than 90º, it is called backscattering or reflectance. The scattering particles in the skin consist of either lipids or proteins embedded in the fluids in and between skin cells. These fluids mainly consist of water. The primary protein scatterers in skin are keratins and melanins in the epidermis, and collagen and elastin fibers in the dermis.[44] The scattering coefficient (μ_s) is a measure of the attenuation due to scattering of light as it traverses a medium containing scattering particles. It is used to describe the interaction of light with a turbid medium like human skin.

Each layer of the skin has different inherent optical properties, primarily due to differences in the concentration of melanin, blood, and keratin between them. The inherent optical properties of a particular layer can be represented by a set of non-dimensional numbers[44]: 1) the optical depth, i.e. the integrated attenuation coefficient of a beam going perpendicularly through a particular layer; 2) the single scattering albedo, i.e. the probability that an attenuation event is a scattering event and 3) the normalized volume scattering function, i.e. the probability of scattering in a particular direction.

2.2 Significance of skin tissue Optical Spectroscopy

The various optical properties of different skin tissue types can be estimated and calculated by the use of optical spectroscopy techniques. These techniques are used to study the optical properties of skin tissue by measuring its interaction with light. Optical Spectroscopy has emerged as an important technique in modern scientific fields like chemistry, astronomy and biomedicine. It has been used in the diagnosis of various diseases.[12, 14, 18, 45-52] Diagnostic techniques based on optical spectroscopy have the

potential to link the biochemical and morphological properties of tissues to individual patient care. In particular, these techniques are fast, noninvasive and quantitative. Furthermore, they can be used to elucidate key tissue features, such as the cellular metabolic rate, vascularity, intravascular oxygenation and alterations in tissue morphology[53]. These tissue features can be interpreted to shed light on a variety of clinical problems and provide valuable information in screening and diagnosis of diseases.

2.3 Optical Spectroscopy - Introduction

Optical Spectroscopy is a useful technique to study the properties of physical objects by measuring its interaction with light. The objects may absorb, reflect or emit light and this information can be used to analyze the properties of physical objects. Various attributes such as chemical composition, temperature, and velocity can be measured by optical spectroscopy. It may involve visible, ultraviolet, or infrared light, alone or in combination during measurements and is a part of a larger group of spectroscopic techniques called electromagnetic spectroscopy. There are three aspects to a spectroscopic measurement: irradiation of a sample with electromagnetic radiation; measurement of the absorption, spontaneous emission (fluorescence, phosphorescence) and/or scattering (Rayleigh elastic scattering, Raman inelastic scattering) from the sample; and analysis and interpretation of these measurements.[53] Detailed study of absorption, spontaneous emission and scattering provides information that can be classified broadly as analytical, structural, dynamic, and energetic.

The visibility of an object depends upon whether it emits or reflects photons and the wavelengths of these photons are governed by the object's composition. The human

eye perceives the existence or non-existence of particular wavelengths by the presence or absence of certain colors. The spectrometer is a device that is used for precise analysis of light interaction with the object. This precise measurement of the different properties of light that different substances produce, reflect, or absorb under various conditions forms the basis of optical spectroscopy.[54]

Different chemical elements and compounds differ in how they interact with light (i.e. absorption, emission or reflection). It is because of the mechanical differences in the atoms and molecules that comprise them. The spectrometer produces spectral lines by measuring how the light has been reflected from, passed through, or emitted by the object being studied. Different substances produce distinctive spectral lines that can be used to identify their presence in a material. Other characteristics like light intensity, temperature and velocity provide useful information about the object and can be measured by a spectrometer.

2.4 Review of conventional skin tissue optical spectroscopy techniques

2.4.1 Diffuse Reflectance spectroscopy

Diffuse reflection is the reflection of light from a surface in which an incident ray is reflected at many angles from the strike point of illumination. Diffuse Reflectance Spectroscopy (DRS), sometimes known as Elastic Scattering Spectroscopy, is a non-invasive technique that measures the characteristic reflectance spectrum produced as light passes through a medium. The primary mechanisms are absorption and scattering that produce the reflectance spectrum that containing information about the optical properties and structure of the medium being measured. Diffuse Reflectance occurs because of the back scattering of light when it passes through a sample. It refers

only to the part of the incident light that is scattered within the sample and returned to the surface. This back scattered light is collected by the detector to study the optical properties of materials.

DRS has found applications in a number of areas. The most prominent is in the field of color measurement and color matching. The paper, paint, dye, textile, printing, and ceramics industries have made use of this technique for the measurement of color in routine quality-control functions.[55] For pharmaceutical applications the technique is being used extensively for production control, formulation studies and for investigations of aging and illumination effects. This rapid spectroscopic technique has also been extensively used in the field of biomedicine. The numerous biomedical applications of DRS include optical biopsy - detection of breast and skin cancer, cancer treatment decisions and defining therapeutic drug levels. Most of these applications utilize the unique ability of DRS to quantify the tissue chromophores, in particular the hemoglobin, lipids and water, which can be used to differentiate between normal and diseased tissue.[56]

2.4.2 Fluorescence spectroscopy

Fluorescence Spectroscopy (FS) is based on the phenomenon of fluorescence. The energy level diagram of a molecule with the ground (S_0) and excited (S_1) electronic energy states and its vibrational energy states is shown in Figure 2.2.[57]

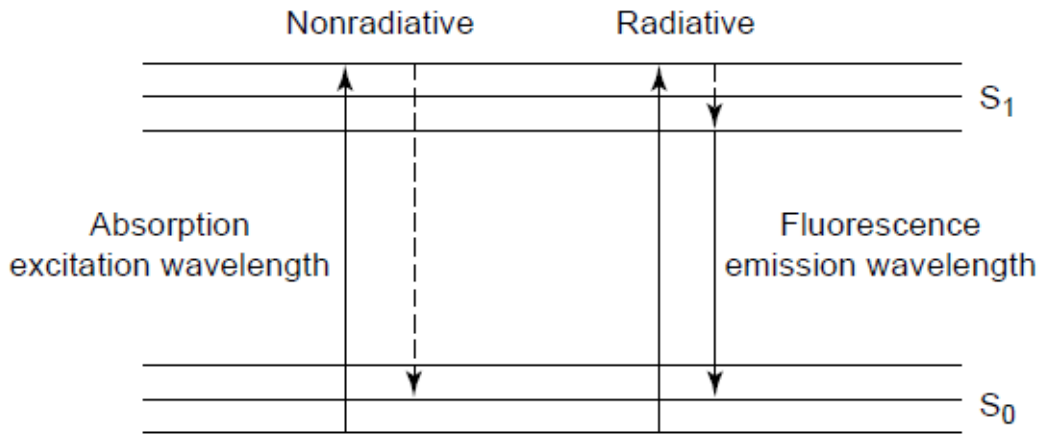

Figure 2.2 Energy level diagram illustrating the phenomena of absorption and fluorescence of a molecule

When a molecule is excited by an illumination wavelength within its absorption spectrum, it absorbs energy and moves from ground state (S_0) to excited energy state (S_1). The molecule relaxes back into the ground state either by emitting radiation or not. The relaxation depends on the local environment and occurs by thermal generation (dotted lines: non radiative) or by fluorescence emission (solid line: radiative) at particular wavelengths. Three different transitions take place during the emission of fluorescence:

1. non radiative transition to lowest vibrational level of first excited state (S_1).
2. radiative (fluorescence emission) transition to a higher vibrational level of ground state (S_0).
3. non radiative transition to the lowest vibrational level of ground state (S_0).

The emitted fluorescence normally has a longer wavelength than the illumination wavelength and is associated with the energy difference between the vibrational energy states in each electronic energy state.

FS has become an important tool in the field of biomedicine due to the presence of numerous endogenous fluorophores in tissues.[58-64] The most common fluorophores in

the human tissues are NADH (nicotinamide adenine dinucleotide), flavins, collagen and elastin and produce autofluorescence (AF) which is the natural emission of light by cellular biological structures when they have absorbed light (additional artificial fluorescent markers are not used to induce fluorescence). Therefore, AF spectroscopy has been utilized extensively in the screening and diagnosis of various diseases.[5, 12, 48, 65-68]

2.4.3 Raman spectroscopy

Raman spectroscopy is an optical vibrational technology capable of probing biomolecular changes of tissue.[47, 69-71] It is based on the Raman effect which was discovered by the Indian physicist Sir Chandrasekhara Venkata Raman (1888-1970) who won the Nobel Prize for physics in 1930. When the energy of the incident photon is not sufficient to excite the molecule to higher energy electronic level, the molecule is excited to the virtual energy level within the electronic level.[72] If the energy of the incident photon is unaltered after the collision with the molecule, the scattering phenomenon is called Rayleigh scattering (elastic scattering). However, a very small proportion of incident photons (~1 in 10^{10}) are scattered with a change in frequency,[73] called inelastic light scattering or Raman scattering technique that resolves the fundamental vibrational frequencies of molecules. If the final vibrational state of the molecule is more energetic than the initial state, the emitted photon will be shifted to a lower frequency for the total energy of the system to remain balanced. This shift in frequency is designated as a Stokes shift. If the final vibrational state is less energetic than the initial state, then the emitted photon will be shifted to a higher frequency, and this is designated as an anti-Stokes shift. Figure 2.3 shows all the energy level transitions involved in Raman scattering.

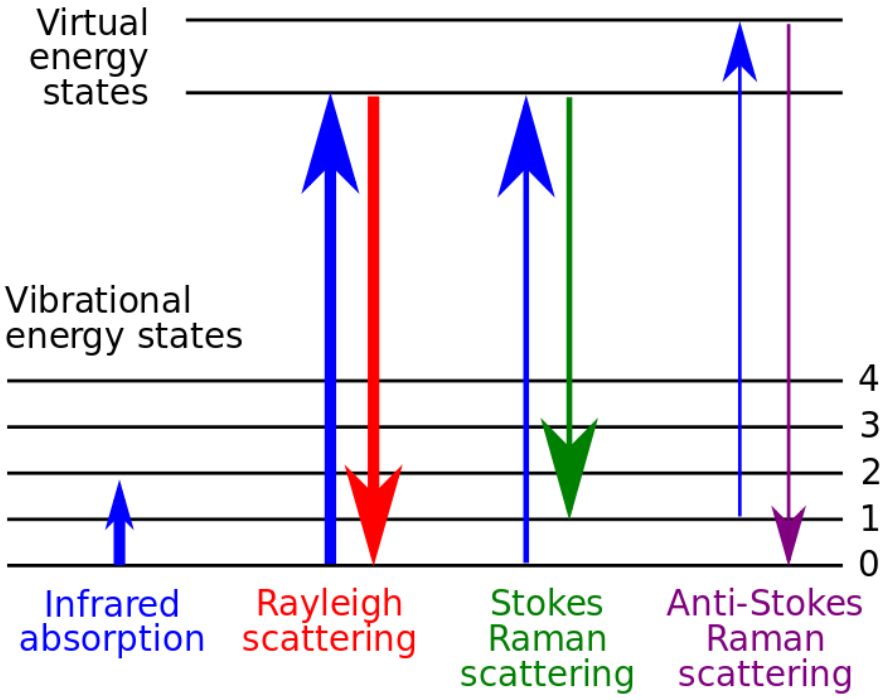

Figure 2.3 Energy-level diagram showing the states involved in Raman signal

Since Raman spectroscopy is a vibrational spectroscopic technique capable of providing details on the chemical composition, molecular structure, and molecular interactions in cells and tissues, it has been used in a variety of applications. Raman spectroscopy is commonly used in chemistry, since vibrational information is specific to the chemical bonds and symmetry of molecules. In solid-state physics, spontaneous Raman spectroscopy is used to characterize materials, measure temperature, and find the crystallographic orientation of a sample. Raman spectroscopy has also been used in various clinical applications to address various biomedical issues such as the early detection of cancers, monitoring of the effect of various agents on the skin, determination of atherosclerotic plaque composition, and rapid identification of pathogenic microorganisms.[74]

2.4.4 Basic instrumentation of fiber-based optical spectroscopy system

The basic instrumentation of a fiber-based optical spectroscopy system consists of three essential units:

1. Illumination unit
2. Detection unit
3. Fiber-optic probes

2.4.5 Illumination unit

The illumination unit consists of a suitable illumination source and an appropriate filter for efficient coupling of light into the probe to provide adequate irradiation to the sample. The required illumination source depends upon the type of spectroscopy. Normally, a broadband white light source is used for DRS. Filters are not required for DRS as the tissue sample is illuminated over the entire broadband visible range of wavelengths. More powerful light sources like lasers are required to induce fluorescence in biological samples. Therefore, lasers of different wavelengths are used to excite specific endogenous fluorophores present in the tissues. A suitable band-pass filter is essential to suppress the laser noise during tissue illumination. However, for Raman Spectroscopy, the illumination source should be strong enough to produce sufficient Raman signals and it should be monochromatized to have little power and to produce uncomplicated spectra.[75] This is because the Raman signals are very weak (only 1 in 10^{10} photons undergo Raman scattering) and a high power laser is required for excitation so that sufficient Raman signals can be collected. The main difficulty for the implementation of *in vivo* tissue Raman diagnosis system is the interference of tissue AF, which is typically of several orders of magnitude stronger than the inherently weak tissue Raman

signals, and the interference of silica fluorescence and Raman signals.[76] To avoid the strong AF interference, lasers in the ultraviolet (UV) range or near infrared (NIR) range are normally used. The UV lasers are typically used to probe superficial layers of tissue (due to its low penetration depth) and NIR lasers are utilized for probing deeper tissue layers.

2.4.6 Detection unit

The detection unit normally comprises of a spectrograph, a charged couped device (CCD) detector to record the spectra and a long pass filter to suppress the strong laser signal from the acquired spectra. The spectrograph is used to separate an incoming light wave into a frequency spectrum.It is used to separate and measure the wavelengths present in Electromagnetic radiation and to measure the relative amounts of radiation at each wavelength. The spectrograph is essential to resolve the incoming light wave into its characteristic spectrum. A CCD detector is used to detect and store the resolved spectrum. The CCD (multi-channel array detector) detection system has replaced other detection systems due to its reduced integration time, spectrum multiplexing capability, enhanced quantum efficiency and reduced etaloning effect over a large wavelength range (e.g., from 400 to 1100nm).[75] CCD also provides improved detection sensitivity due to very low dark count rate and vertical binning.[50, 77] Suitable long-pass filters are required to suppress the scattered laser light (which is several orders of magnitude higher than Raman and fluorescence signals) and to prevent the strong laser signal from interfering with the acquired spectra.

2.4.7 Fiber-optic probes

Various types of fiber-optic probes have been designed for specific applications. The probes are usually bifurcated and comprise of several collection fibers surrounding a central excitation fiber. Different types of probes can be employed to acquire diffuse reflectance and fluorescence signals because these signals are very strong. However, special probes are required to acquire Raman signals and there are several critical design considerations for fiber-optic Raman probes:[78-80] (i) The probe must have high collection efficiency to acquire Raman signal in very short acquisition time (<0.5 sec) with high SNR and low laser excitation power. (ii) Integration of filters to reduce laser noise, Rayleigh scattered light as well as fused-silica Raman and fluorescence interference. (iii) Constrained geometry for flexible clinical use to fit into the instrument channel of the desired medical equipment (e.g., endoscope, bronchoscope, colonoscope etc.). (iv) Bio-compatible and capable to withstand medical sterilization. Controlling the probing depth and sampling volume is of great clinical importance during disease diagnosis because diseases like cancer typically initiates in the epithelial layer. Several design strategies such as beveled collection fibers, graded-index (GRIN) lens or distal ball lens have been proposed to maximize tissue spectral measurements in the epithelial tissue. Thus, it is of critical importance to choose the type of fiber-optic probe depending upon the type of application.

2.5 Need for pressure sensitive probe in optical spectroscopy

Optical spectroscopy techniques make use of fiberoptic probes during spectral measurements. [36, 37] The fiberoptic probes are generally in contact with the target skin tissue throughout the data acquisition process. Probe pressure contact reduces the

refractive index mismatch and eliminates specular reflection from the tissue.[30, 35, 36]It also reduces spectral variations in acquired data compared to non-contact measurements. Moreover, the deformable nature of the skin results in compression of the tissue when pressure is applied resulting in changes in tissue optical properties.[30] Disparities in data acquisition and inaccuracies in diagnosis arise if there is variation in the applied probe pressure. The probe-tissue contact pressure is a user-dependent parameter that is difficult to control as the operator does not have any information about the applied probe pressure. Hence it is essential to quantify the exerted probe-tissue contact pressure and provide feedback to the operator in order to mitigate the pressure induced distortions in the acquired spectral data. The need for real-time monitoring and quantification of applied probe pressure can be accomplished by the development of a pressure sensitive probe that is capable of establishing dynamic probe pressure control by providing quantitative probe pressure feedback to operators during spectroscopic measurements.

2.6 Confounding effect of probe pressure

Various groups have attempted to study the effects of probe-tissue contact pressure on the spectral profiles of the acquired optical spectra. The probe pressure is an important parameter because many diagnostic or therapeutic applications that use optical fiber probes, pressure is often applied to the tissue to reduce index mismatch and increase light transmittance.[35] It has been reported that optical properties like transmittance, reflectance, absorption coefficient and scattering coefficients showed considerable variations with changes in applied probe pressure.[81] The effects of probe pressure on diffuse reflectance spectroscopy have been investigated extensively in the last two decades. Eric Chan et al. were the first to study the effects of probe pressure on in vitro

human skin and reported that the overall reflectance decreased with applied probe pressure.[35] Shangguan et al. measured the effects of probe tissue contact pressure on in vitro elastin biomaterial and showed the reflectance signal decreased with increase in exerted probe pressure.[81] Reif et al. carried out the first in vivo probe pressure reflectance studies on mouse high muscle and reported that the probe-tissue contact had a significant effect on the reflectance spectra.[82] Ti Et al. investigated the in vivo probe pressure induced reflectance measurements on mouse heart and liver tissue and reported that no statistically significant changes in diffuse reflectance spectra were observed.[29] The first reflectance measurements on in vivo human skin (palm tissue) were carried out by Chen et al. who reported that the reflectance signal decreased with applied probe pressure.[36] Clinical studies were carried out by Atencio et al. who measured reflectance signals from in vivo human volar forearm at different pressures and their reported results were in agreement with Chen et al.[37] However, Randeberg et al. reported an increase in reflectance signal with applied probe pressure.[83] Recent studies by Lim et al. have shown that the effect of probe-tissue contact pressure on in vivo human skin is site-specific.[32] They reported that the applied probe pressure produced contrasting effects on the forehead and neck reflectance signal. Cugmas et al. have shown that the significant variations in reflectance measurements with applied probe pressure can be used as valuable information for soft tissue classification (i.e. skin above muscle, skin above veins and skin above bone).[31] The above studies that report on the effects of probe-tissue contact pressure on diffuse reflectance measurements show that the probe pressure is a confounding variable and it is important to monitor the applied probe pressure in real-time to mitigate its effects on the acquired spectral data.

Similar probe pressure studies on fluorescence spectroscopy have already been carried out but these studies are very limited in number. Fluorescence spectra acquired at different probe pressures during in vivo FS from cervical and breast tissues showed that though the variations in probe pressure resulted in differences in fluorescence intensity; it was not large enough to affect the diagnostic capacity of fluorescence spectroscopy.[34, 84, 85] Probe pressure studies which were carried out by Ti et al. during in vivo FS on rat liver and heart issue showed that the fluorescence intensity clearly increased with applied probe pressure. They also reported that a minimum tissue-dependent threshold pressure is required to induce statistically significant alterations in the fluorescence spectra.[29] Lim et al. reported that the effect of probe pressure is site-specific with no increasing or decreasing trend.[32] These aforementioned studies show that more investigation has to be carried out to characterize the effects of probe-tissue contact pressure on in vivo FS.

Till date (up to our knowledge), there has been no detailed studies that have analyzed the influence of probe pressure on in vivo Raman spectroscopy. The existing literature show that probe pressure has negligible effect on Raman signals if it is maintained below clinically extreme pressures of 55 kPa.[86, 87] However, more detailed studies are required to evaluate the effect of probe-tissue contact pressure on in vivo Raman spectroscopy.

The concurrent probe pressure spectroscopic studies discussed above suffer from the following shortcomings:

i) Many of these studies used arbitrarily defined pressure values which were operator-dependent (i.e. the pressure was not quantified and so it is impossible to know how much pressure was applied).

ii) Some studies utilized spring loaded devices in which pre-set pressure levels were utilized to perform spectroscopic measurements. These devices could only be used to measure probe pressures at specific pre-set pressure levels while pressure monitoring or measurement over a wide range is not possible. Moreover, these devices were difficult to use because they had to be calibrated every time before conducting experiments due to the mechanical properties of the spring.

iii) Some studies also depended upon the extent of tissue compression (in mm) to apply pre-set pressure levels on the tissue. These measurements may not be accurate due the inter-subject differences in tissue deformability.

Therefore, in this dissertation, the focus is on the development of a pressure sensitive fiber-optic probe for real-time quantitative monitoring of probe-tissue contact pressure, evaluation of the probe pressure effects on various optical spectroscopic techniques and the discussion of improvements in pressure measurements by the utilization of the developed pressure sensitive spectroscopic platform.

2.7 Conventional Pressure Sensors

There are different types of pressure sensors that have been developed over the years. Pressure sensors are typically used to determine the magnitude of applied pressure. Most pressure sensors have the ability to sense a wide range of pressures (zero to few hundred kilo Pascals).

2.7.1 Types of pressure sensors

2.7.1.1 Piezo-resistive strain gauge

The piezoresistive effect of bonded or formed strain gauges are used to detect strain due to applied pressure. Common technology types are Silicon (Monocrystalline),

Bonded Metal Foil and Thick Film. This is the most commonly employed sensing technology for general purpose pressure measurement. Generally, these technologies are suited to measure absolute, gauge, vacuum, and differential pressures.

2.7.1.2 Capacitive

A variable capacitor is created by the use of a diaphragm and pressure cavity to detect strain due to applied pressure. Common technologies use metal, ceramic, and silicon diaphragms. Generally, these technologies are most applied to low pressures.

2.7.1.3 Electromagnetic

The displacement of a diaphragm is measured by means of changes in inductance, Hall Effect, or by eddy current principle.

2.7.1.4 Piezoelectric

The piezoelectric effect in certain materials such as quartz is used to measure the strain upon the sensing mechanism due to pressure. This technology is commonly employed for the measurement of highly dynamic pressures.

2.7.1.5 Optical

Techniques include the use of the physical change of an optical fiber to detect strain due to applied pressure. A common example of this type utilizes Fiber Bragg Gratings. This technology is employed in challenging applications where the measurement may be highly remote, under high temperature, or may benefit from technologies inherently immune to electromagnetic interference. Another analogous technique utilizes an elastic film constructed in layers that can change reflected wavelengths according to the applied pressure (strain).

2.7.1.6 Potentiometric

The motion of a wiper along a resistive mechanism is used to detect the strain caused by applied pressure.

The real-time monitoring of applied probe pressure in biomedical spectroscopic applications has been challenging due to the non-availability of appropriate pressure sensors that could be integrated into the probe during spectral data acquisition. This is because the traditional pressure sensors were large and bulky and could not be coupled with the small probes that are used in optical spectroscopy. Moreover, the commercially available pressure sensors were mostly utilized to measurement of extreme pressure (> 100 kPa) and therefore these sensors had a very low sensitivity to measure clinically relevant low pressures (< 100 kPa).

2.7.2 Thin film pressure sensors

Thin film pressure sensors are piezo-resistive sensors that have been recently developed and work on the principle of transduction of mechanical strain into an impedance change providing simple read-out of the applied pressure.[88]Many of the reported resistive-type sensors function based on bulk piezoresistivity and employ composites of insulating polymers and conductive additives as the active layer.[89] These pressure sensors are small (3-9 mm sensing area diameter) and flexible having high sensitivity (upto 50 mV/kPa) and very low response time (< 5μs). Figure 2.4 shows a picture of two types of thin film pressure sensors. These sensors are useful for biomedical spectroscopic applications due to their small size and high sensitivity to measure low pressures (0- 100kPa). We employed these thin film sensors during the development of the pressure sensitive probe and utilized the pressure sensor coupled probe to evaluate the probe pressure induced distortions on the spectral profiles of various optical spectroscopy

techniques.

Figure 2.4 Examples of thin-film piezo-resistive pressure sensors

2.8 Data pre-processing

Devices like gratings, detectors, beam splitters, lenses and other components that are used for analysing light are, by their very nature wavelength-dependent. The response of these individual components is collectively termed as the instrument response. Whenever it is necessary to define the precise shape of spectral features, the instrument effects must be removed from data. Instrument corrections adjust the observed intensity value of each data point in a spectrum by a factor that represents the relative response of the instrument at that point. Etaloning in the CCD, modal interference in optical filters, variation in the CCD pixel sensitivity and particularly, gradual change in quantum efficiency of the detector across the spectral range can cause a significant change in instrument sensitivity that varies slowly with wavelength, resulting in rapid oscillation in the sensitivity of the spectroscopy instrument with changing wavelength.[90] Therefore, the acquired spectra must first be corrected for wavelength dependence of the system. A stable white light source such as a tungsten-halogen lamp or flashlight with tungsten bulb is normally used to correct for the instrument dependence of the spectra. Spectra are acquired using the standard white light source whose spectral distribution is already

known and this information is utilized to correct for the instrument response of the system. Furthermore, the background noise must be subtracted from the acquired spectral data. This can be done by blocking the source and scanning the dark data and subtracting it from the original spectral data. This process is automated in many software packages. For Raman spectroscopy, further data processing is required to extract the Raman signals from the intensity corrected raw data. The intensity corrected raw data is a combination of prominent tissue AF background, weak tissue Raman scattered signals, and noise. Hence, the intensity corrected spectra has to be further smoothed (e.g., Savitzky-Golay) to reduce the uncorrelated noise.[91, 92] Since, the AF is typically several orders of magnitude more intense than the Raman signal, accurate subtraction of this AF signal is necessary to obtain the pure Raman signal and is still a challenge.[93] A number of methodologies have been proposed for effectively removing the tissue AF background.[94-97] However, polynomial fitting is one of the most commonly used methods and found to be the simplest and accurate to describe the broad AF line shape and retain the Raman spectral features.[95] Therefore, data processing has to be carefully carried out to obtain the required spectral data from the acquired raw spectra.

2.9 Multivariate statistical analysis

Multivariate statistical analysis refers to multiple advanced techniques for examining relationships among multiple variables at the same time. Multivariate procedures are often used in studies that involve more than one dependent variable (also known as the outcome or phenomenon of interest), more than one independent variable (also known as a predictor) or both. This type of analysis is desirable because most research problems are affected or influenced by more than one variable. In spectroscopy,

multivariate algorithms are employed to study the dependence of the acquired spectra over a wide range of independent wavelengths.

2.9.1 Classification algorithms

Several multivariate classification algorithms like principal component analysis-linear discriminant analysis (PCA-LDA)[71, 98, 99] and partial least squares-discriminant analysis (PLS-DA)[22, 100, 101] have been utilized to classify the spectroscopic data based on different parameters. Classification of normal tissue from abnormal tissue[102, 103] and soft tissue classification (i.e. skin above muscle, skin above veins and skin above bone)[31, 56] have been performed by utilizing the aforementioned statistical algorithms. In this dissertation, we use PLS-DA to classify the spectral data based on the magnitude of the applied pressure (i.e. LP, MP, and HP). The goal of PLS-DA is to predict or analyze a set of a set of dependent variables from a set from a set of independent variables or predictors. This prediction is achieved by extracting from the predictors a set of orthogonal factors called *latent* variables (LVs) that are essentially loading values having the best predictive power[104]. PLS-DA is based on the PLS model in which the dependent variable is chosen to represent the class membership.[105] The class membership for each sample is usually coded with zeros (i.e., sample does not belong to a particular class) and ones (i.e., denoting the presence of sample to a particular class). PLS-DA utilizes the pre-defined class membership information to maximize the group separation. It extracts the latent variables in a decreasing order of their respective singular values from the input dataset. PLS-DA follows the principle of PCA, but further rotates the components (latent variables (LVs)) to achieve maximum group separation.[103] Unlike PCA, PLS-DA correlates the variations in the dataset with the response variable. Therefore, PLS-DA

makes use of relevant variations in the dataset rather than the most significant differences and can be used to provide diagnostically relevant predictions. The optimum number of components is estimated based on the local minimum of cross-validation classification error values. The latent scores, loadings and weights are extracted for the corresponding number of components selected. In PLS-DA, the complexity of the model is controlled by the number of components selected and the number of optimal components is determined from CV error values. The CV error plot is a curve plotted between the number of LVs and the estimated error in the prediction model. The objective is to choose the optimum number of components that minimizes the error in prediction. By selecting the optimum number of components it is possible to avoid over fitting and under fitting. Thus, these multivariate algorithms are used for in-depth analysis of the acquired spectral data and to determine the statistical significance of the datasets.

Chapter 3. Development of a pressure sensitive fiber-optic probe for real-time, quantitative monitoring of probe-tissue contact pressure on *in vivo* autofluorescence spectroscopy

This chapter is divided into two major parts. The first part focuses on the development of the real-time pressure sensitive fiber probe for *in vivo* optical spectroscopy and the utilization of the developed pressure sensitive probe for evaluation of probe-tissue contact pressure effects on *in vivo* UV/visible AF at 405 nm laser excitation. The second part of this chapter deals with the assessment of probe pressure effects on *in vivo* NIR AF spectroscopy under laser excitation of 785 nm.

3.1 Probe-tissue contact pressure effects on *in vivo* UV/visible autofluorescence spectroscopy

A novel miniaturized probe design integrated with a customized piezo-resistive pressure sensor is presented in this study for real-time, quantitative monitoring of probe-tissue contact pressure effects during *in vivo* skin optical spectroscopy measurements. The developed pressure sensitive probe with sensitivity of ~20.6 mV/kPa and short response time of < 5 μs was then utilized to investigate the probe pressure induced spectral variations on *in vivo* skin autofluorescence (AF) spectroscopy at clinically relevant probe contact pressures (i.e., 0 to 200 kPa). High-quality *in vivo* AF spectra (λ_{ex}=405 nm; λ_{em}=450-650 nm) were acquired from fingertip and volar forearm skin sites (n=10 subjects) at three reference pressure levels (i.e., low pressure (LP) ~10 kPa, moderate pressure (MP) ~50 kPa and high pressure (HP) ~130 kPa). The emission peak intensity (I_{467nm}) of skin AF spectra showed that MP affected fingertip AF appreciably ($p < 5X10^{-4}$)

compared to volar forearm ($p > 0.05$). Multiclass partial least squares-discriminant analysis (PLS-DA) could accurately classify 56.41% (22/39) of the fingertip spectra and 12.82% (5/39) of volar forearm spectra measured under MP from LP and HP, which reconfirmed the site-specific effect of probe pressure (i.e., MP influenced fingertip AF considerably, but not the volar forearm AF). The PLS-DA analysis could further accurately separate 70.59% (24/34) of fingertip and 86.11% (31/36) of volar forearm AF acquired at LP from MP and HP, which suggested that the probe pressure affected *in vivo* skin AF significantly. The instant, quantitative probe pressure feedback provided by the developed pressure sensitive fiberoptic probe could be used to mitigate the probe pressure induced site specific spectral variations on *in vivo* skin tissue AF.

3.1.1 Introduction

Skin is an important organ in the human body that is highly vulnerable to diseases such as cancer. The skin is a complex structure with a unique tissue biochemical composition that has to be carefully monitored for biochemical changes to detect and diagnose various skin diseases[58, 106] Recently, fiberoptic spectroscopy techniques (e.g., reflectance, fluorescence and Raman spectroscopy) capable of probing changes in tissue optical properties that can reflect physiological parameters and tissue composition have been recognized as promising candidates for *in vivo* disease diagnosis in various organs of the human body.[1, 3, 8, 23, 28, 66] The spectroscopy diagnostic instruments employ fiberoptic probe as an integral part of system, enabling non-invasive or minimally-invasive access to remote internal organs. The probe is placed against the target tissue and remains unchanged during *in vivo* spectral measurements. This ensures probe-tissue contact, avoids inconsistent illumination-detection geometry, reduces refractive index mismatch,

and increases light penetration depth into tissue to enhance the diagnostic capability of spectroscopy instruments.[29] High probe contact pressure, however, alters the optical properties of tissue[31, 32] by producing following effects on tissue under compression: decreased thickness, reduced blood volume and oxygen saturation, vasodilation, microcirculation impairment, densely packed scatterers and occlusion under the probe tip.[30] Furthermore, it is hard to control the applied probe pressure particularly in clinical scenario (e.g., *in vivo* diagnosis in endoscopic organs) due to difficulty in accessibility of internal organs. Thereby, utilization of hand-held fiberoptic probe in tissue optical spectroscopy may introduce operator-induced variations in the magnitude of probe pressure exerted onto the tissue.[32, 33] This may lead to potential concerns such as changes in tissue spectral profiles, disparities in data collection and calibration[34] and possible inaccuracies in diagnosis. Hence, acquisition of high-quality *in vivo* tissue spectra in sub-seconds (<1 sec) together with real-time probe handling advice about probe contact pressure and its effects are highly paramount to mitigate user-induced tissue spectral profile variations.

Very few limited studies have investigated the effect of exerted probe pressure on *in vivo* tissue spectral measurements.[29, 32, 84, 85] For instance, the varying fiberoptic probe pressure exhibited insignificant changes in cervical tissue fluorescence.[84, 85] Ti et al. have reported that the site-specific effects of high probe pressure on *in vivo* fluorescence of rat liver and heart tissue can be minimized with the application of short-term low pressure (LP).[29] Lim et al. also disclosed that short-term, light probe pressure has negligible effects (i.e., within 0 ± 10% for all extracted physiological properties) on *in vivo* skin fluorescence and reflectance.[32] However, till date (up to our knowledge), most of the

reported studies in fluorescence spectroscopy modalities are limited to employing pre-calibrated spring loaded device for exerting arbitrary pressure onto tissue[32, 84] or utilizing subjective, operator determined light, medium or firm pressures[84]. In this study, we report on the development of a novel pressure sensitive piezo-resistive fiberoptic probe applicable for various biomedical spectroscopy platforms (e.g., Raman, fluorescence, and reflectance) to quantitatively monitor the effects of probe-tissue contact pressure *in vivo* in real-time. We further tested the capability of the developed pressure sensitive piezo-resistive fiberoptic probe for assessing contact pressure effects on *in vivo* skin autofluorescence (AF) spectroscopy. Since skin acts as a highly scattering medium in visible to near-infrared region, it presents one of the most challenging organs with complex inhomogeneous morphological structures to demonstrate the probe pressure effects. Multivariate analysis including partial least squares-discriminant analysis (PLS-DA) was executed on skin AF spectra to elicit the spectral information associated with probe pressure variability.

3.1.2 Materials and methods

3.1.2.1 Pressure sensitive UV/visible AF spectroscopic platform

Figure 3.1.1 shows the schematic of pressure sensitive *in vivo* tissue AF spectroscopy platform developed for real-time, quantitative monitoring of probe-tissue contact pressure effects. The spectroscopy system consists of a spectrum-stabilized 405-nm diode laser (maximum output: 100 mW, Power Technology Inc., Alexander, AR, USA), a transmissive imaging spectrograph (QE65000, Ocean Optics Inc., Dunedin, FL, USA) equipped with a back-thinned charge-coupled device (CCD) detector (S7031-1006, 1024X58with pixel sizes of 24.6mm, QE > 90%, Hamamatsu, Shizuoka, Japan), and a

customized piezo-resistive sensor coupled bifurcated fiberoptic probe.

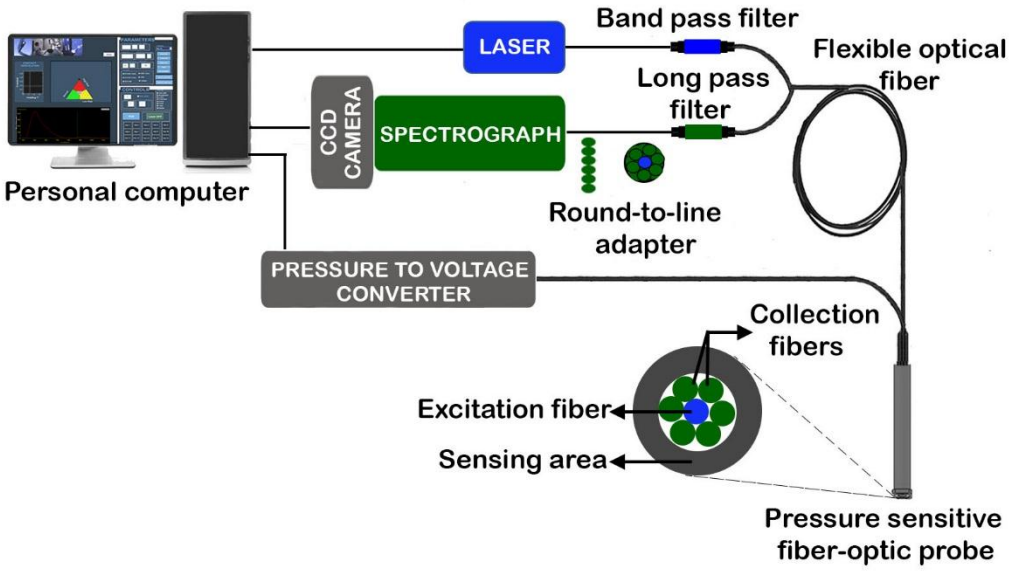

Figure 3.1.1 Schematic of the pressure sensitive fiber-optic autofluorescence (AF) spectroscopy system

The hand-held bifurcated fiber probe (2 m in length, 6.35 mm in outer diameter, R200-7-VIS/NIR, Ocean Optics Inc., Dunedin, FL, USA) consists of a tight bundle of 200 μm silica fibers in a 6-around-1 configuration (i.e., 6 collection fibers surrounding the central laser light delivery fiber). The excitation and emission fibers at the proximal ends of fiberoptic probe were coupled into two separate filter modules: the excitation fiber is integrated with a narrow band-pass filter (FBH 405, Thorlabs Inc., Newton, NJ, USA) to suppress laser noise and to reduce fused-silica noise generated in the excitation fiber before the excitation beam hits the tissue; the collection fiber bundle is integrated with a long-pass filter (HQ 430, Thorlabs Inc., Newton, NJ, USA) to further reduce the scattered laser light, while permitting tissue AF signals to pass toward the spectrograph through a specially designed round-to-line fiber bundle adapter (28×50μm, NA=0.22).

The round-to-line fiber bundle adapter further improves the signal-to-noise ratio of the measured *in vivo* tissue NIR AF signal of up to 7.6-fold (√58) by vertical binning of entire CCD. The hand-held fiberoptic probe is customized by coupling a piezo-resistive flexiforce pressure sensor (sensing area outer diameter of 6.35 mm, length of 51 mm, thickness of 0.203 mm, Tekscan Inc., South Boston, MA, USA) to the probe tip to facilitate real-time, quantitative monitoring of probe pressure exerted on the tissue and its effects. The relative contact area (i.e. ~0.6 cm^2) is equal to the sensing area of the pressure sensor. The standard thin film pressure sensor is made of a piezo-resistive polyester substrate that changes its resistance with applied pressure on the sensing area. The pressure sensor has large working range of 0-25 lbs, sensitivity of ~20.6 mV/kPa for measuring clinically relevant pressures (0-200 kPa), very short response time of <5μs, and operating temperature of -9°C to 60°C, greatly facilitating the adoption of piezo-resistive sensor coupled pressure sensitive fiberoptic probe for real-time quantitative monitoring of probe pressure and its effects on *in vivo* tissue spectroscopy. The pressure sensor is connected to a force/pressure-to-voltage circuit and analog to digital converter (ADC) to promptly quantify the magnitude of exerted probe pressure onto the tissue. The force-to-voltage circuit consists of a voltage divider circuit with a fixed reference resistance of 1.5 MΩ followed by an inverting amplifier with an adjustable gain and DC bias (0 to 5 V) to produce an analog output based on the resistance of the sensor. The ADC further converts the sensor's analog output to a digital voltage value. The sensitivity of the sensor can be adjusted either by changing the reference resistance or drive voltage. The lower reference resistance or drive voltage allows the sensor to be less sensitive with large active force range. The entire control of the system is implemented by a personal

computer using in-house developed graphical user interface (GUI) under Matlab environment (Mathworks Inc., Natick, MA, USA) that triggers data acquisition and analysis including laser power control, CCD shutter and camera readout synchronization, CCD dark-noise subtraction, outlier detection, wavelength calibration, system spectral response calibration, normalization, and real-time display of *in vivo* skin spectra together with the quantified probe contact pressure applied.[38]

3.1.2.2 Calibration of the fiber-optic pressure sensor

Precise calibration of fiberoptic pressure sensor is essential for accurate real-time quantification of applied probe pressure during *in vivo* tissue spectroscopic measurements. Standard weights were utilized for the calibration process. The sensor was pre-calibrated using standard weights in the range of 0-2 kg with small increments of 50 g and the response of the sensor was noted. The standard weights were first placed on the sensing area of the pressure sensor (starting from 50g to 2g) in steps and the response of the sensor was noted. The force (mass X acceleration of gravity) and pressure (force / sensing area) values corresponding to the weight applied were calculated. The resistance of the sensor gradually decreases with applied pressure and causes an increase in the output voltage. The relationship between the applied probe pressure and the output voltage was calculated and plotted in Figure (3.1.2). The calibration procedure was repeated three times and standard deviation of the measured pressure was calculated and plotted in Figure 3.1.2

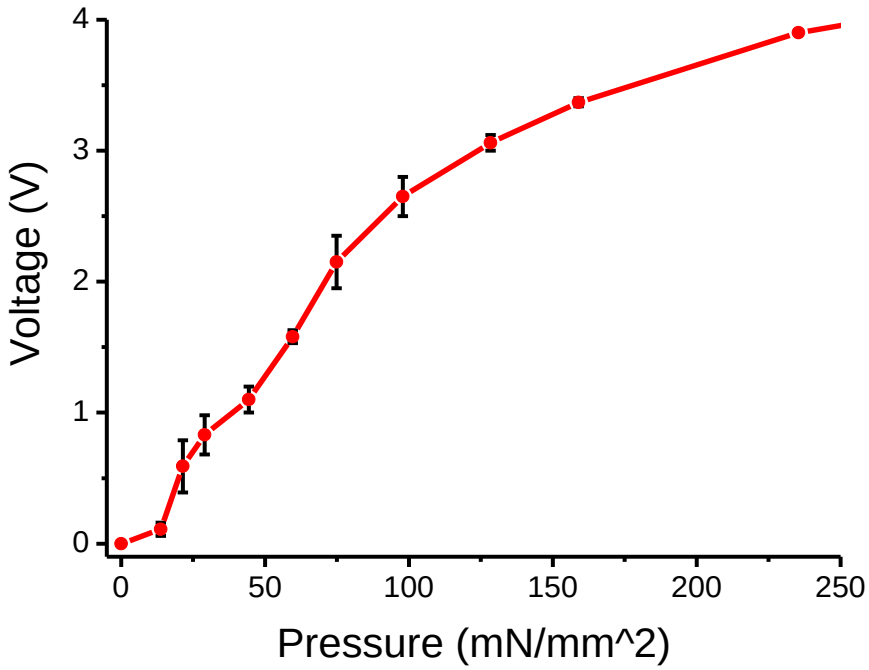

Figure 3.1.2 Typical response curve ± standard deviation (SD) of thin film piezo-resistive pressure sensor calibrated for range of pressures (0 – 200 kPa)

The picture of the final piezo-resistive fiberoptic probe attached to the pressure sensor is shown in Figure 3.1.3 (a). A central aperture (seen in Figure 3.1.3) in the sensing area of the pressure sensor allows the unhindered passage of light into the tissue. Figure 3.3.3 (b) shows the experimental setup and Figure 3.3.3 (c) shows the schematic of the human arm indicating the various measurement sites.

The flexiforce sensor and the probe tip were integrated by using a suitable adhesive. However, care should be taken to use an adhesive that does not react chemically with the substrate of the pressure sensor. Additionally, the pressure sensor should be able to provide unhindered passage of light into the tissue as shown in *Figure 3.1.3 a.*

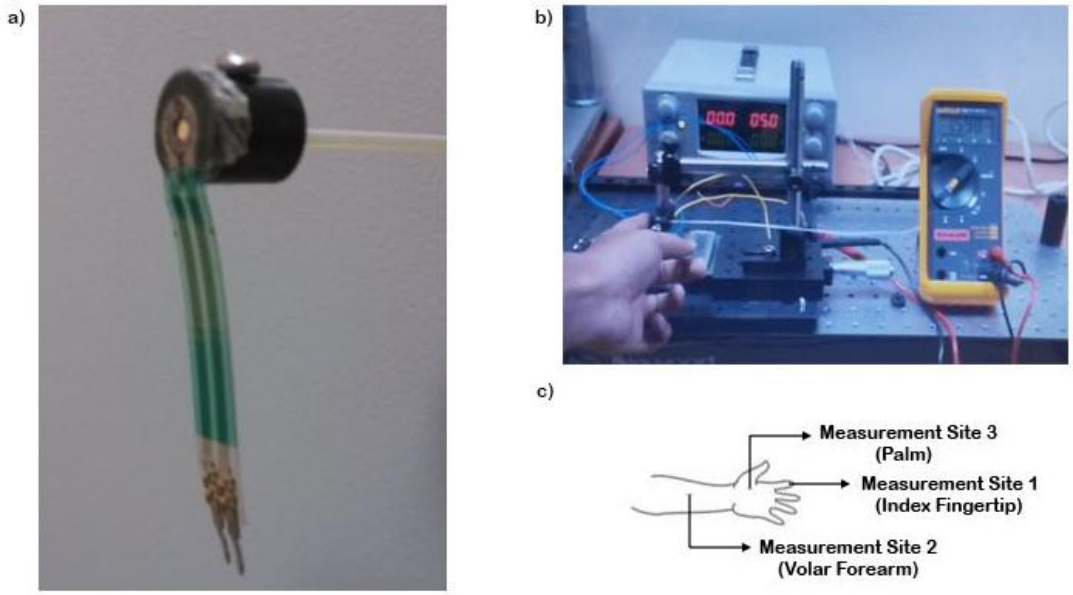

Figure 3.1.3 a) Picture of the pressure sensor attached with the piezo-resistive fiberoptic probe. The central aperture in the pressure sensor allows the unhindered passage of light into the tissue b) Picture of the experimental setup c) Schematic of the human arm showing the various skin measurement sites.

3.1.2.3 In vivo pressure sensitive skin AF measurements

The pre-calibrated pressure sensor coupled piezo-resistive fiberoptic probe was mounted horizontally on a translation stage. The tissue site to be measured (i.e., index fingertip or volar forearm) was fixed perpendicular to probe tip to restrict the mobility and to avoid variations in exerted probe pressure due to orientation of probe during spectral measurements. Movement of the hand will cause variations in the applied probe pressure and will be reflected in the real-time pressure value that is measured by the pressure-sensitive probe. Therefore, care was taken to avoid sudden motion of the hand during the experiment by placing the measurement site between a fixed immovable stage (on one side) and the horizontally displaceable probe tip (on the other side). The translation stage was promptly displaced to employ desirable probe pressures (i.e., LP – 10 kPa, moderate pressure (MP) – 50 kPa and high pressure (HP) – 130 kPa) on *in vivo*

target tissue site. The applied probe pressure was instantaneously displayed in the real-time diagnostic software,[38] guiding the operator to continue holding the probe against the tissue at desired reference pressure level during *in vivo* tissue spectral acquisition. High-quality *in vivo* tissue AF spectra were subsequently measured from fingertip (n=113) and volar forearm (n=115) of 10 healthy volunteers at the aforementioned three reference pressures within an integration time of 1 sec under 405 nm laser excitation. Multiple spectra (~3-4) were obtained from each site for all the three pressure levels to include inter- and/or intra-tissue variability for data analysis. Pronounced spectral changes have been previously reported due to diverse skin phototype and associated variations in melanin and hemoglobin content across individuals (i.e., race, age, and sun exposure).[68] The volunteers were therefore restricted to single race (i.e., Chinese) with the age limit of 18-35 and no history of skin cancer.

3.1.2.4 Multivariate statistical analysis

Multi-class probabilistic PLS-DA was performed to realize *in vivo* discrimination among skin AF spectra acquired at different pressure levels. PLS-DA employs the fundamental principle of principal component analysis (PCA), but further rotates the components (latent variables (LVs)) by maximizing the covariance between AF spectral variations and applied probe pressure in order to exclusively explain probe pressure related spectral variability.[107] The performance of PLS-DA model was validated using leave-one volunteer-out, cross validation methodology. In this validation procedure, the spectral data of one volunteer was left out and the PLS-DA model was redeveloped from the spectra measured from remaining volunteers. The redeveloped model was used to classify the withheld spectral data of one volunteer and this process was repeated

iteratively until withheld spectral data of all volunteers were classified. The complexity of the developed PLS-DA model (i.e., number of LVs required to develop the model) was determined on the basis of minimum classification error.[105] The one-against-all multi-class terminology was further utilized to classify the tissue spectra measured under different pressure levels.[108] The multivariate statistical analysis was performed using the PLS toolbox (Eigenvector Research, Wenatchee, WA) in the Matlab (Mathworks Inc., Natick, MA, USA) programming environment.

3.1.3 Results

High quality *in vivo* skin tissue AF emission spectra were acquired (< 1 sec) in the range 450 – 650 nm using the developed novel pressure sensitive piezo-resistive fiberoptic probe coupled AF spectroscopy platform under 405 nm-excitation. Figure 3.1.4 shows the *in vivo* mean skin AF spectra ±1 standard error (SE) of index fingertip (n=113) and volar forearm (n=115) acquired from 10 healthy volunteers at three defined reference pressure levels [10 kPa (LP), 50 kPa (MP) and 130 kPa (HP), (Table 3.1.1)]. The measured AF spectra essentially exhibited intense, broadband, but an overall decreasing curve with varying intensities for each pressure level. The tissue AF spectra presumably emerged due to the superposition of light re-emission from excited endogenous skin fluorophores (e.g., nicotinamide adenine dinucleotide (NADH), flavin adenine dinucleotide (FAD), and collagen), usually distorted by the re-absorption of intrinsic tissue pigments (e.g., blood in dermis).[109] The AF emission maximum intensity (over the range 450-470 nm, peaked at ~467 nm, $p < 1X10^{-8}$) of fingertip and volar forearm skin spectra showed substantial increase with applied probe pressure (Figure 3.1.4).

Pressure Level	Load (g)	Force (N)	Pressure (kPa)
Low Pressure (LP)	50	0.490	10
Medium Pressure (MP)	350	3.430	50
High Pressure (HP)	800	7.840	130

Table 3.1.1 The range of pressures applied on skin tissue (i.e., index fingertip and volar forearm) using the pressure sensitive fiber-optic probe (sensing area= 0.6 cm^2) during autofluorescence (AF) spectral measurements together with the equivalent load and force

Besides emission maximum (~467 nm), significant changes ($p < 0.0001$, one-way ANOVA with Bonferroni correction at 5%) with probe pressure were evident around 518-526 nm ($p < 1X10^{-4}$) and 540-570 nm ($p < 1X10^{-7}$), reconfirming that the observed AF changes primarily contain signals related to NADH (λ_{em}~460nm), FAD (λ_{em}~520nm), dermal collagen (λ_{em}~460nm) and blood (i.e., oxy/deoxy-hemoglobin in blood, λ_{em}~540, 557, 577 nm).[29, 59, 110] Furthermore, the fingertip and volar forearm AF spectra measured under LP exhibited considerably less spectral variance (~ 2 %) compared to HP (~ 10 %), signifying that LP causes trivial changes in tissue optical properties.[32, 87] The intensity bar plot comparing the maximum fluorescence emission (~467 nm) intensity for different probe pressure levels ± 1 SD (Figure 3.1.5) denotes that the effect of probe pressure is site-specific. For instance, fingertip AF changed significantly for MP as well as HP. On the other hand, volar forearm showed substantial changes only for HP, but not for MP.

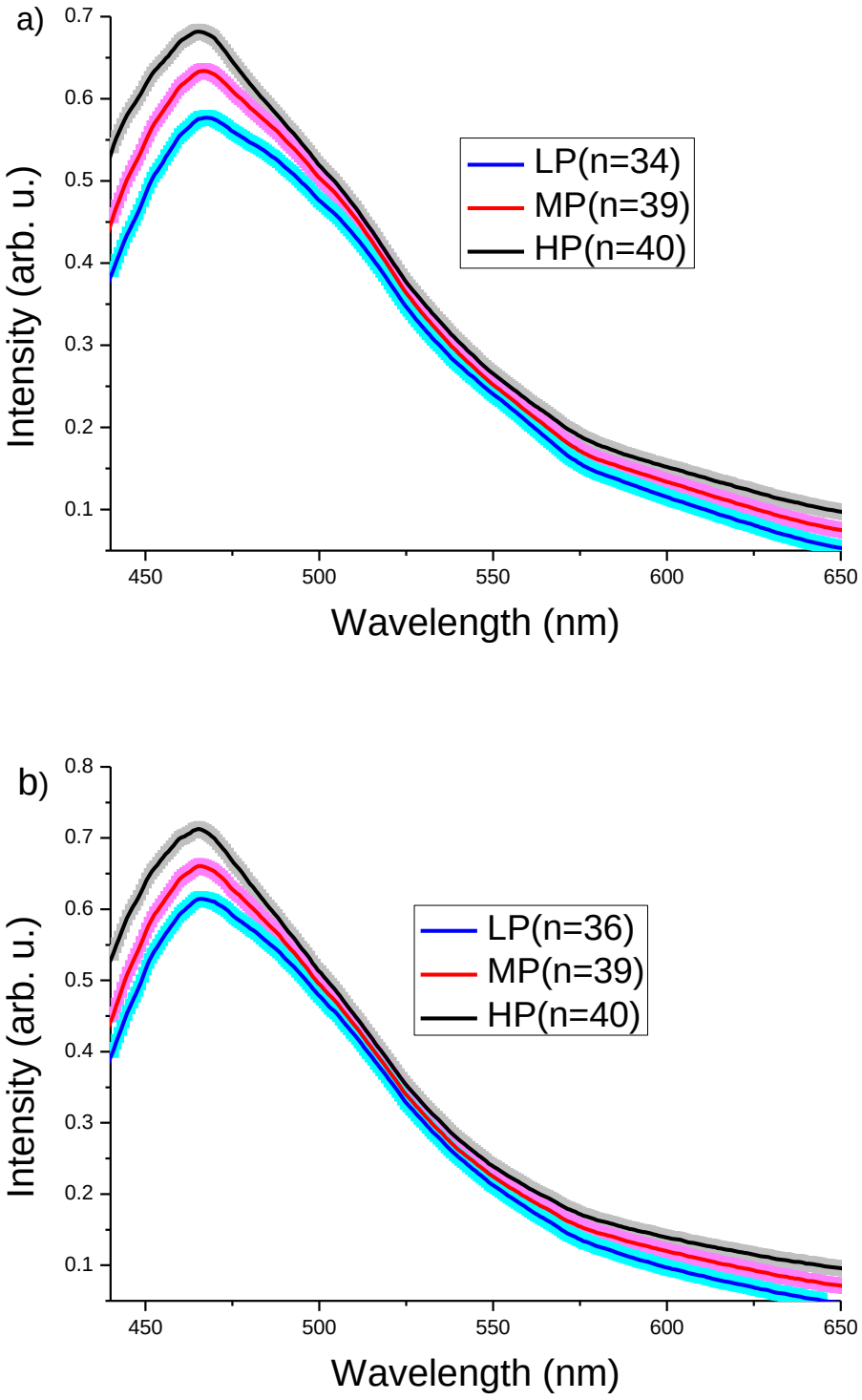

Figure 3.1.4 The mean *in vivo* autofluorescence (AF) spectra ± 1 standard error (SE) acquired from (a) fingertip (n=113) and (b) volar forearm (n=115) of 10 healthy volunteers at LP (10 kPa), MP (50 kPa) and HP (130 kPa). (LP, low pressure; MP, medium pressure; HP, high pressure). [The Standard Error appears as a coloured shade]

To further understand the AF spectral profile changes associated with user-induced probe contact pressure variability, multivariate algorithms including PLS-DA together with leave-one volunteer-out, cross validation, was employed. The dataset was arranged with each wavenumber being in columns and individual case rows. The PLS-DA class membership for each sample was predefined by coding with zeros (i.e., sample does not belong to a particular class) and ones (i.e., denoting the presence of sample to a particular class) to maximize the group separation.

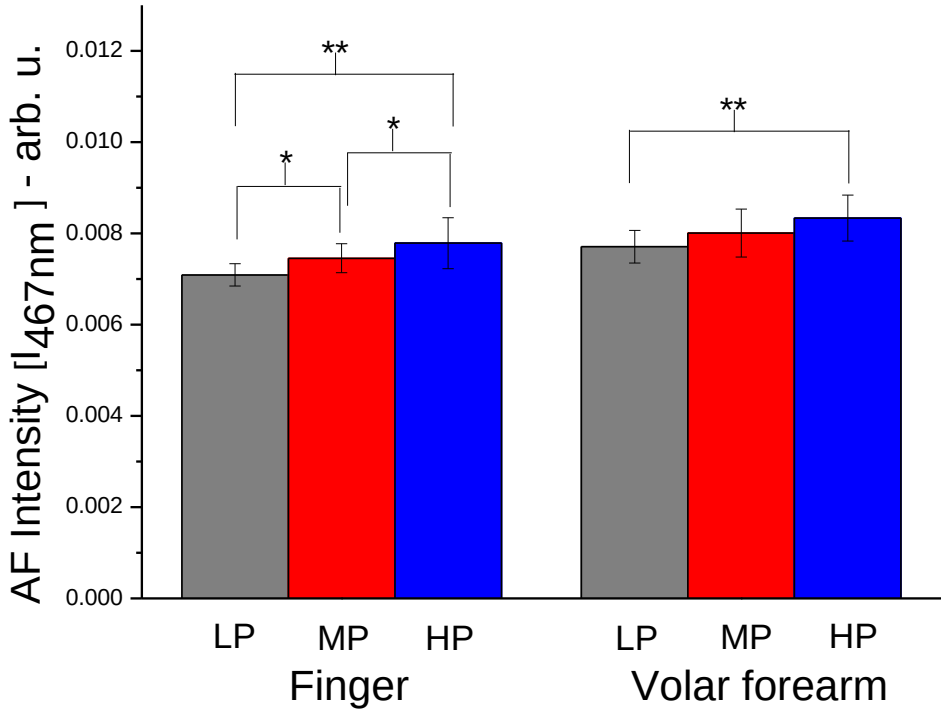

Figure 3.1.5 Bar plot displaying the peak AF intensity [I_{467nm}] of the acquired fingertip and volar forearm AF spectra among three pressure levels (LP ~10 kPa, MP ~50 kPa and HP ~130 kPa). The one standard error (SE) confidence interval is shown for each model component. Note: (*) indicates a significant difference ($p < 1X10^{-3}$); whereas (**) indicates a significant difference ($p < 1X10^{-7}$) for discriminating the fingertip and volar forearm AF spectra measured under different pressure levels

The arranged dataset was mean-centered to eliminate common variance. Outlier analysis based on PCA coupled with Hotelling's T2 and Q-residual statistics was further utilized to remove the spectra with unusual variations (e.g., light interference).[38] Following the spectral quality verification, the leave-one volunteer-out, cross-validated PLS-DA multi-class diagnostic models were developed for fingertip and volar forearm dataset using optimum number of components. The optimum number of components was found to be 3 LVs for fingertip and 1 LV for volar forearm dataset (see Figure 3.1.6), accounting for 99.47% and 83.39% of total AF spectral variations, respectively, for differentiating pressure induced changes in skin AF.

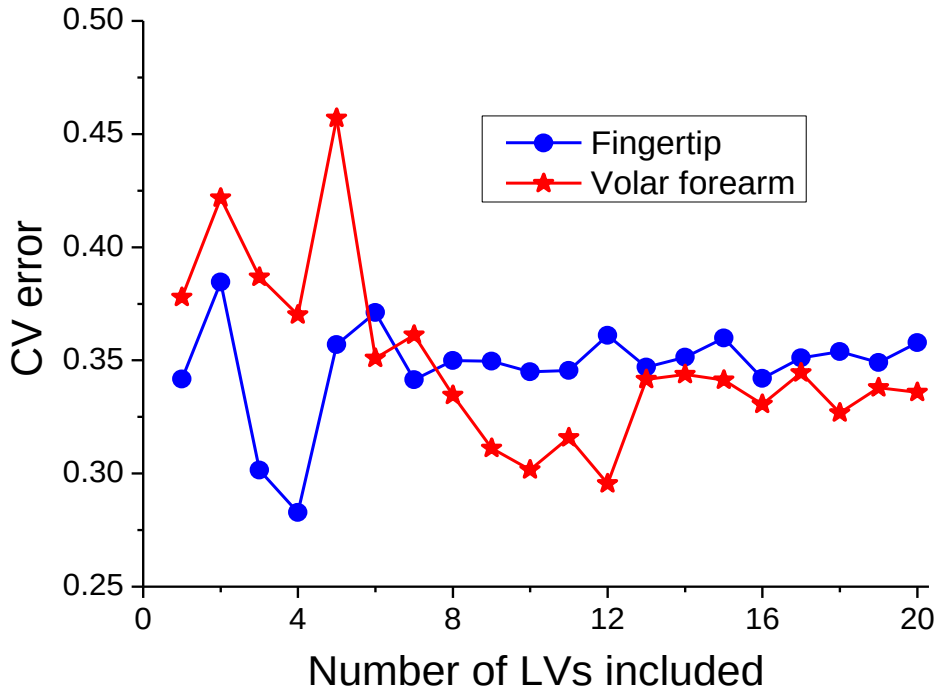

Figure 3.1.6 The number of latent variables (LVs) against cross-validation error for identifying ideal number of LVs to be utilized for classifying spectra measured at different probe-tissue contact pressures (LP ~10 kPa, MP ~50 kPa and HP ~130 kPa)

The loading vectors are related to the basic spectrum by their corresponding score which represent the weight of that loading vector against the basis spectrum. Therefore, they provide significant insights into the underlying spectral shape which can be useful for resolving spectral variations in the data. The corresponding LV loadings for fingertip and volar forearm dataset (Figure 3.1.7) exemplifies that the prominent spectral variations are located around the emission peaks ~465, 529, 540, 557, and 572 nm, representing the native skin tissue chromophores such as collagen, NADH, FAD, and blood oxy/deoxy-hemoglobin. The posterior probability values were further calculated for fingertip and volar forearm datasets using the developed PLS-DA multi-class models and shown as a 2-D ternary scatter plot (Figure 3.1.8).

The generated models for fingertip and volar forearm dataset classify the AF spectra measured under LP from MP + HP with a correct rate of 70.59% and 86.11%, respectively; the spectra acquired at MP from LP + HP with a correct rate of 56.41% and 12.82%, respectively (Table 3.1.2). The above results suggest that the probe-pressure effect on *in vivo* skin AF is site-specific and causes a significant change in both fingertip and volar forearm AF. Thus, the developed novel pressure sensitive piezo-resistive fiberoptic probe has great potential to mitigate the high probe pressure induced variations on native skin AF by quantitatively monitoring the probe-tissue contact pressure in real-time during clinical spectroscopy measurements.

	AF prediction					
	Fingertip			Volar forearm		
	LP	MP	HP	LP	MP	HP
LP	24	10	0	31	0	5
MP	9	22	8	24	5	10
HP	6	13	21	15	5	20
Correct classification rate (%)	70.59	56.41	52.50	86.11	12.82	50.00

Table 3.1.2 Classification results for discriminating *in vivo* skin tissue (fingertip and volar forearm) autofluorescence spectra measured at low-pressure, medium pressure and high pressure using PLS-DA algorithms, together with the leave-one volunteer-out, cross-validation method. [The diagonals are correct predictions while the off diagonals are the false predictions].

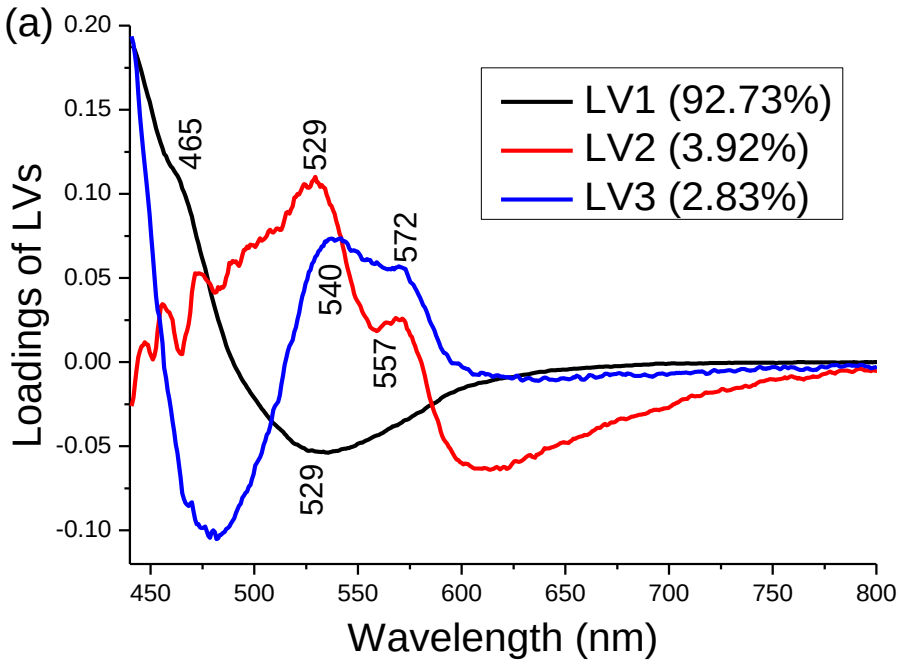

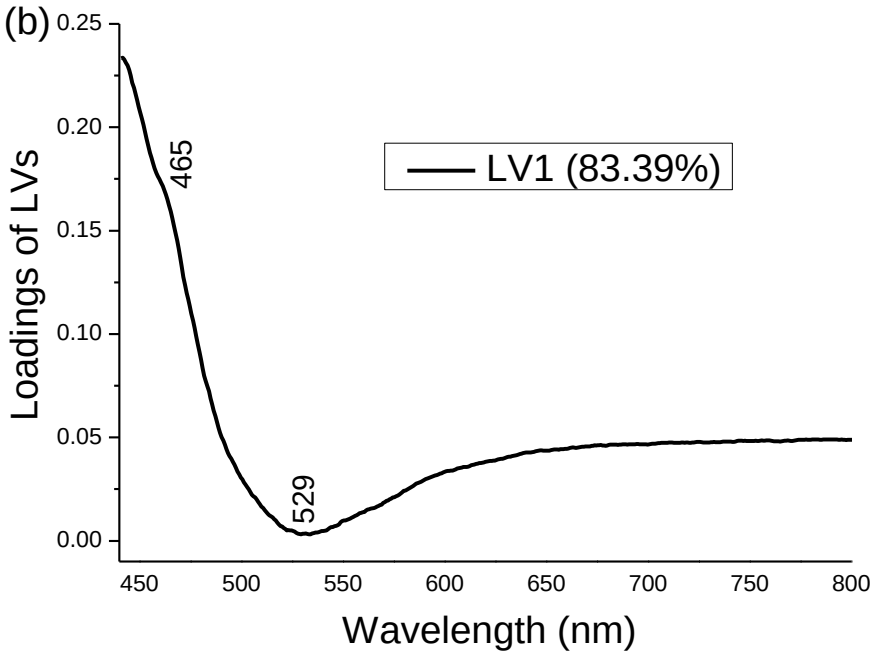

Figure 3.1.7 The diagnostically significant LVs calculated from the autofluorescence (AF) spectra of (a) fingertip and (b) volar forearm measured at three different probe pressure levels (LP ~10 kPa, MP ~50 kPa and HP ~130 kPa)

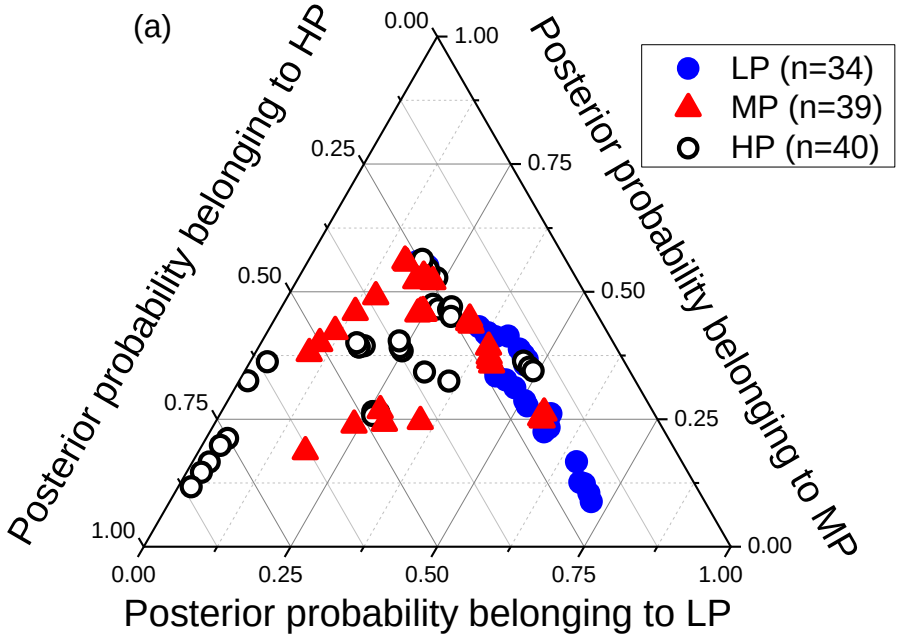

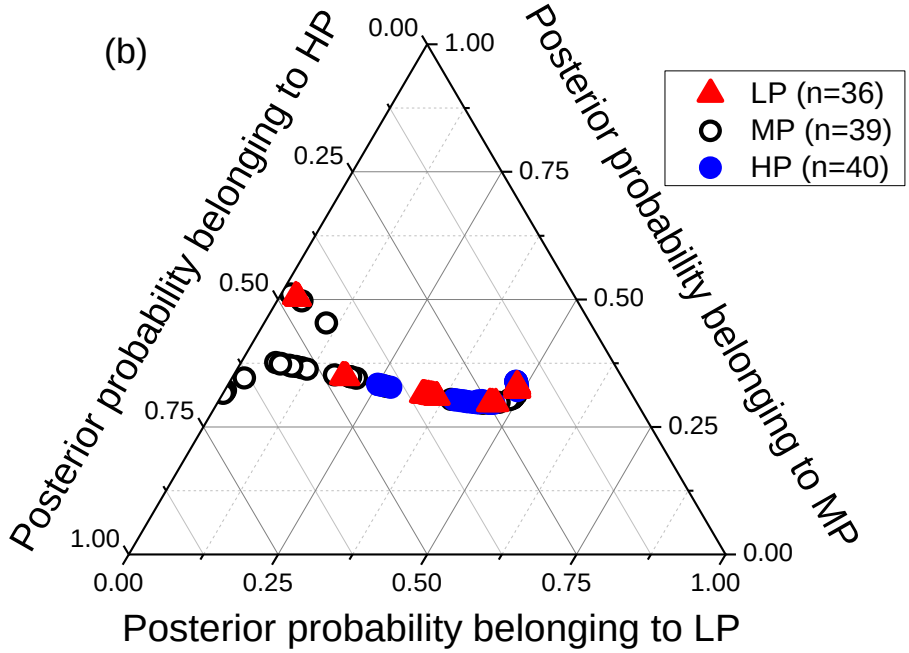

Figure 3.1.8 Two-dimensional ternary plot of the posterior probabilities belonging to low pressure (LP), medium pressure (MP), and high pressure (HP) categories calculated from the PLS-DA models together with leave-one patient-out, cross validation, generated from *in vivo* autofluorescence (AF) spectra of (a) fingertip and (b) volar forearm

3.1.4 Discussion

Fiberoptic spectroscopy techniques including reflectance, fluorescence and Raman have recently emerged as a compelling tool for early cancer diagnosis at the molecular level.[1, 3, 8, 23, 28, 66] The latest technical advances including high-performance spectroscopy instrumentation, fiberoptic probe design, and real-time implementation of chemometric techniques play a pivotal role in making these spectroscopy modalities as a robust diagnostic tool in clinical settings.[38] These potential clinical spectroscopy modalities require hand-held fiberoptic probes to perform contact spectral measurement from remote internal organs. The probe-tissue contact spectral measurement reduces the refractive index mismatch between the probe tip and tissue, thus providing less spectral variability compared to non-contact measurements.[30, 35, 36] It has been, however, reported

that the probe-tissue contact pressure is a user-dependent variable that affects the local optical properties of tissue.[35, 82] The precise control of applied probe pressure during spectroscopic measurements is particularly hard in clinical scenario and may induce variations in the tissue spectral profiles. The pressure induced spectral alterations can dilute the diagnostic variations present across the tissue spectra and further lead to reduced diagnostic accuracy, raising potential concerns in the use of spectroscopy diagnostic modalities for clinical disease diagnosis. .

In this study, we developed for the first time a novel pressure sensitive piezo-resistive fiberoptic probe for quantitative monitoring of magnitude of exerted probe-tissue contact pressure and its effects in real-time during *in vivo* tissue AF spectroscopic measurements. The improvements made by the developed pressure sensitive fiberoptic probe over existing systems are:

i) The high sensitivity (20.6 mV/kPa) and short response time time (<5 μs) of the piezo-resistive pressure sensor enable precise and accurate pressure measurements.

ii) The setup be used to monitor probe pressure in real-time and provide instantaneous probe pressure feedback to operators during spectral data acquisition.

iii) The setup can be also used as a dynamic probe pressure control mechanism for spectroscopy measurements.

We further tested the developed pressure sensitive fiber probe coupled AF spectroscopy on *in vivo* skin tissue to identify spectral variations associated with physiological changes in skin induced by varied probe pressure. The use of visible-excited spectroscopy (λ_{ex}=405nm) holds potential benefits for safe tissue diagnosis such as non-carcinogenic and deeper light penetration into tissue compared to ultraviolet

excitation. In addition, skin tissue blanches when pressure is applied,[32] creating a challenging experimental scenario to test our developed novel pressure sensitive spectroscopy platform. Moreover, spectroscopic studies on skin have reported that the typical pressure used in clinical measurements is ~9 kPa[32] and the spectral changes have only been observed for the spectra measured under clinically extreme pressure (>55 kPa).[87] Hence, we chose three well-defined reference pressure levels of 10 kPa as LP, 50 kPa (<55 kPa) as MP and 130 kPa (>55 kPa) as HP in our study. We successfully acquired high-quality *in vivo* skin tissue AF spectra (n=228) from index fingertip (n=113) and volar forearm (n=115) within 1 sec at three reference pressure levels. The AF spectra (450-650 nm) measured from fingertip and volar forearm (Figure 3.1.4) exhibited notably increased intensity for high probe pressure over the range 450-480 nm with substantial variations particularly around ~450-470, 518-526, and 540-570 nm ($p < 0.0001$, one-way ANOVA with Bonferroni correction at 5%). The pressure-induced enhancement in skin AF may be primarily associated with the increase of epithelial fluorescence (e.g., free/bound NADH (λ_{em}~460nm), and FADH (λ_{em}~520nm)),[10, 13, 26] because the penetration depth of 405-nm excited laser on skin tissue is ~50-100 μm.[111] The pressure-related accumulation of epithelial fluorophores can most likely be attributed to the reduction in metabolic activity caused by local ischemia at the tissue site under pressure.[29] The blood is also squeezed out of the dermis while compressing the underlying tissue, leading to decreased blood absorption and increased AF signals that may arise from dermal collagen (λ_{em}~460nm).[29, 32, 109] The AF changes that occur at 540-570 nm may correspond to re-absorption of blood oxy/deoxy-hemoglobin and transition of oxy-hemoglobin to deoxy-hemoglobin with applied probe pressure onto the tissue.[32]

Additional interesting features such as minor blue-shift of AF emission peak (467 to 464 nm) due to pressure induced increase in rigidity of chromophore environment[112] and narrowing of skin AF spectra can also be noted with the increase of probe pressure.

Although the pressure related changes such as increased AF intensity and narrowing of AF can be noticed in both fingertip and volar forearm skin, the effect of probe pressure induced spectral variability is site-specific (Figure 3.1.5). For instance, the AF intensity at emission peak (I_{467nm}) demonstrates that the MP has high implications on fingertip AF spectra ($p < 5X10^{-4}$) compared to volar forearm ($p > 0.05$). The multivariate analysis based on PLS-DA diagnostic modeling further rendered a correct classification rate of 56.41% (22/39) and 12.82% (5/39) for discriminating fingertip and volar forearm AF spectra measured at MP from those measured at LP and HP (Table 3.1.2), reaffirming the site-specific effect of probe-tissue contact pressure. The differences in the concentration of absorbers (e.g., hemoglobin and melanin) in fingertip and volar forearm skin may contribute to the site-specific effect of probe pressure on *in vivo* skin AF. For instance, high blood content at the fingertip requires less pressure (i.e., MP) to cause changes in fingertip AF. In contrast, volar forearm require HP to cause substantial changes in its AF due to increased concentration of melanin. The 2D ternary plots shown in Figure 3.1.8 graphically represent how efficiently spectra acquired at the different pressure levels (i.e. L.P, M.P and H.P) can be differentiated by the PLS-DA model. The separation accuracy determines the impact/effect of the parameter that is being evaluated statistically (i.e. probe pressure in this case) on the specific dataset (i.e acquired AF spectra in this case). It implies that if the separation accuracy is high, the effect of probe pressure on the acquired spectral data is also high which signifies that variations in the probe-tissue contact

pressure causes prominent distortions in the measured spectral data. Figure 3.1.8 shows that there is fairly good separation between LP *vs*. HP compared to LP *vs*. MP or MP *vs*. HP which indicates that the AF spectra acquired at LP and HP are quite different from each other. The AF spectra of fingertip and volar forearm measured under LP can further be accurately discriminated with a rate of 70.59% (24/34) and 86.11% (31/36), respectively, from the spectra acquired with MP and HP, demonstrating that the native skin tissue AF changes significantly with high probe pressure. Thus the developed pressure sensitive spectroscopy platform can mitigate the probe pressure induced spectral variability by assisting the user with real-time, quantitative feedback of applied probe pressure and its effects during *in vivo* AF spectroscopy measurements. The automated probe handling feedback to clinicians further ensures the contact between the probe and tissue, as well as application of constant LP during spectral acquisition, enabling objective disease diagnosis by preserving only the diagnostically relevant variations. Furthermore, the pressure sensitive spectroscopy platform can easily be adapted to other *in vivo* tissue optical spectroscopic modalities (e.g., diffuse reflectance, Raman spectroscopy), particularly appealing for challenging endoscopic applications in clinical settings. However, this work warrants further investigation with a large number of volunteers in each pressure category with biological dimension of skin color (i.e., various level of pigmentation) to evaluate the true clinical merit of pressure sensitive skin AF spectroscopy. We hope that by incorporating the probe pressure induced spectral variations in the diagnostic models, the diagnostic efficacy of spectroscopy techniques can further be enhanced.

3.1.5 Conclusion

In summary, we report for the first time on the development of a novel pressure sensitive piezo-resistive fiberoptic probe for biomedical diagnostic spectroscopy platform to quantitatively monitor *in vivo* probe-tissue contact pressure and its effects in real-time (<1 sec). The successful utilization of the developed probe for characterizing probe pressure induced changes on *in vivo* skin AF has been demonstrated. The results showed that the probe pressure effect on *in vivo* skin AF is significant and site-specific and the integration of pressure sensitive piezo-resistive fiberoptic probe with the rapid spectroscopy diagnostic technique can greatly reduce the spectral changes associated with probe pressure variability, opening a new pathway for improving real-time *in vivo* tissue diagnosis.

3.2 Probe- tissue contact pressure effects on *in vivo* near infrared autofluorescence spectroscopy

The aim of this study is to investigate in real-time the biochemical changes associated with probe tissue contact pressure variations during near infrared (NIR) skin tissue autofluorescence (AF) spectroscopy. An *in vivo* pressure sensitive spectroscopy platform that includes a novel custom-designed pressure sensitive confocal fiber-optic probe was utilized to exert real-time dynamic control of external probe contact pressure during spectral data acquisition. The probe pressure induced NIR AF spectral response of 20 subjects were acquired from three measurement sites on the skin (i.e. index fingertip, palm and volar forearm) and studied at three reference pressure levels (i.e., low pressure (LP - 10 kPa), medium pressure (MP - 50 kPa) and high pressure (HP - 130 kPa)). The mean AF signal intensity progressively increased with the magnitude of applied probe

pressure for all measurement sites. Although clear differences in NIR AF was observed at different pressure levels; one-way ANOVA statistical analysis with Bonferroni correction at 5% yielded insignificant p-values ($p>0.05$) for the entire spectral range. However, multiclass partial least squares (PLS)-discriminant analysis (DA) modelling could accurately discriminate ~ 50 - 65% of AF spectra acquired under LP *vs.* MP and HP; suggesting that increased probe pressures (i.e. MP or HP) affected NIR AF to a certain extent. These NIR AF variations can be mitigated if the applied probe pressure is maintained at LP which substantiates the need for real-time, quantitative monitoring of probe-tissue contact pressure during *in vivo* NIR AF measurements.

3.2.1 Introduction

NIR AF spectroscopy is an effective tool for various biomedical applications as it is used to study the optical window in biological tissues where the scattering of light is the dominant phenomenon. This is because the absorption of light is considerably weak in the optical window which facilitates the deeper penetration of light. Additionally, NIR light has the advantage of being non-carcinogenic compared to ultraviolet (UV) light and is considered more safe in therapeutic and diagnostic applications. Studies have shown that NIR AF spectroscopy provides useful, complementary information in tissue characterization and disease diagnosis[8, 67, 102] and makes use of a fiber-optic probe that is in contact with the target tissue site during spectral data acquisition.[31, 32, 35-37, 82] Ensuring probe-tissue contact is essential in order to reduce interferences due to refractive index mismatch, specular reflection, to increase light penetration and transmittance and to avoid inconsistent illumination-detection geometry during spectral acquisition which results in the enhancement of the diagnostic capability of the system.[29, 35, 36] Therefore, a certain

amount of probe pressure is applied onto the measurement site when spectral data is collected. The applied probe pressure is a confounding, user-dependent (i.e., operator-dependent) parameter that can potentially alter the optical properties of biological tissues.[29, 36] In addition, increase in probe pressure causes tissue compression which leads to the following effects: decreased thickness, reduced blood volume and oxygen saturation, vasodilation, microcirculation impairment, densely packed scatterers and occlusion under the probe tip and these effects may introduce pressure induced distortions in the acquired spectra.[30] Improper control of exerted probe pressure may lead to potential concerns such as changes in tissue spectral profiles, disparities in data collection and calibration and potential inaccuracies in diagnosis.[32-34] Hence, it is necessary to control the applied probe pressure carefully by establishing a dynamic probe pressure control mechanism for real-time, quantitative monitoring of exerted probe pressure to mitigate the pressure induced spectral variability on NIR AF spectral profiles.

A few studies have been carried out to evaluate the effects of probe-tissue contact pressure on UV/visible AF spectra.[29, 32, 84, 85] However, the effects of probe pressure on NIR AF have not been studied so far. Moreover, the existing studies on probe pressure have been limited to static pressure measurements utilizing a pre-calibrated spring loaded device, or making use of the extent of tissue compression (in mm) as a criterion for applying a particular pressure or operator-dependent arbitrary probe pressures. The dynamic changes in applied probe pressure that occur due to differences in deformability of various measurement sites on skin tissue, inter-subject variations in the extent of tissue compression (in mm) and orientation of the probe are important sources of variation in the exerted probe pressure that have not been analyzed sufficiently. Hence, in this study,

we highlight the significance of real-time, quantitative monitoring of dynamic changes in the applied probe pressure by providing dynamic real-time probe pressure control during spectral measurements. We successfully utilized the custom-designed pressure sensitive fiber-optic probe to quantitatively monitor the dynamic pressure induced variations in real-time on *in vivo* human skin DR spectroscopy. Three measurement sites (i.e., fingertip, volar forearm and palm) on the skin tissue were chosen specifically because skin tissue acts as a highly scattering medium in visible to near-infrared region, representing one of the most challenging organs with complex and inhomogeneous morphological structures. Multivariate statistical models (PLS-DA) were used for in-depth analysis of the spectral information acquired at various pressure levels.

3.2.2 Materials and Methods

3.2.2.1 Pressure sensitive NIR AF spectroscopy platform

The pressure sensitive *in vivo* spectroscopy platform utilized for real-time, quantitative monitoring of probe-tissue contact pressure has been reported in detail elsewhere (refer chapter 3.1.2.1 Pressure sensitive UV/visible AF spectroscopy platform). A spectrum stabilized 785-nm diode laser (maximum output: 300 mW, B&W TEK Inc., Newark, Delaware) and appropriate filters replaced the laser and filters in the aforementioned system (refer chapter 3.1.2.1 Pressure sensitive UV/visible AF spectroscopy platform) to perform NIR AF spectroscopy. A custom designed hand-held confocal Raman probe with an NIR-coated sapphire ball lens (5 mm in diameter, refractive index n= 1.77) mounted on the probe tip. The confocal probe is specially designed to collect signals particularly from the epithelial layer (< 300 Um). The acquired spectra were over the range of 800−1800 cm^{-1} with a spectral resolution of 9 cm^{-1}. Each

spectrum in this study was measured with an integration time of 1 sec under the 785 nm laser excitation.

3.2.2.2 Subjects

The *in vivo* NIR AF spectra were acquired from index fingertip, palm and volar forearm of 20 healthy subjects using the pre-calibrated piezo-resistive pressure sensor coupled confocal fiber-optic probe. The subjects who were recruited had no previous history of skin cancer and a total of 1436 high-quality *in vivo* tissue AF spectra were subsequently measured from fingertip (n=481), palm (n=485) and volar forearm (n=470) at three reference pressure levels (i.e., low pressure (LP) -10 kPa, moderate pressure (MP) – 50 kPa and high pressure (HP) – 130 kPa). Probe pressure variations due to orientation of the probe and movement of target tissue site were avoided by fixing the target tissue perpendicular to the probe tip during spectral data acquisition. Different probe pressures (LP, MP and HP) applied on to the target tissue site were displayed instantaneously in the developed real-time Raman diagnostic platform during spectroscopic measurements.[38] Spectral data can be acquired at constant probe pressures by making use of the real-time instantaneous probe pressure display during spectral data acquisition.

3.2.2.3 Data processing and multivariate statistical analysis

The acquired raw spectrum is a composite signal that was a combination of Raman signals, intense AF and noise. The noise was suppressed by the use of first-order Savitsky–Golay smoothing filter (window width of 5 pixels). A fifth-order polynomial fitting was found to be optimal for extracting the autofluorescence signal from the raw

spectrum. The extracted AF datasets from the fingertip, palm and volar forearm were subjected to multi-class probabilistic PLS-DA for differentiation among spectra acquired at different pressure levels (refer chapter 3.1.2.4 multivariate statistical analysis).

3.2.3 Results

Figure 3.2.1 shows the mean *in vivo* NIR AF spectra ±1 standard error (SE) acquired from skin tissue (index fingertip (n=481), palm (n=485), and volar forearm (n=470)) of 20 healthy volunteers at various pressure levels of ~10 kPa (LP), 50 kPa (MP) and 130 kPa (HP). The mean AF spectra of the three measurement sites (i.e., fingertip, palm and volar forearm) had higher signal intensities with progressive increase in applied probe-tissue contact pressure. The NIR AF signals also showed a uniform, average spectral variation of ~ 10% at each pressure level for the entire spectral range. The mean AF intensity was found to be the strongest when high probe pressure (i.e., HP – 130 kPa) was applied on to the tissue.

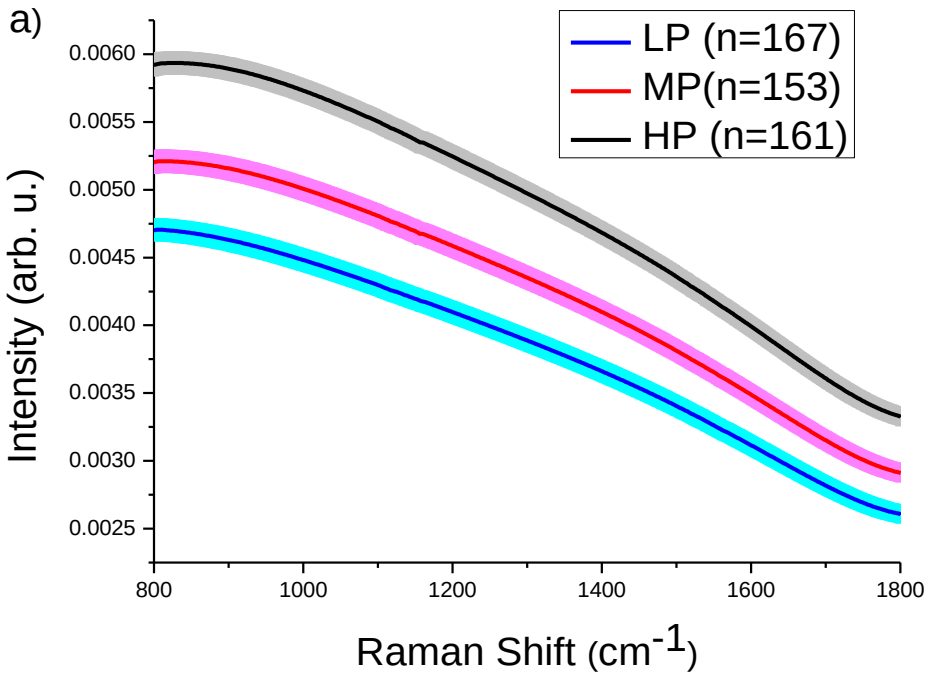

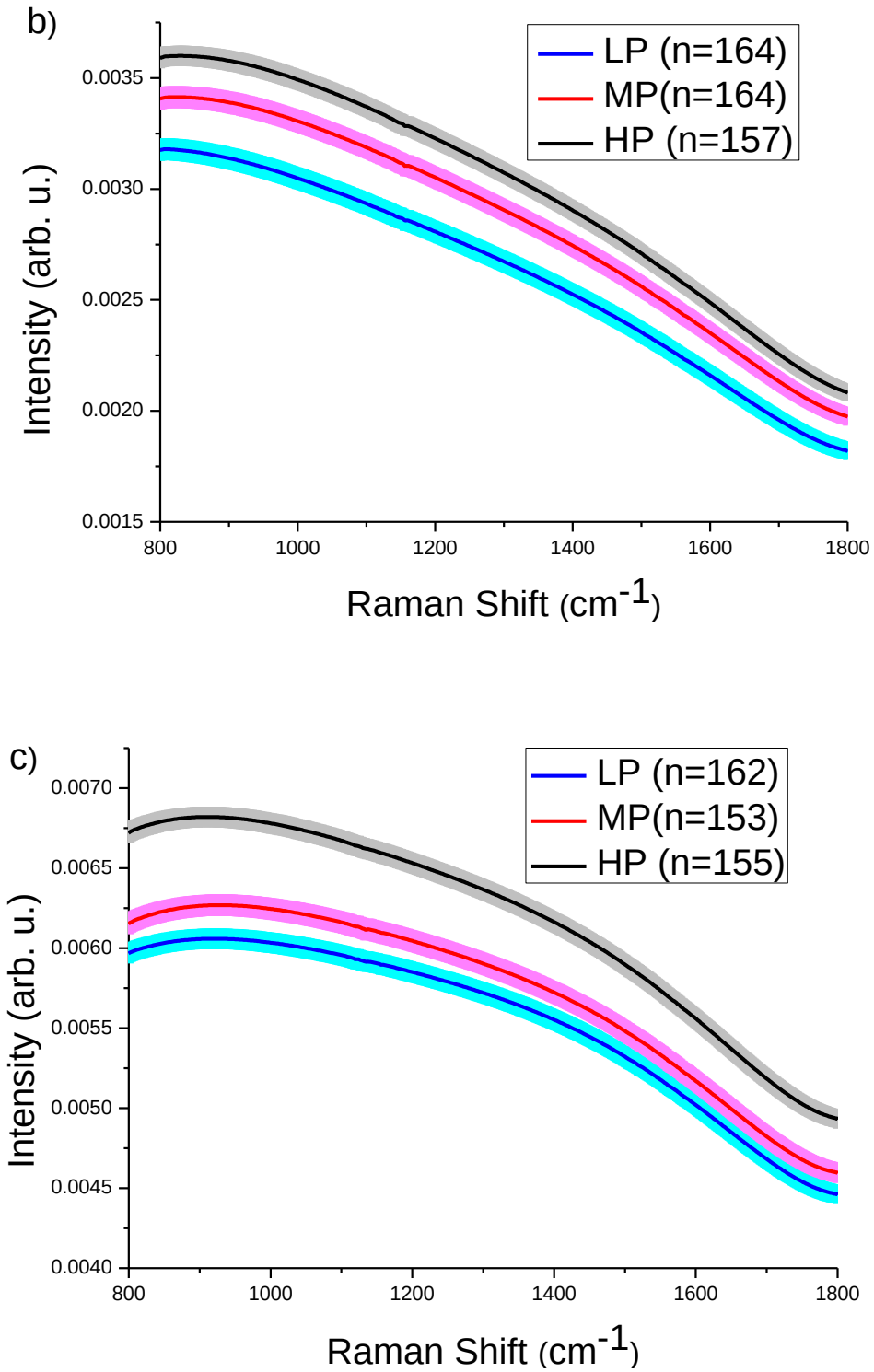

Figure 3.2.1 The mean *in vivo* NIR AF spectra ± 1 standard error (SE) measured from (a) fingertip (n=481) (b) palm (n=485) and (c) volar forearm (n=470) skin of 20 healthy volunteers at LP (10 kPa), MP (50 kPa) and HP (130 kPa). (LP, low pressure; MP, medium pressure; HP, high pressure). [The Standard Error appears as a coloured shade]

The MP (50 kPa) level caused an AF signal increase of 10.63%, 9.67% and 1.34% while the HP (130 kPa) level caused an increase of 25.43%, 13.88% and 9.21% for the fingertip, palm and volar forearm spectra respectively; suggesting that the extent of AF signal variation is dependent on the skin tissue type. The differences in spectral signal intensities also indicate that variations in the exerted probe pressure affect the acquired AF spectra to a certain extent. These results demonstrate that the probe pressure is an important parameter that warrants careful monitoring in order to avoid pressure induced variations in the acquired spectra. However, statistical analysis (i.e. one-way ANOVA with Bonferroni correction at 5%) of the AF spectra yielded insignificant p-values (i.e. $p>0.05$) for the entire AF spectral range.

Multivariate statistical analysis (i.e., PLS-DA) was performed on the fingertip, palm and forearm spectral datasets to further explore spectral changes associated with operator-induced probe pressure variability. Outlier analysis based on PCA coupled with Hotelling's T2 and Q-residual statistics was further utilized to remove the spectra with unusual variations (e.g., light interference).[38] After spectral quality verification, PLS-DA together with leave-one patient-out, cross validation, was employed to realize *in vivo* discrimination of AF spectra acquired at the different reference pressure levels. The optimum number of components (i.e. latent variables- LVs) that were included in the analysis was determined from the cross validation (CV) classification error plot which is shown in Figure 3.2.2.

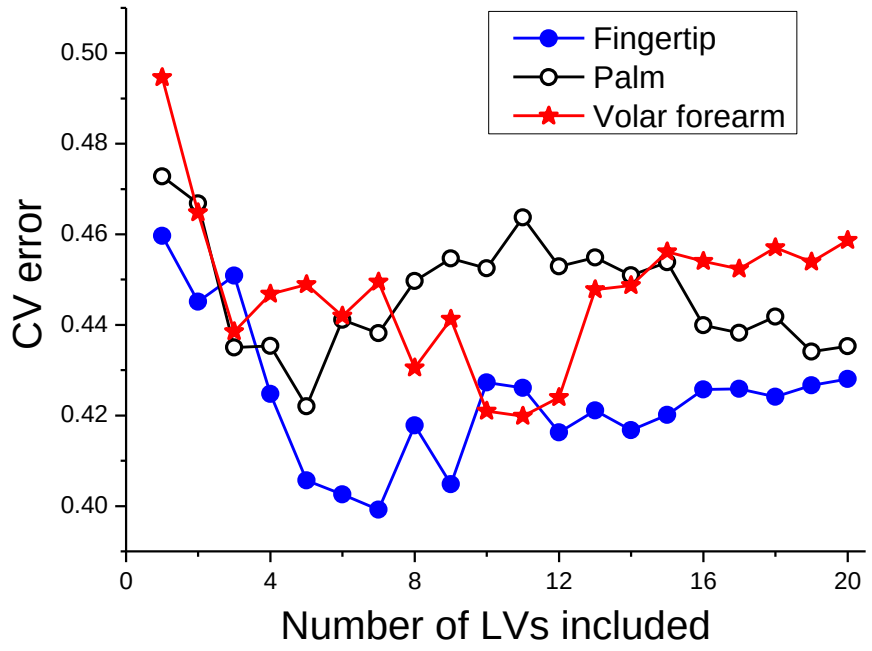

Figure 3.2.2 The number of latent variables (LVs) *vs.* cross-validation error for identifying optimum number of LVs to be utilized for developing PLS-DA diagnostic models for differentiating spectra acquired at different reference pressure levels (LP ~10 kPa, MP ~50 kPa and HP ~130 kPa).

The optimum number of components was found to be 2 LV (LV1 - 99.72%; LV2 - 0.27%) for fingertip, 3 LVs (LV1 - 99.73%; LV2 - 0.19%; LV3 – 0.08%) for palm and 3 LVs (LV1 – 99.98%; LV2 – 0.11%; LV3 – 0.01%) for volar forearm dataset, representing the variations in the AF spectral profiles which may be due to the changes in concentrations of the endogenous fluorophores with increase in applied probe pressure. The first latent variable (LV1) which closely resembles the AF signals in the fingerprint region (800 – 1800 cm^{-1}); contribute to the greatest variations in the AF signal (i.e., 99.72% - fingertip; 99.73% - palm and 99.88% - volar forearm) and is shown in Figure 3.2.3.

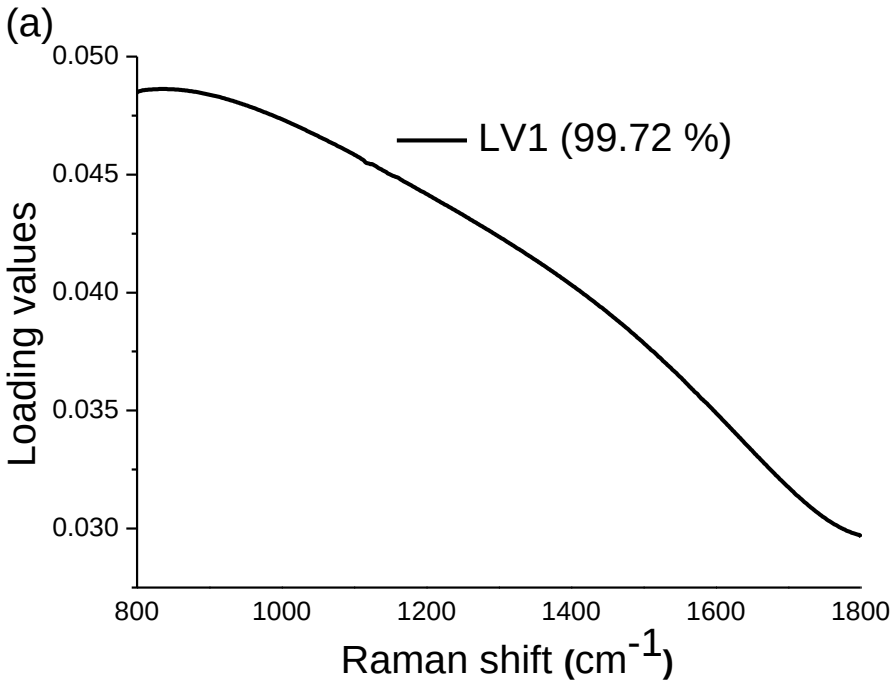
(a)
0.050
0.045
0.040
0.035
0.030
Loading values
LV1 (99.72 %)
800
1000
1200
1400
1600
1800
Raman shift (cm-1)

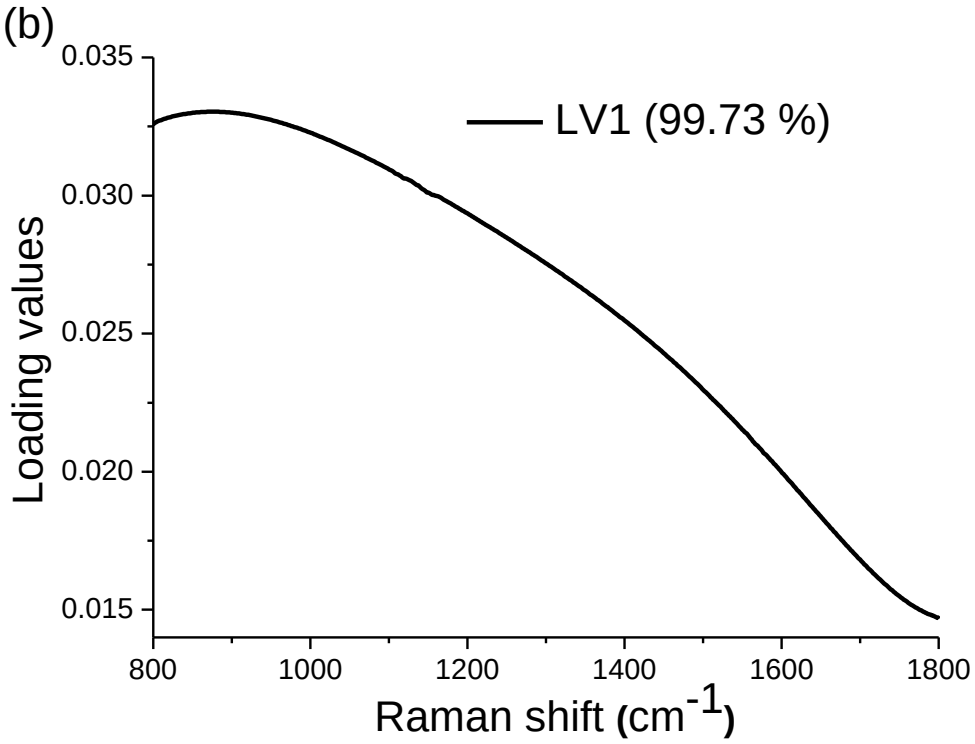
(b)
0.035
0.030
0.025
0.020
0.015
Loading values
LV1 (99.73 %)
800
1000
1200
1400
1600
1800
Raman shift (cm-1)

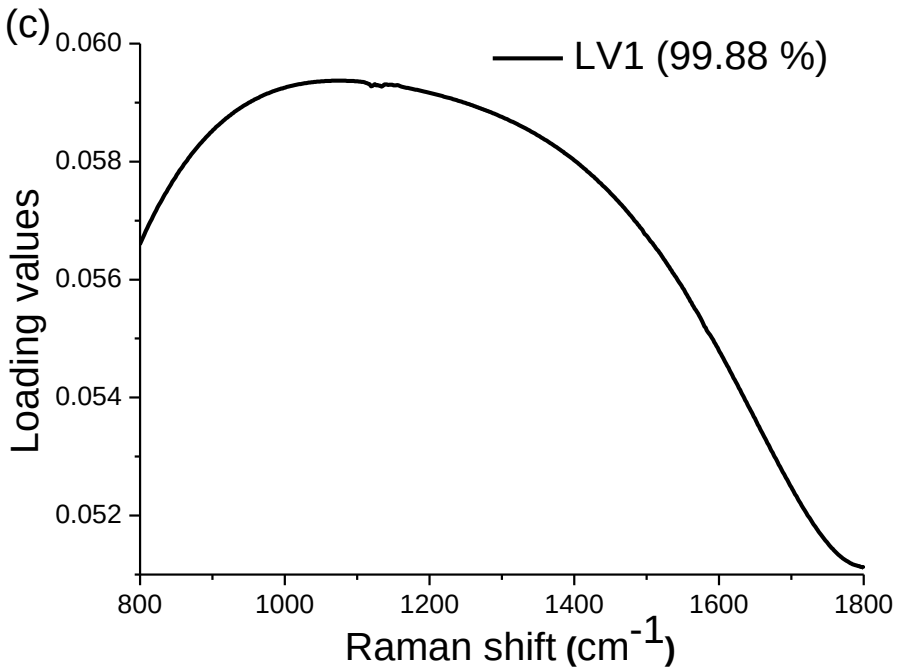

Figure 3.2.3 The diagnostically significant latent variables (LVs) calculated from the NIR AF spectra of (a) fingertip, (b) palm, and (c) volar forearm measured at three different probe pressure levels (LP ~10 kPa, MP ~50 kPa and HP ~130 kPa).

	AF prediction								
	Fingertip			Palm			Volar forearm		
	LP	MP	HP	LP	MP	HP	LP	MP	HP
LP	88	54	54	102	21	41	87	53	46
MP	25	37	25	20	59	43	48	60	56
HP	54	2	82	42	77	80	27	40	53
Correct classification rate (%)	52.69	24.18	50.93	62.19	35.97	50.95	53.70	39.21	34.19

Table 3.2.1 Classification results for discriminating *in vivo* skin (fingertip, palm and volar forearm) NIR AF spectra measured at low-pressure, medium pressure and high pressure using PLS-DA algorithms, together with the leave-one patient-out, cross-validation method. [The diagonals are correct predictions while the off diagonals are the false predictions].

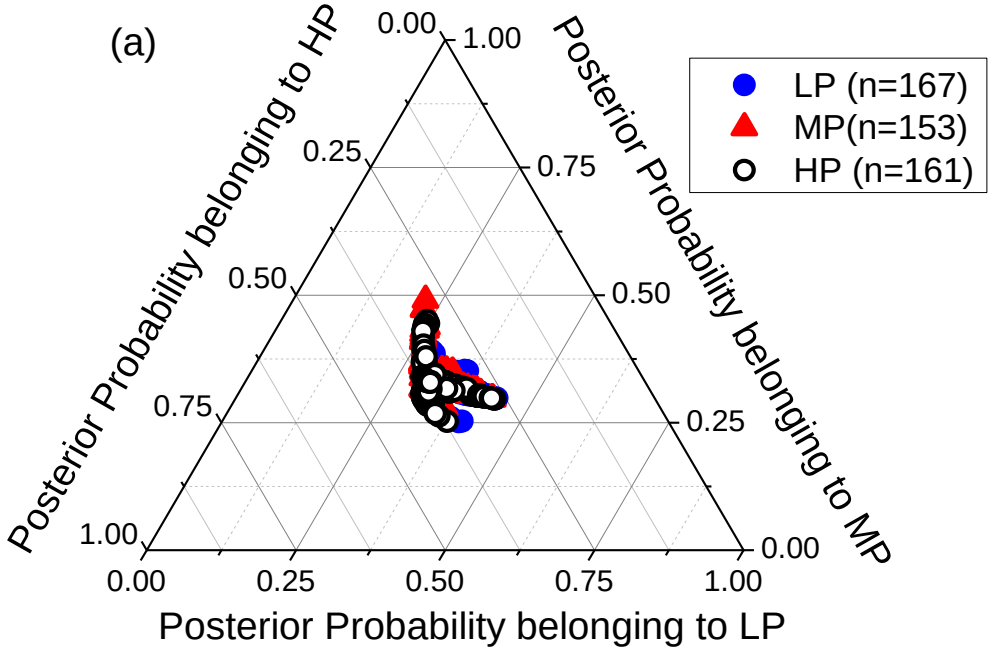
(a)
Posterior Probability belonging to HP
Posterior Probability belonging to MP
Posterior Probability belonging to LP
0.00
0.25
0.50
0.75
1.00
LP (n=167)
MP(n=153)
HP (n=161)

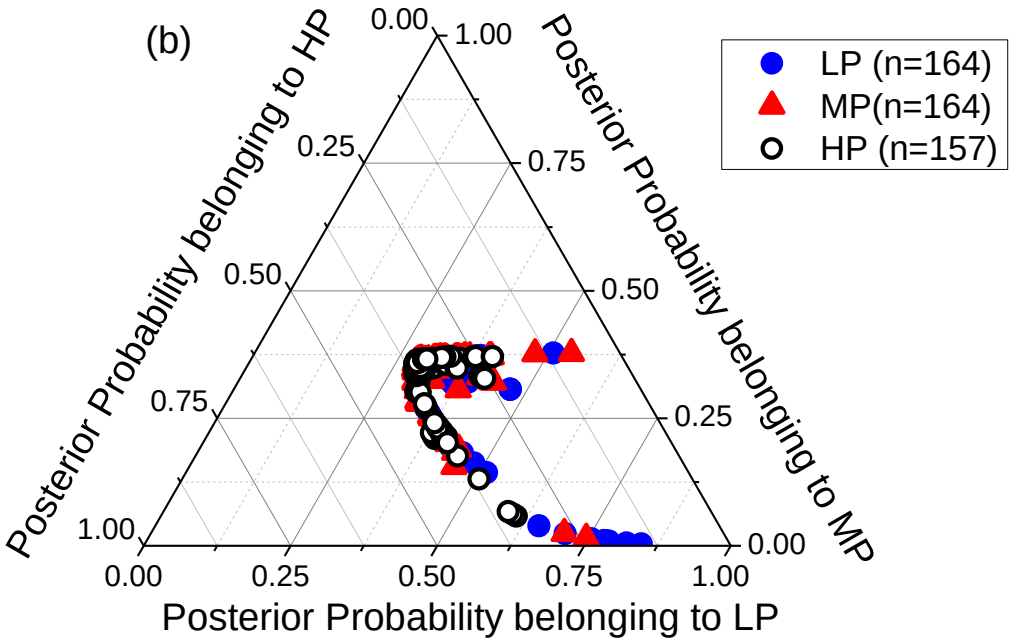
(b)
Posterior Probability belonging to HP
Posterior Probability belonging to MP
Posterior Probability belonging to LP
0.00
0.25
0.50
0.75
1.00
LP (n=164)
MP(n=164)
HP (n=157)

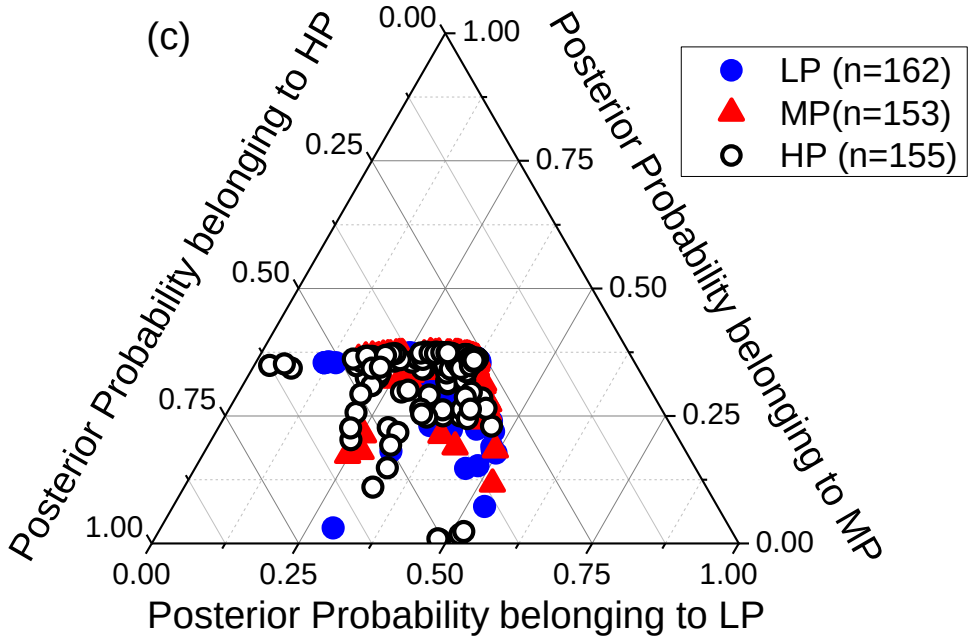

Figure 3.2.4 Two-dimensional ternary plot of calculated posterior probabilities belonging to *in vivo* (a) fingertip, (b) palm, and (c) volar forearm NIR AF spectra measured under low pressure (LP ~10 kPa), medium pressure (MP ~50 kPa), and high pressure (HP ~130 kPa) using PLS-DA models together with leave-one patient-out, cross validation

The generated PLS-DA models from the AF spectra of fingertip, palm and forearm provided correct classification rate of 52.69%, 62.19% and 53.70% for separating LP spectra from MP + HP; accuracies of 21.18%, 35.97% and 50.95% for differentiating MP spectra from LP + HP and accuracies of 50.93%, 50.95% and 34.19% for differentiating HP spectra from LP + MP respectively (Table 3.2.1). These classification results were plotted in a 2-D ternary scatter plot shown in Figure 3.2.4 for visualization of the classification results. From the results, it can be observed that the applied probe pressures produces notable variations (~50-60% discrimination between LP *vs.* MP + HP) in the AF spectroscopic properties of skin tissue. The observed probe pressure variations on skin tissue AF spectra can be minimized by applying short-term (< 1sec) constant LP against the tissue which can be achieved by real-time quantitative

monitoring of probe-tissue contact pressure using the developed pressure sensitive probe. This enhances the capability of NIR AF spectroscopy platform in disease diagnosis by providing probe pressure feedback to operators during spectral data acquisition; enabling the operators to perform spectroscopic measurements at constant pressure levels.

3.2.4 Discussion

NIR AF spectroscopy makes use of the therapeutic optical window to study the optical properties of biological tissues. NIR excited spectroscopy has been extensively utilized in a variety of biomedical applications as it is non-carcinogenic and considered safe.[22, 25, 67, 99, 113-115]. Moreover, it holds other potential benefits such as being relatively insensitive to tissue water content compared to ultraviolet (UV)-visible-excited spectroscopy and also provides complementary information for *in vivo* disease diagnosis.[8, 102, 116] Therefore, NIR AF has a great potential to be an effective tool for tissue characterization and disease diagnosis. However, operator-dependent factors like probe-tissue contact pressure must be carefully monitored to prevent pressure induced distortions from affecting the acquired NIR AF spectral data. It has been reported that the probe handling variations (e.g., probe pressure) is one of the major sources of spectral variations in spectroscopy modalities including fluorescence, diffuse reflectance and Raman spectroscopy.[33, 36, 82, 117] Hence, the effect of probe handling variations on *in vivo* fiber-optic optical spectroscopy is always a point of contention in biomedical community, which hasn't been studied in detail till now. In this study, real-time monitoring of the probe pressure is accomplished by establishing a dynamic probe pressure control using a custom-designed pressure sensitive fiber-optic confocal probe. Pressure induced spectral variability was studied over a wide range of pressure values (10 – 130 kPa). The range of

pressure levels were LP – 10 kPa (i.e., typical clinical pressure - ~9 Pa), MP - 50 kPa (i.e., slightly less than clinical extreme pressure - 55 kPa[87]) and HP – 130 KPa (i.e., far higher than clinical extreme pressure). 1436 high quality *in vivo* NIR AF spectra were acquired from three measurement sites of human skin (i.e., index fingertip (n=481), palm (n=485) and volar forearm (n=470)) with an integration time of 1 second from 20 healthy subjects who volunteered to take part in the spectroscopic experiment.

The mean NIR AF spectra (Figure 3.2.1) showed notable AF signal intensity variation with increase in exerted probe pressure. The strongest AF signal was observed when HP (i.e., 130 kPa) was applied on the tissue. This may be due to the increase in concentration of endogenous fluorophores when tissues are subjected to compression due to the exerted probe pressure.[31, 32, 56] Although specific endogenous fluorophores that have fluorescence emission peaks in the NIR range have not been identified; studies have reported that tissue spectra measured at 785 or 830 nm excitation display residual broadband signal that is believed to be fluorescence background.[113] This residual fluorescence background that is observed in the NIR range has been reported to be due to fluorophores such as porphyrins and melanin.[118-121] It can also be observed that the extent of AF signal variation with applied probe pressure is different for the three measurement sites (i.e., fingertip, palm and volar forearm); suggesting that the AF signal variance is dependent on the skin tissue type. Additionally, MP level causes an AF signal increase of 1.34% (i.e., considerably less compared to fingertip - 10.63 % and palm - 9.67%) in volar forearm which may due to the increased concentration of melanin (i.e., a strong fluorescence absorber) in volar forearm compared to fingertip and palm.[122] The absorption spectra of melanin shows that there is strong absorption in the spectral range

between 800- 850 nm which may be responsible for the slight difference in the mean NIR AF spectral shape of volar forearm.[123] Therefore, the concentrations of endogenous fluorophores affect the NIR AF spectral data to a certain extent.

Further analysis of the pressure-induced variations in NIR AF spectra was performed by generating multiclass PLS-DA models for the fingertip, palm and volar forearm datasets. From Figure 3.2.4, it can be seen that the spectra belonging to different pressure levels are clustered together; indicating that the classification algorithm could not efficiently discriminate the spectra belonging to the different pressure levels due to the statistical insignificance of the AF spectra ($p > 0.05$). The generated PLS-DA models for fingertip, palm and volar forearm dataset provided correct classification rate of 52.69%, 62.19% and 53.70% respectively, for classifying the spectra obtained at LP resembling the natural skin AF from MP + HP. The spectra obtained at HP can be separated from LP + MP with correct classification rate of 50.93%, 50.95% and 34.19%. The classification results show that the native tissue AF (i.e. AF spectra acquired at LP) differed substantially (~50-60 % discrimination for LP vs. MP + HP) from compressed tissue AF (i.e. AF spectra acquired at MP or HP) demonstrating that MP (~50kPa) that is proximate to the clinically extreme pressure (>55 kPa) and HP (~130 kPa) influences the skin NIR AF properties to an extent. Although clear differences in mean AF intensity can be observed in Figure 3 at different pressure levels; these differences when statistically analysed (i.e. one-way ANOVA with Bonferroni correction at 5%) were found to be insignificant. The obtained p-values were not significant (i.e. $p > 0.5$) for the measured spectral range. Hence the poor accuracy in classification. We also obtained similar trend with applied probe pressure for the NIR AF spectra acquired from fingertip, palm and

forearm under LP, MP and HP using the volume probe (probing depth of ~800 um)[117] (unpublished data), substantiating the real-time monitoring of quantitative probe pressure during NIR AF spectral measurements particularly during clinical applications. Thus the developed pressure sensitive spectroscopy platform enables quantitative assessment of probe-tissue contact pressure in real-time during *in vivo* spectroscopy measurements and can be used to mitigate the probe pressure induced spectral variability during *in vivo* NIR AF spectroscopy. Furthermore, the real-time feedback of applied pressure can guide the operator/clinician to precisely maintain the magnitude of probe pressure, eliminating the possibility of observed site-specific changes associated with probe pressure variability during NIR AF spectral measurements. This automated probe handling (i.e., real-time probe pressure feedback) may further enable effective clinical decision making using *in vivo* NIR AF spectroscopy even in the hands of inexperienced clinicians.

3.2.5 Conclusion

In conclusion, for the first time, the effects of exerted probe pressure on *in vivo* NIR AF spectroscopy were thoroughly studied in real-time by the dynamic control of external probe pressure using the pressure sensitive NIR AF spectroscopic platform. The results showed that higher probe pressures (i.e. MP or HP) affected NIR AF to a certain extent. These variations can be mitigated by pressure sensitive fiber-optic NIR AF spectroscopy that could provide instantaneous probe pressure feedback to operators and help in maintaining the probe pressure at LP level during NIR AF spectral measurements.

Chapter 4. Real-time monitoring of probe-tissue contact pressure effects on in vivo Raman spectroscopy

The aim of this study is to evaluate the real-time effects of probe pressure induced spectral variations during *in vivo* skin tissue confocal Raman spectroscopy by the dynamic quantitative monitoring of the applied probe-tissue contact pressure. High-quality *in vivo* Raman spectra were measured from fingertip, palm and volar forearm skin sites of 20 volunteers at three different pressure levels (i.e., low pressure (LP - 10 kPa), medium pressure (MP - 50 kPa) and high pressure (HP - 130 kPa)) using a dynamic pressure-sensitive fiberoptic probe. The Raman spectral signatures of fingertip showed subtle variations ($p < 0.05$) only when HP was applied. However, spectral data acquired from the palm showed subtle changes ($p < 0.05$) at both MP and HP levels around various protein Raman bands (i.e., ~1244-1247, 1275-1295, 1335-1360, 1400-1420, 1617-1630 and 1650-1680 cm^{-1}). In contrast, the spectra measured from volar forearm exhibited no significant variations at the various reference pressures ($p > 0.05$), revealing that the probe pressure effect is site-specific. Partial least squares (PLS)-discriminant analysis (DA) could accurately discriminate ~ 45 – 55% of Raman spectra acquired under LP *vs.* MP and HP; demonstrating that the higher probe pressures (i.e. MP or HP) caused some trivial changes to *in vivo* skin Raman spectral profiles. These observed small spectral changes caused by probe handling variations can be eliminated if probe pressure is maintained at LP. As the probe pressure is arduous to control especially during clinical endoscopy procedures, pressure sensitive Raman spectroscopy that incorporates real-time, quantitative, monitoring of probe-tissue contact pressure can be used to control the applied probe pressure during Raman spectral measurements.

4.1.1 Introduction

Raman spectroscopy is a unique analytical technique that has opened a new line of approach for fighting against cancer based on early detection at the biomolecular level *in vivo*. With the technical hallmarks of today's Raman instruments such as near-infrared (NIR) diode lasers, NIR-enhanced deep-depletion charge-coupled device (CCD) detectors and miniaturized fiber-optic Raman probes, the point-wise fiber-optic Raman spectroscopy has recently been emerged as a promising non-invasive, *in vivo* diagnostic tool in the field of cancer diagnostic medicine.[22, 23, 47, 86] The use of fiber-optic probes permits non-invasive access to remote internal organs and gently placed against target tissue during *in vivo* Raman measurements to eliminate specular reflection and reduce refractive index mismatch.[29] The contact between probe and tissue further increases light penetration into living tissue, enhancing the diagnostic capability of the spectroscopy modalities. This probe-tissue contact creates a light pressure on underlying tissue, however, preserving the light pressure constantly on target tissue throughout the spectroscopic measurements is extremely difficult, particularly during challenging clinical endoscopic applications. The change in the magnitude of probe pressure may induce variations on fiber-based *in vivo* tissue spectroscopic measurements due to pressure-induced alterations in tissue optical properties and lead to possible inaccuracies in diagnosis.[31-33]

The effects of probe pressure on diverse spectroscopy modalities such as fluorescence and diffuse reflectance spectroscopy have already been well documented.[29, 32, 82, 84] Very recent work from our group has also reported for the first time on the development of a novel pressure sensitive fiber-optic probe for real-time, quantitative

monitoring of probe-tissue contact pressure and its effect on *in vivo* skin fluorescence (refer chapter 3). Recently, most of the studies based on optical-diagnostics of diseases have been directed towards Raman spectral diagnostics that can provide extensive information about the changes of biochemical/biomolecular structures and conformations in tissue for molecular discrimination of cancer and precancer.[23, 38, 86, 124-127] In spite of the great potential of fiber-optic Raman spectroscopy for *in vivo* disease diagnosis, the probe pressure effects on *in vivo* tissue Raman spectra have been studied the least.[86, 87] For instance, the *in vivo* Raman spectra measured from gastrointestinal tissue (i.e., esophagus, colon) at different pressures controlled manually by an endoscopist exhibited insignificant changes.[86] On the other hand, the differences across skin tissue Raman spectra measured under extreme pressure (> 55kPa) was found to be significant compared to different arbitrary probe pressures (i.e., user-dependent- low, medium or high pressures).[87] In this study, for the first time, we quantitatively monitor the exact probe pressure applied onto *in vivo* skin tissue (i.e., fingertip, palm and volar forearm) and its effect in real-time during Raman spectroscopic measurements. Multivariate analysis including partial least squares (PLS)-discriminant analysis (DA) together with leave-one patient-out, cross-validation was performed on *in vivo* skin Raman spectra to actualize the probe handling variations (i.e., probe pressure-induced spectral variability).

4.1.2 Materials and Methods

4.1.2.1 Pressure sensitive Raman spectroscopy platform

The pressure sensitive *in vivo* tissue Raman spectroscopy platform utilized for real-time, quantitative monitoring of probe-tissue contact pressure has been reported in detail elsewhere (refer chapter 3.1.2.1 pressure sensitive UV/visible AF spectroscopy

platform).[100, 117] A spectrum stabilized 785-nm diode laser (maximum output: 300 mW, B&W TEK Inc., Newark, Delaware) and appropriate filters replaced the laser and filters in the aforementioned system (refer chapter 3.1.2.1 Pressure sensitive UV/visible AF spectroscopy platform) and is coupled to a custom designed hand-held confocal Raman probe with an NIR-coated sapphire ball lens (5 mm in diameter, refractive index n = 1.77) mounted on the probe tip. The confocal Raman probe comprises of two single fibers (200 μm diameter each, NA = 0.22), one for laser light delivery, and another for signal collection and high-index miniaturized ball lens at probe tip, enabling selective interrogation and scattered tissue Raman photons collection from epithelial layer (< 300 μm). The probe was integrated with optical filtering modules for suppressing laser noise, Rayleigh scattered light, while allowing only the frequency-shifted tissue Raman signal to pass towards the spectrograph. A customized piezo-resistive pressure sensor is coupled to the hand-held fiber-optic probe tip to facilitate real-time, quantitative monitoring of applied probe-tissue contact pressure during *in vivo* Raman measurements (refer chapter 3.1.2.1 pressure sensitive UV/visible AF spectroscopy platform). The system acquires *in vivo* skin tissue Raman spectra over the range 800-1800 cm^{-1} with an acquisition time of 1 sec and a spectral resolution of 9 cm^{-1}.

4.1.2.2 Volunteer profile

The volunteer profile is explained in detail elsewhere (refer chapter 3.2.2.2 subjects).

4.1.2.3 Multiclass diagnostics

The in-house developed GUI triggers data acquisition and analysis including laser power control, spectrometer, CCD shutter and camera readout synchronization, CCD

dark-noise subtraction, probe background subtraction, outlier detection, wavelength calibration, system spectral response calibration, autofluorescence subtraction, normalization, and real-time display of *in vivo* skin tissue Raman spectra together with the magnitude of applied probe-tissue contact pressure.[38] Multi-class probabilistic PLS-DA was further performed on the dataset to realize *in vivo* discrimination among skin tissue spectra acquired at different pressure levels (refer chapter 3.1.2.4 multivariate statistical analysis).

4.1.3 Results

Figure 4.1 shows the mean *in vivo* Raman spectra ±1 standard deviation (SD) acquired from skin tissue (i.e., (a) index fingertip (n=481), (c) palm (n=485), and (e) volar forearm (n=470)) of 20 healthy volunteers at various pressure levels of ~10 kPa (LP), 50 kPa (MP) and 130 kPa (HP). The mean difference spectra (i.e. HP-LP, HP-MP and MP-LP) of fingertip (b), palm (d) and volar forearm (f) are also plotted in Figure 4.1. The Raman spectra of skin tissue show prominent Raman peaks at 858 and 938 cm^{-1} (υ(C-C) of proteins), 1005 cm^{-1} (υ(C-C) of symmetric ring breathing of phenylalanine), 1070 cm^{-1} (υ(C-C) of lipids), 1255 cm^{-1} (amide III υ(C-N) and δ(N-H) of proteins), 1323 cm^{-1} (CH_3CH_2 twisting of proteins), 1457 cm^{-1} (δ(CH_2) of proteins and lipids) and 1661 cm^{-1} (amide I υ(C=O) of proteins).[45, 128] Additionally, subtle Raman spectral variations (i.e. $p<005$, one-way ANOVA with Bonferroni correction at 5%) in the difference spectra (see Figure 4.1 (b), (d) and (f)) were observed only at certain Raman peaks (i.e. 1255 cm^{-1}, 1323 cm^{-1} , 1457 cm^{-1} and 1661 cm^{-1}). The Raman spectra acquired on various sites of skin tissue (i.e., finger, palm and volar forearm) indicated differences in spectral properties associated with variability in applied probe pressure (Figure 4.1(b), 4.1(d), and

4.1(f)). For instance, Raman spectra acquired from fingertip expressed subtle changes only for HP (($p < 0.005$, one-way ANOVA with Bonferroni correction at 5%). Palm showed subtle changes ($p < 0.05$, one-way ANOVA with Bonferroni correction at 5%) with probe exerted pressure (i.e., MP and HP) around the major Raman peaks particularly related to proteins ~1244-1247, 1275-1295, 1335-1360, 1400-1420, 1617-1630 and 1650-1680 cm^{-1}. In contrast, the spectral changes associated with probe pressure variability were found to be negligible ($p > 0.05$) for volar forearm. The above pressure-related changes observed in Raman active components of skin tissue reveals that the probe pressure effects are site-specific.

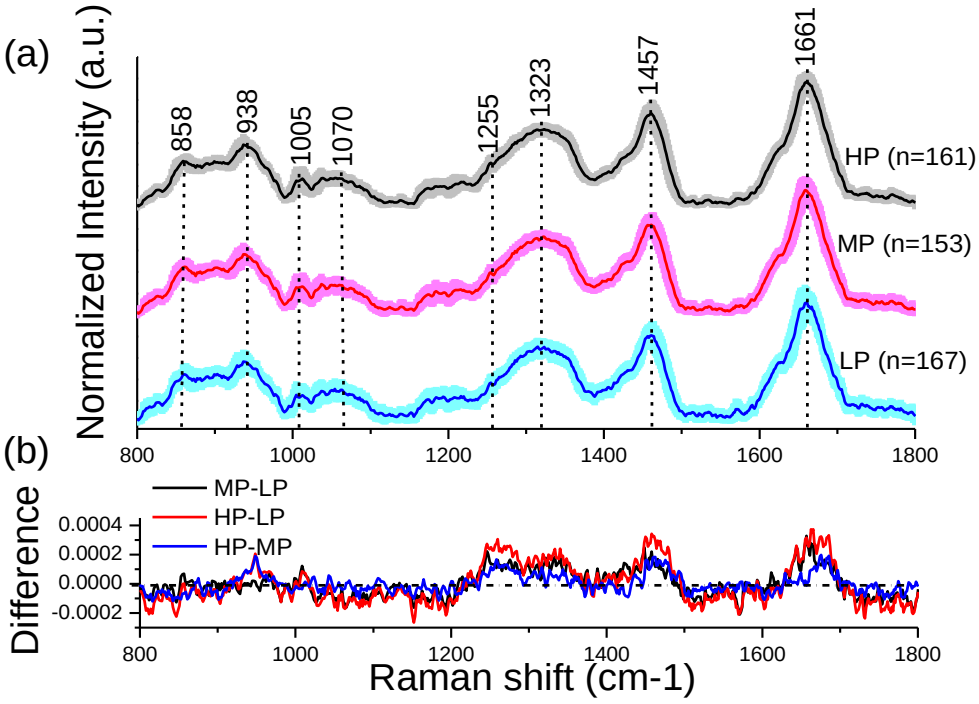

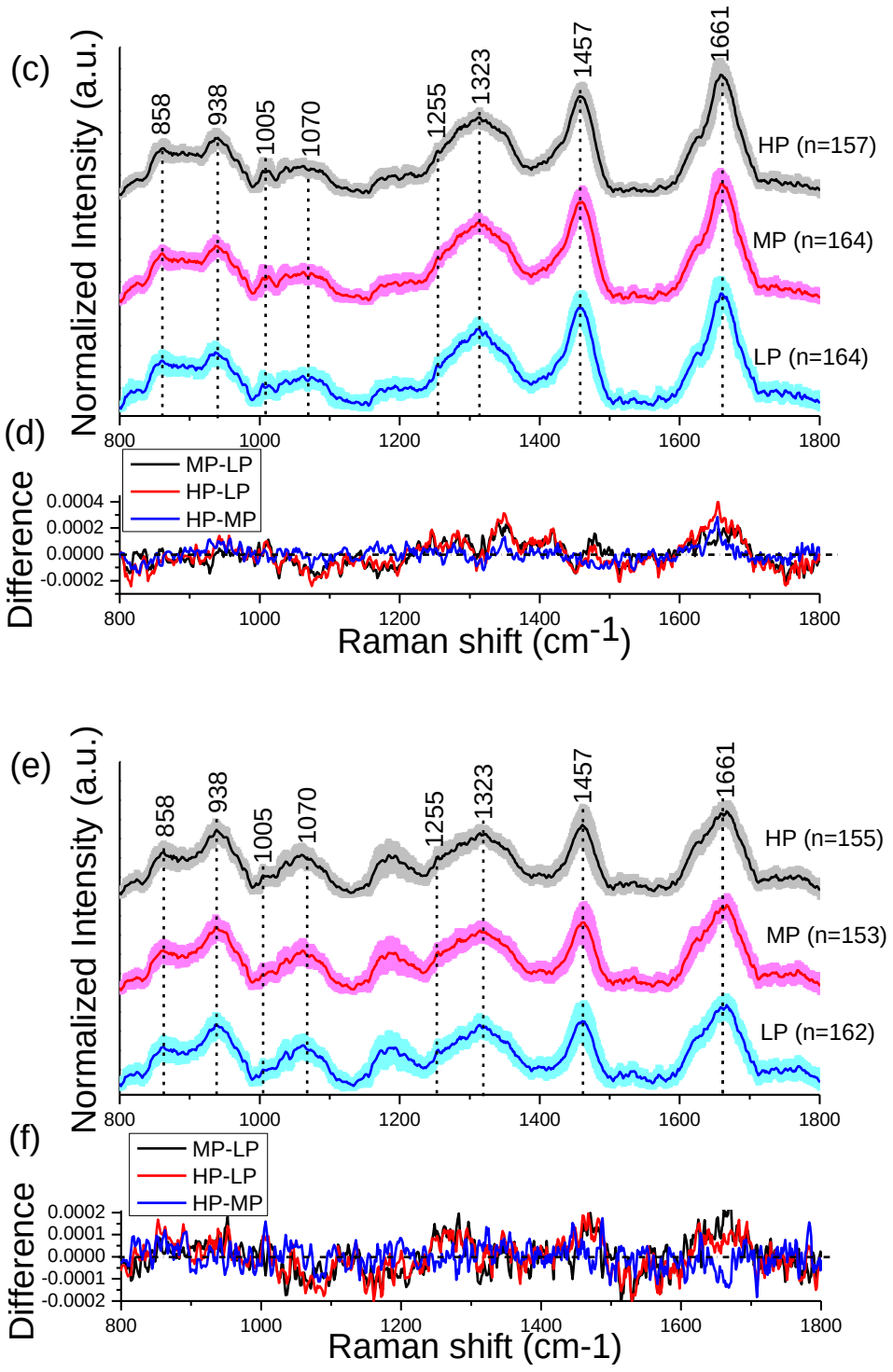

Figure 4.1 The mean *in vivo* Raman spectra ± 1 standard deviation (SD) measured from (a) fingertip (n=481) (c) palm (**n**=485) and (e) volar forearm (n=470) skin of 20 healthy volunteers at LP (10 kPa), MP (50 kPa) and HP (130 kPa). (LP, low pressure; MP, medium pressure; HP, The mean difference spectra for fingertip (b), palm (d) and volar forearm (f) show ~2-3 % variation for most Raman peaks while a maximum variation of ~5-6 % was observed for Raman peaks at 1457 cm^{-1} and 1661 cm^{-1} [The Standard Deviation appears as a coloured shade. Also, the Raman spectra acquired at different pressure levels are displaced vertically for better visualization]

Multivariate PLS-DA models were further generated from fingertip, palm and forearm spectral dataset to further explore these site-specific spectral changes associated with operator-induced probe pressure variability. The measured Raman spectra were first mean-centered and spectrum quality was assured with outlier analysis (i.e., principal component analysis (PCA) coupled with Hotelling's T2 and Q-residual statistics), where Hotelling's T2 represents the major variations in the data and Q-residuals represents the random noise or variations that are not present in the dataset (e.g., new variations).[38] Thereby, the spectra with unusual variations (e.g., light interference) were successfully removed from the spectral database of three skin tissue sites. The PLS-DA multi-class models together with leave-one patient-out, cross-validation were further developed for fingertip, palm and volar forearm dataset using optimum number of components. The optimum number of components was found to be 1 LV (14.23%) for fingertip, 5 LVs (LV1 - 25.60%; LV2 - 13.64%; LV3 – 3.25%; LV4 – 3.93%; LV5 – 2.52%) for palm and 2 LVs (LV1 – 25.13%; LV2 – 7.43%) for volar forearm dataset (Figure 4.2), representing the variations around Raman peaks (~853, 936, 1004, 1012, 1260, 1313, 1345, 1451, 1468, 1618, 1642, 1656, and 1665 cm^{-1}) corresponding to major skin tissue Raman-active biomolecules (Figure 4.3). The generated PLS-DA models from the Raman spectra of fingertip, palm and forearm correctly classified 55.09%, 45.73% and 51.23%, respectively, for separating LP spectra from MP + HP; correct classification rate of 75.78%, 57.32% and 5.81% for differentiating HP spectra from LP + MP, respectively (2-D ternary scatter plot, see Figure 4.4, Table 4.1).

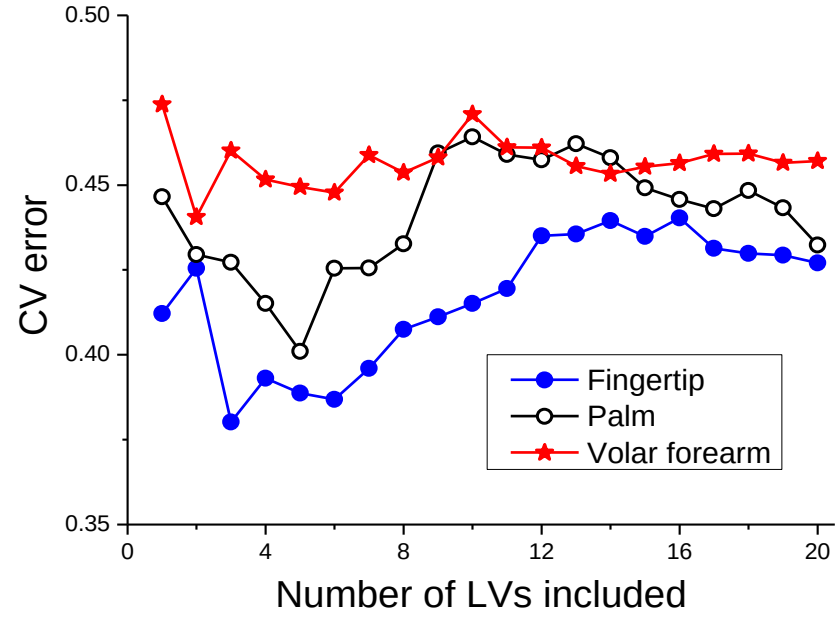

Figure 4.2 The number of latent variables (LVs) *vs.* cross-validation error for identifying optimum number of LVs to be utilized for developing PLS-DA diagnostic models for differentiating spectra measured at different reference pressure levels (LP ~10 kPa, MP ~50 kPa and HP ~130 kPa

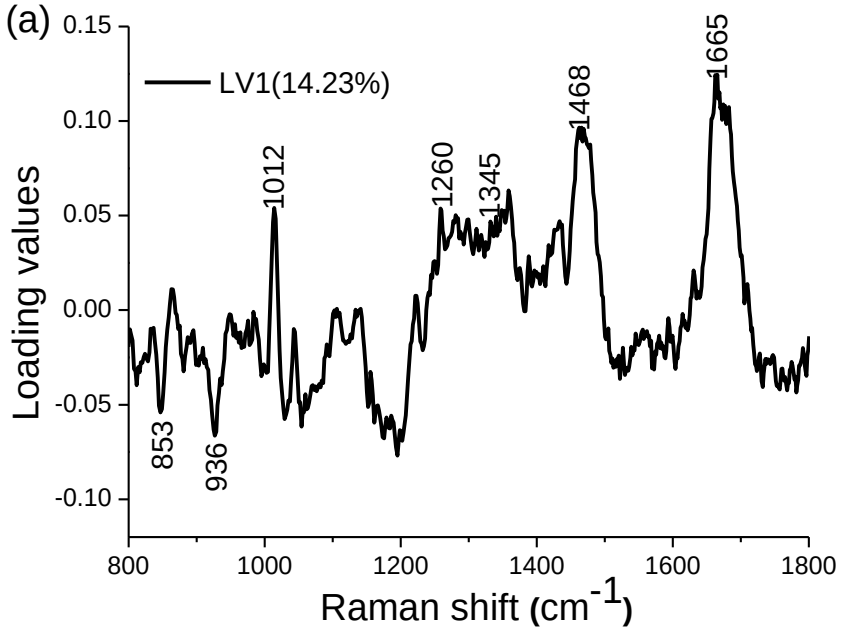

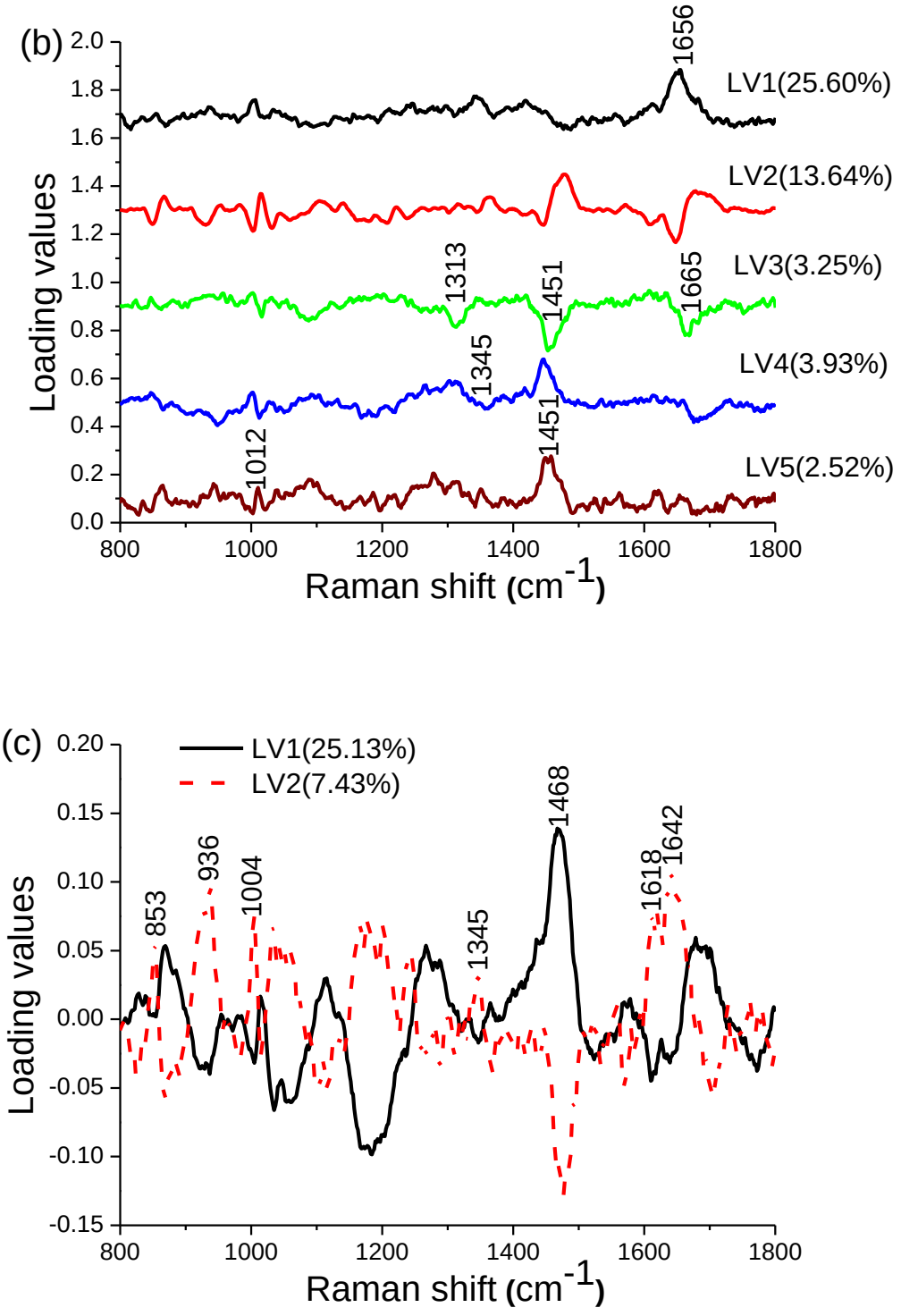

Figure 4.3 The diagnostically significant latent variables (LVs) calculated from the Raman spectra of (a) fingertip, (b) palm, and (c) volar forearm measured at three different probe pressure levels (LP ~10 kPa, MP ~50 kPa and HP ~130 kPa). The significant LVs of palm (b) have been shifted vertically for better visualization

From the results, it can be noted that the applied probe pressures cause slight variations in the Raman spectroscopic properties of skin tissue. The observed small probe pressure variations on skin tissue Raman spectra can further be eliminated by applying short-term (< 1sec) LP against the tissue through monitoring the probe-tissue contact pressure in real-time using the developed pressure sensitive Raman probe, moving the capability of novel pressure sensitive Raman spectroscopy one step forward in disease diagnosis by preserving only the diagnostically relevant variations.

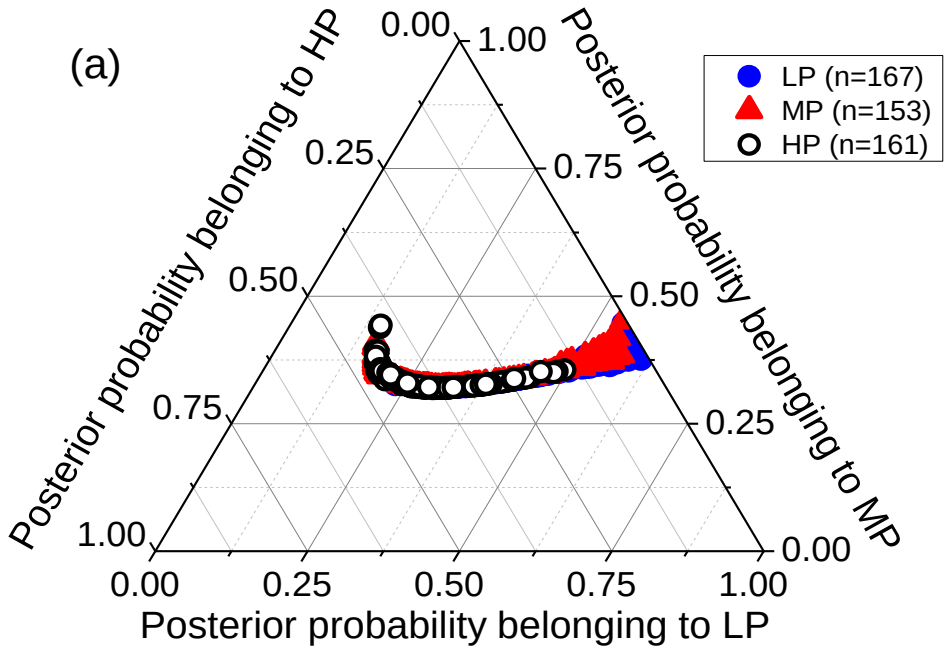

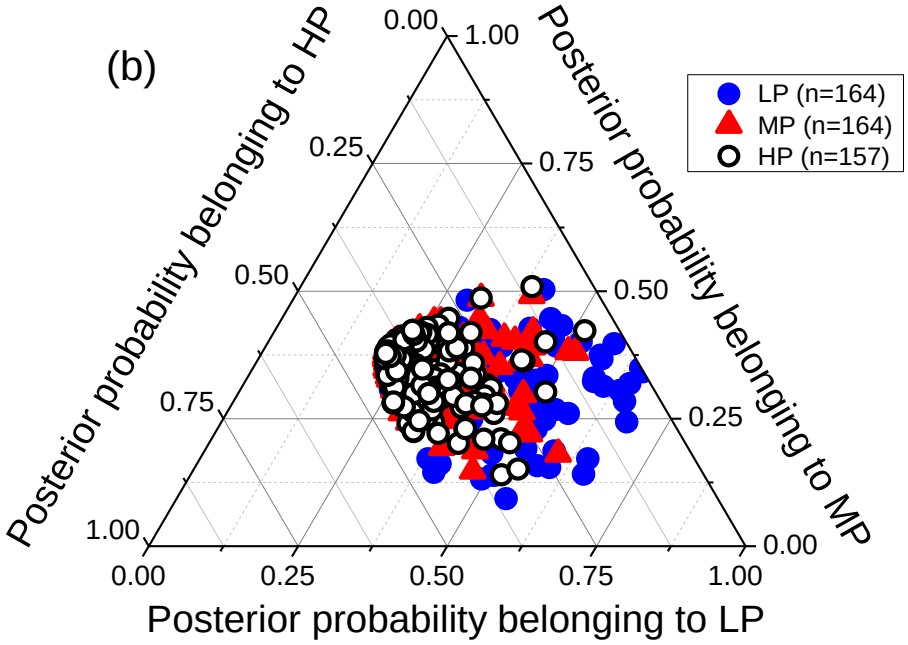

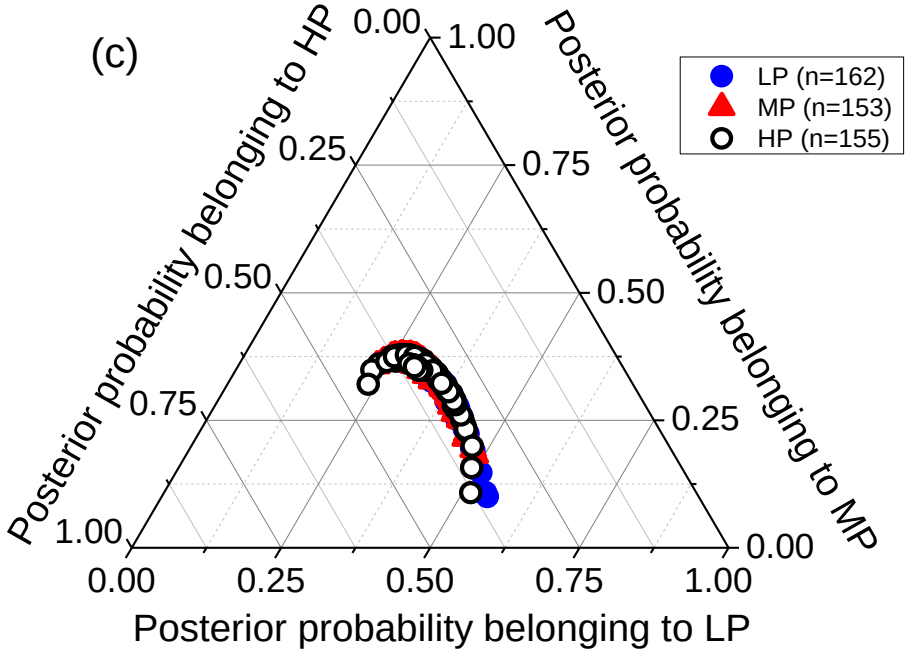

Figure 4.4 Two-dimensional ternary plot of calculated posterior probabilities belonging to *in vivo* (a) fingertip, (b) palm, and (c) volar forearm Raman spectra measured under low pressure (LP ~10 kPa), medium pressure (MP ~50 kPa), and high pressure (HP ~130 kPa) using PLS-DA models together with leave-one patient-out, cross validation

	Raman prediction								
	Fingertip			Palm			Volar forearm		
	LP	MP	HP	LP	MP	HP	LP	MP	HP
LP	92	0	75	75	34	55	83	73	6
MP	56	0	97	34	57	73	45	96	12
HP	37	2	122	30	37	90	53	93	9
Correct classification rate (%)	55.09	0.00	75.78	45.73	34.76	57.32	51.23	62.75	5.81

Table 4.1 Classification results for discriminating *in vivo* skin (fingertip, palm and volar forearm) Raman spectra measured at low-pressure, medium pressure and high pressure using PLS-DA algorithms, together with the leave-one patient-out, cross-validation method. [The diagonals are correct predictions while the off diagonals are the false predictions].

4.1.4 Discussion

Raman spectroscopy is a vibrational spectroscopic technique that can noninvasively capture specific biomolecular information for tissue diagnosis and characterization in its native state. The difficulty in capturing weak tissue Raman signals, slow spectral acquisition speed (>1 sec) and manufacturing of miniaturized fiber-optic Raman probes to access remote internal organs presented great challenges in pushing Raman spectroscopy for non-invasive, *in vivo* disease diagnosis. The very recent advancements in modern Raman instrumentation have opened a new frontier in Raman spectroscopic diagnosis of early cancer screening *in vivo* in real-time (<1sec). Accumulating evidences reported signify the potential of Raman spectroscopy for non-invasive diagnosis of cancer and precancer *in vivo* in internal organs.[23, 38, 124, 125, 127] However, it has been

reported that the probe handling variations (e.g., probe pressure) is one of the major sources of spectral variations in spectroscopy modalities including fluorescence, diffuse reflectance, especially for biomedical applications due to difficulty in accessibility of internal organs.[29, 32, 82, 84] Hence, the effect of probe handling variations on *in vivo* fiber-optic Raman spectroscopy is always a point of question in biomedical community, which hasn't been studied in detail till now. In this work, we quantitatively monitor the probe pressure applied on the tissue and its effect in real-time during *in vivo* Raman spectroscopic measurements. Moreover, NIR-excited spectroscopy holds potential benefits for safe tissue diagnosis, such as non-carcinogenic and relatively insensitive to tissue water content compared to ultraviolet (UV)-visible-excited spectroscopy. In this study, we utilize the typical pressure used in clinical procedures (~9 kPa) as LP; pressure lower than the clinically extreme pressure (55 kPa)[87] as MP (50 kPa); and 130 kPa as HP, which is far higher than the clinically extreme pressure (55 kPa). As a result, we successfully acquired Raman spectra (n=1436) from index fingertip (n=481), palm (n=485) and volar forearm (n=470) *in vivo* within 1 sec at the defined three reference pressure levels.

The measured Raman spectra showed site-specific changes with applied external probe pressure. For instance, the spectra acquired from fingertip showed subtle changes on all wavenumbers for HP ($p<0.005$). However, these spectral changes were insignificant for MP. Interestingly, palm showed pressure-associated spectral variations for both MP and HP, primarily around the protein Raman bands (i.e., 1244-1247, 1275-1285, 1335-1360, 1416-1419, 1617-1630, and 1650-1670 cm^{-1}). On the other hand, the forearm spectra were not influenced by the probe exerted pressure ($p>0.05$). The

important Raman spectral changes for all the measured three skin sites were noted loosely around 1345 (proteins and nucleic acids), 1450 (proteins and lipids), 1627 (amide I - β-sheet) and 1650 cm^{-1} (amide I – α-helix). It has been demonstrated that the pressure above 5.5kbar broadens and lowers the frequency of amide I band, mainly related to environmental changes around the protein, leading to pressure-induced protein-precipitation, random organization, unfolding and denaturation.[129-131] The pressure-related increase in the frequency of CH_2 bending mode of methylene chain of lipids ($1450cm^{-1}$) is also observed, likely associated with the conformational and orientational ordering of methylene chains.[130] However, our data do not show any major differences in the position of prominent Raman peaks (e.g., amide I, amide III, and CH_2 bending mode of lipids, see Figure 4.1) because the utilized pressure range is far less compared to the pressure required for protein precipitation, unfolding or denaturation (e.g., ~5.5 kbar pressure required for inducing denaturation and precipitation in lysozyme).[129] The small changes noticed in the intensities of the measured skin Raman spectra (i.e., increased intensity approximately at 1245 cm^{-1} (amide III), 1345 cm^{-1} (α-helix) and 1637 (amide I - β-sheet))[129]could be because the applied pressure is nearly equal (MP ~50kPa) or extremely high (HP ~130kPa) compared to the clinically acceptable extreme pressure (~55kPa).[87] This exerted probe-tissue contact pressure (i.e., MP and HP) may have induced minor structural disruption in the protein secondary structures (α-helix and β-sheet), especially in the poly-peptide backbone of protein or the hydrogen/deuterium (H/D) exchange behaviour in the individual secondary-structure elements under HP, resulting in trivial variations in the measured Raman spectra.[129, 131] The pressure-related changes also occurs in phosphate stretching bands (e.g., nucleic acids ~1345 cm^{-1}), likely

be related to characteristic of hydrogen-bonded or non-hydrogen-bonded functional groups.[129]

The mean difference spectra shown in Figure 4.1 - (b) fingertip, (d) palm and (f) forearm were plotted to resolve the subtle inter-pressure (i.e. HP-LP, HP-MP and MP-LP) Raman spectral variations. Subtle Raman spectral variations (i.e. $p<005$, one-way ANOVA with Bonferroni correction at 5%) in the difference spectra were observed only at certain Raman peaks (i.e. 1255 cm^{-1}, 1323 cm^{-1} , 1457 cm^{-1} and 1661 cm^{-1}). Moreover, the difference spectra showed an average variation of ~2-3 % for most Raman peaks while a maximum variation of ~5-6 % was observed for Raman peaks at 1457 cm^{-1} and 1661 cm^{-1}; suggesting that these pressure induced subtle Raman spectral variations were minimal.

To further differentiate and provide deep insight into these subtle probe pressure-induced changes on *in vivo* skin tissue Raman spectra, PLS-DA multi-class models for the entire Raman spectral datasets (i.e. finger, palm and forearm) were generated. From Figure 4.4, it can be seen that the spectra belonging to different pressure levels are clustered together; indicating that the classification algorithm could not efficiently discriminate the spectra belonging to the different pressure levels. This may be because the entire Raman spectra was used for classification and not individual Raman peaks (i.e. individual Raman peaks showed non-uniform site-specific spectral variation. For e.g. At 1402 cm^{-1}, Raman spectral intensity increased for HP but at 1661 cm^{-1}, Raman spectral intensity decreased for HP).

However, the generated PLS-DA models could accurately classify 55.09%, 45.73% and 51.23% of fingertip, palm and volar forearm, respectively, measured at LP

resembling the natural skin molecular content from MP+HP. The fingertip, palm and volar forearm spectra obtained at HP could be separated from LP + MP with classification rate of 75.78%, 57.32% and 5.81%, respectively. The classification results (i.e. ~45-55 % discrimination for LP vs. MP + HP) demonstrate that the MP (~50kPa) that is proximate to the clinically extreme pressure (>55 kPa) and HP (~130 kPa) induce subtle variations in the skin Raman spectroscopic properties (i.e. especially for fingertip and palm but not forearm). We also obtained similar trend with applied probe pressure for the Raman spectra acquired from fingertip, palm and forearm under LP, MP and HP using the volume probe (probing depth of ~800 um)[20] (unpublished data).

The subtle pressure induced Raman spectral distortions might affect the diagnostic efficacy of Raman spectroscopy as it is extremely sensitive to slight changes in tissue biochemical composition. However, these effects become negligible if probe pressure is maintained below clinically extreme pressure level. Therefore Raman spectroscopy without pressure measurement can be performed for the measured skin sites (i.e. fingertip, volar forearm and palm) as long as probe pressure is maintained below clinically extreme pressure. However, it is still unclear if there will be any major pressure induced variations in Raman spectra in internal organs during endoscopy, laparoscopy etc. and therefore; more studies are required to prove that probe pressure does not affect Raman spectral measurements. Pressure sensitive *in vivo* Raman spectroscopy for other organs might be useful in the future.

4.1.5 Conclusion

In conclusion, for the first time, we quantitatively monitored in real-time (<1 sec) the exact probe pressure applied on to the skin tissue during *in vivo* Raman spectroscopic measurements. The results showed that the probe handling variations (i.e., probe pressure variability) caused trivial changes to the tissue Raman spectra at high pressures (i.e. MP or HP). However, these trivial changes can be eliminated if probe pressure is maintained at LP. As the probe pressure is arduous to control especially during clinical endoscopy procedures, pressure sensitive Raman spectroscopy that incorporates real-time, quantitative, monitoring of probe-tissue contact pressure can be used to control the applied probe pressure during Raman spectral measurements.

Chapter 5. Real-time, quantitative evaluation of dynamic probe-tissue contact pressure effects on in vivo skin diffuse reflectance spectroscopy

In this study, we aim to characterize the effects of dynamic probe pressure induced variations in the acquired reflectance spectra during *in vivo* skin tissue diffuse reflectance (DR) spectroscopy. The exerted probe-tissue contact pressure is controlled by utilizing a custom-designed pressure sensitive fiber-optic probe that can be used to quantitatively monitor the applied probe pressure. The DR spectral response was studied at three different sites of the human hand (fingertip, volar forearm and palm) over three reference pressure levels (i.e., low pressure (LP - 10 kPa), medium pressure (MP - 50 kPa) and high pressure (HP - 130 kPa)). The diffuse reflectance signal intensity significantly decreased with progressive increase in the magnitude of applied probe pressure due to the probe pressure induced alterations in concentrations of major chromophores like hemoglobin, water, fats and lipids. Multiclass partial least squares-discriminant analysis (PLS-DA) models were used to differentiate spectra acquired at different pressure levels and yielded accuracies of 82.11% (fingertip), 82.40% (volar forearm) and 76.01% (palm) for differentiating spectra measured at low pressure LP vs. MP and HP; suggesting that the applied probe pressure affects the DR spectra significantly. Additionally, the differences in melanin concentration at the different measurement sites (i.e. fingertip, volar forearm and palm) also play an important role in contributing to the extent of variation of the reflectance signal at different probe pressures (i.e. MP spectra affects volar forearm more when compared to fingertip and forearm). This study demonstrates the need for real-time

quantitative probe-tissue contact pressure monitoring in order to mitigate the probe pressure induced spectral variations during *in vivo* DR spectroscopy.

5.1.1 Introduction

Fiber based Diffuse Reflectance (DR) spectroscopy is a rapid, non-invasive spectroscopy technique that has been used in various biomedical applications like characterization of tissue biochemical content, studying the optical properties of biological tissues as well as disease diagnosis in a number of organs[10, 11, 36, 106, 123, 132, 133] The diagnostic capability of DR spectroscopy is predominantly due to its excellent sensitivity to reflect changes in biochemical concentration in target tissues. Fiber-based DR spectroscopy makes use of a fiber-optic probe that is in contact with the target tissue to reduce interferences due to refractive index mismatch, specular reflection, increases light penetration and transmittance and avoids inconsistent illumination-detection geometry during spectral acquisition which results in the enhancement of the diagnostic capability of the system.[29, 35, 36] The applied probe tissue contact pressure is a complex, operator dependent variable that can cause alterations in the optical properties of underlying tissue (refer chapter 3.1.1 introduction).[31, 32] Hence, it is necessary to control the applied probe pressure carefully to minimize the pressure induced spectral variation. Improper control of exerted probe pressure may lead to potential concerns such as changes in tissue spectral profiles, disparities in data collection and calibration and potential inaccuracies in diagnosis.[32-34] Therefore, it is highly imperative to accomplish dynamic real-time probe pressure control and quantitatively monitor the probe-tissue contact pressure to mitigate the pressure induced spectral variability.

A number of studies have been carried out to analyze the confounding effect of

the applied probe pressure on DR spectroscopy.[29, 32, 35-37, 82] Existing studies have shown that the variation of DR is tissue site specific and that short-term (< 2s), low probe pressures (<9 kPa) have negligible effect on skin tissue DR signal[32, 37]. However, the aforementioned studies have been limited to static pressure measurements utilizing a pre-calibrated spring loaded device, or making use of the extent of tissue compression (in mm) as a criterion for applying a particular pressure or operator-dependent arbitrary probe pressures. The dynamic changes in applied probe pressure that occur due to differences in deformability of various measurement sites on skin tissue, inter-subject variations in the extent of tissue compression and orientation of the probe are important sources of variation in the exerted probe pressure that have not been analyzed sufficiently. The limited reports in existing literature about dynamic probe pressure effects on DR assert that the variations in probe pressure are a viable source of information for soft tissue classification (i.e. skin above muscle, skin above veins and skin above bone).[31, 56] Hence, in this study, we highlight the significance of real-time, quantitative monitoring of dynamic changes in the applied probe pressure and providing dynamic real-time probe pressure control during spectral measurements. We successfully utilized the custom-designed pressure sensitive fiber-optic probe [ref] to quantitatively monitor the dynamic pressure induced variations in real-time on *in vivo* human skin DR spectroscopy. Three measurement sites (i.e., fingertip, volar forearm and palm) on the skin tissue were chosen specifically because skin tissue acts as a highly scattering medium in visible to near-infrared region, representing one of the most challenging organs with complex and inhomogeneous morphological structures. Multivariate statistical models (PLS-DA) were used for in-depth analysis of the spectral information

acquired at various pressure levels.

5.1.2 Material and Methods

5.1.2.1 Pressure sensitive DR spectroscopy platform

Figure 5.1 shows the schematic diagram of the pressure sensitive *in vivo* tissue diffuse reflectance (DR) spectroscopy platform developed for real-time, quantitative probe-tissue contact pressure measurement.

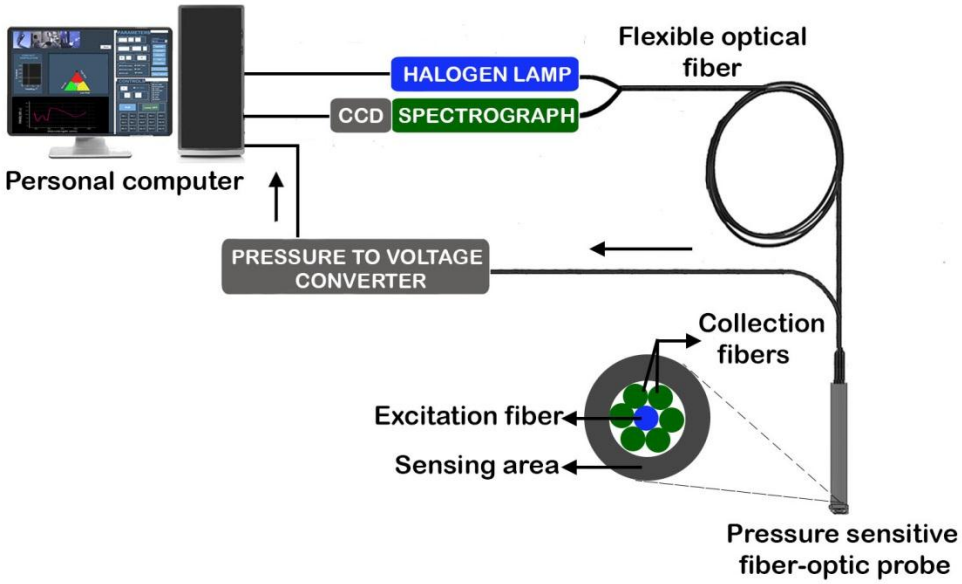

Figure 5.1 Schematic of the pressure sensitive fiber-optic diffuse reflectance (DR) spectroscopy system

The basic setup of the pressure sensitive spectroscopy system is explained in detail elsewhere (refer chapter 3.1.2.1 pressure sensitive UV/visible AF spectroscopy platform). The pressure sensitive DR spectroscopy system utilizes a tungsten halogen lamp (LS1LL, Ocean Optics Inc., Dunedin, FL, USA) and a transmissive imaging spectrograph (QE65000, Ocean Optics Inc., Dunedin, FL, USA) equipped with a back-thinned charge-coupled device (CCD) detector (S7031-1006, 1024X58with pixel sizes of

24.6mm, QE > 90%, Hamamatsu, Shizuoka, Japan) that replaces the laser, filters and the spectrograph used in the pressure sensitive AF spectroscopy system. The DR spectra were acquired within the spectral bandwidth 375-1150 nm with an integration time of 10 ms and tungsten light incident power of 0.1mW on tissue surface. DR spectra measurements were carried out on the skin surface of ten healthy volunteers at three different measurement sites (the index fingertip, volar forearm and palm skin on abductor pollicis muscle). Desirable probe pressures (i.e., low pressure (LP) -10 kPa, moderate pressure (MP) – 50 kPa and high pressure (HP) – 130 kPa) were applied upon *in vivo* target tissue site by mounting the sensor coupled probe on a translation stage and controlling its movement appropriately (refer chapter 3). The probe pressure was instantaneously displayed in the real-time diagnostic software,[38] guiding the operator to acquire spectra at required pressure levels. High-quality *in vivo* tissue DR spectra were subsequently measured from fingertip (n=145), volar forearm (n=130) and palm (n=145) at the aforementioned three reference pressures. Multiple spectra (~4-5) were obtained from each site for all the three pressure levels to include inter- and/or intra-tissue variability for data analysis.

5.1.2.2 Multivariate statistical analysis

Multi-class probabilistic PLS-DA modeling was performed to realize *in vivo* discrimination among skin tissue spectra acquired at different pressure levels (refer chapter 3.1.2.4 multivariate statistical analysis).

5.1.3 Results

The custom designed pressure sensitive fiber optic probe was used to acquire high quality *in vivo* DR spectra in the spectral range 375-1150 nm from three measurement

sites on the human hand (fingertip, volar forearm and palm). Figure 5.2 shows the *in vivo* mean skin DR spectra ±1 standard deviation (SD) of index fingertip (n=145), volar forearm (n=130) and palm (n=145) acquired from 10 healthy volunteers at three defined reference pressure levels [10 kPa (LP), 50 kPa (MP) and 130 kPa (HP)]. The reference pressure levels were chosen such that it included clinically relevant probe pressures (LP and MP) as well as an extreme, intense high pressure level (HP) to study the pressure induced spectral distortions over a wide pressure range (0-150 kPa).

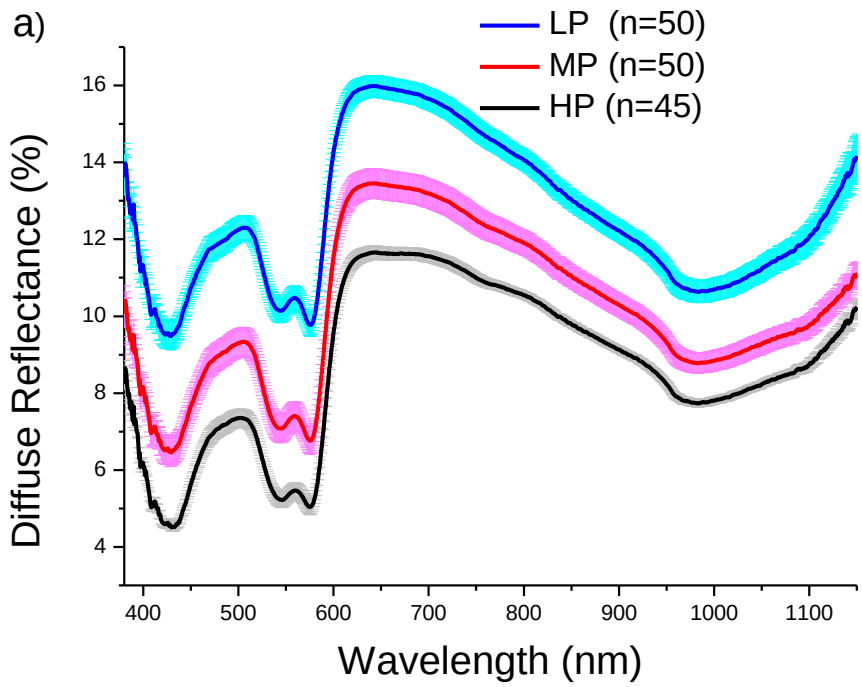

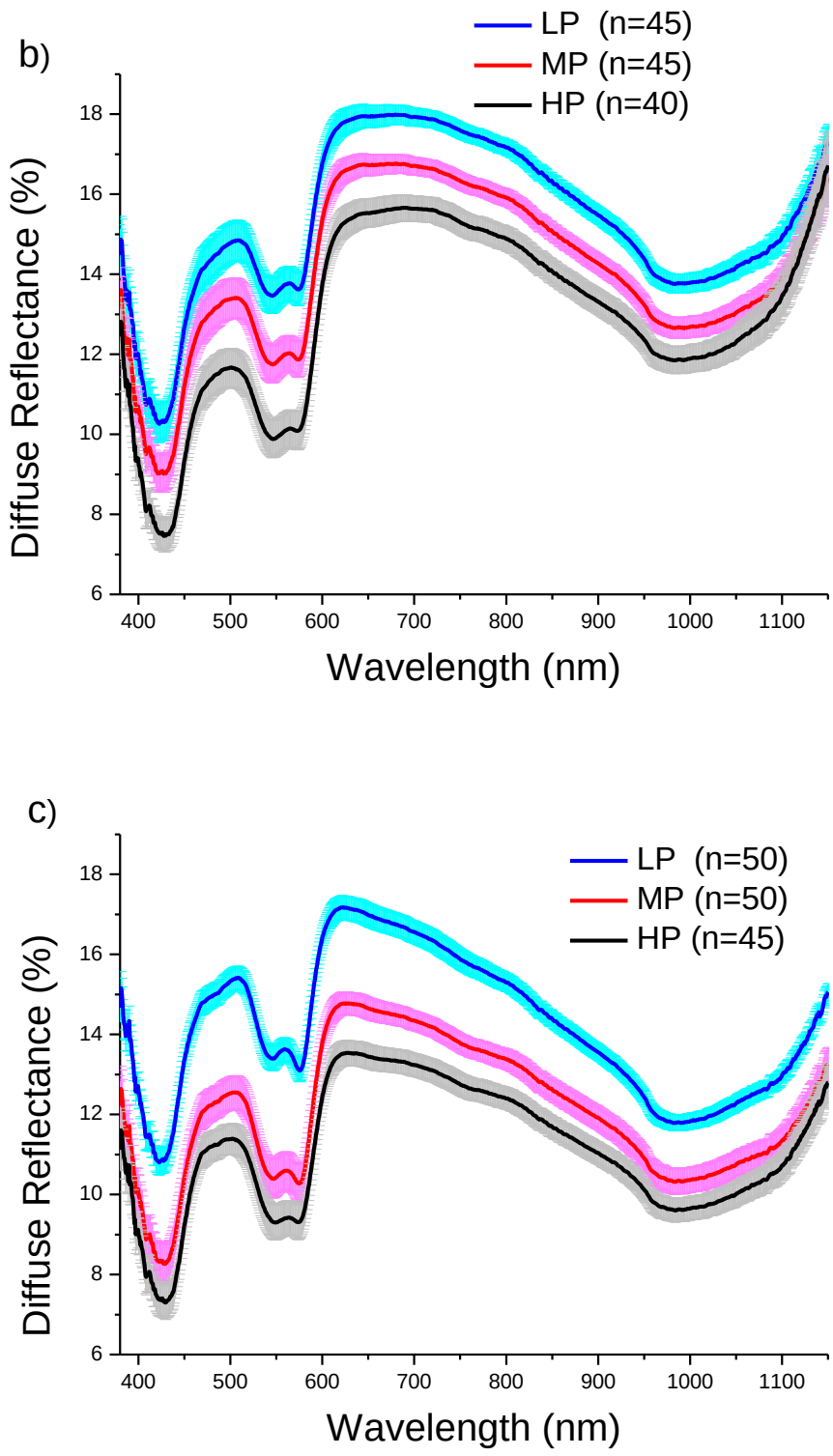

Figure 5.2 The mean *in vivo* diffuse reflectance (DR) spectra ± 1 standard deviation (SD) acquired from (a) fingertip (n=145) (b) volar forearm (n=130) and (c) palm (n=145) of 10 healthy volunteers at LP (10 kPa), MP (50 kPa) and HP (130 kPa). (LP, low pressure; MP, medium pressure; HP, high pressure. [The Standard Deviation appears as a coloured shade]

The acquired DR spectra contained distinct characteristic minima (eg. 420 nm (Soret Band), 540, 578, 750, 815, 920, 980, 1090 nm) that correspond to major endogenous chromophores like hemoglobin, fats, lipids, water and melanin, in agreement with existing literature.[31, 32, 37] However, the DR spectra exhibited an overall decreasing trend with the increase of applied probe pressure. Also, the dual peak of oxy-hemoglobin (540 and 578 nm) decreases in its height with applied probe pressure, indicating a gradual transition from oxy-hemoglobin to deoxy-hemoglobin. Moreover, the excitation peaks of porphyrins (400 nm), flavins (460 nm), lipo-pigments (435 nm) and melanin (1090 nm) also overlap with the peaks in the acquired DR spectra.[64, 123] These results confirm that the observed variation in DR signal may be primarily due to pressure induced changes in the concentration of blood (i.e., oxy/deoxy-hemoglobin - λ_{ab}~540, 560, 578 nm, fat - λ_{ab}~750, 815, 900 nm, lipids - λ_{ab}~920 nm and water - λ_{ab}~980 nm) with minor contributions from other endogenous chromophores.[87, 109, 110] Moreover, the fingertip, volar forearm and palm DR spectra measured under MP and HP exhibited considerably higher spectral variance compared to LP, signifying that LP applied against the tissue causes trivial changes in tissue optical properties, in agreement with the reported literatures.[32, 109] Moreover, The reflectance signals showed a uniform, average spectral variation of ~ 10% at each pressure level for the entire spectral range. Additionally, significant p-values ($p<0.05$; one-way ANOVA with Bonferroni correction at 5%) were obtained for certain wavelengths (i.e. 420, 540, 578, 980 nm).

The DR spectra were further analyzed using multivariate statistical algorithms for in-depth understanding of pressure induced DR spectral distortions and to differentiate DR spectra acquired at different pressure levels. PLS-DA together with leave-one patient-

out, cross validation, was employed for classification of the DR spectra based on the applied probe pressure during spectral data acquisition. Outlier analysis based on PCA coupled with Hotelling's T2 and Q-residual statistics was further utilized to remove the spectra with unusual variations (e.g., light interference).[38] After verification of the spectral quality, the leave-one patient-out, cross-validated PLS-DA multi-class diagnostic modeling was performed on the fingertip, volar forearm and palm DR datasets using optimum number of components, estimated based on the local minimum of cross-validation classification error values. The optimal number of components differed for each measurement site and was found to be 1 (fingertip), 4 (volar forearm) and 1 (palm) as shown in Figure 5.3.

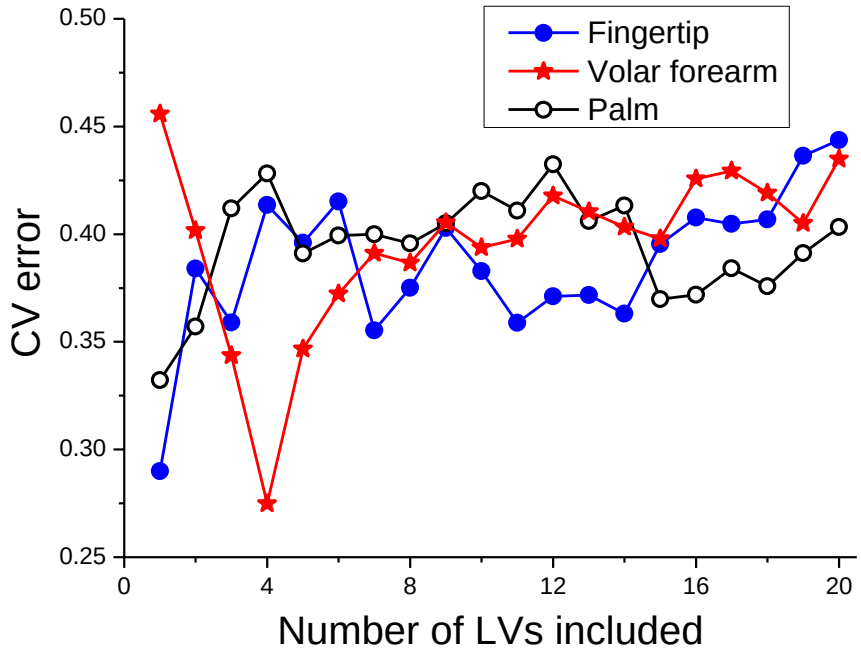

Figure 5.3 The number of latent variables (LVs) against cross-validation error for identifying ideal number of LVs to be utilized for classifying spectra measured at different probe-tissue contact pressures (LP ~10 kPa, MP ~50 kPa and HP ~130 kPa)

The principal components accounted for 92.95% (fingertip), 99.32% (volar forearm) and 91.27% (palm) of total DR spectral variations for differentiating pressure induced changes in the measured skin tissue DR spectra. The loading vectors (see Figure 5.4) clearly show spectral changes that occur at prominent wavelengths located around 420, 540, 578, 750, 815, 920, 980 and 1090 nm of the acquired reflectance signal which are associated with blood (oxy/deoxy-hemoglobin), water, fats and lipid absorption spectra.

The posterior probability values were further calculated for each dataset, using the developed PLS-DA multi-class models and are shown as a 2-D ternary scatter plot (Figure 5.5). The generated models for fingertip, volar forearm and palm dataset classify the DR spectra measured under LP from MP + HP with accuracies of 82.11%, 82.40% and 76.01%; the spectra acquired at MP from LP + HP with accuracies of 49.48%, 64.90% and 52.00%; the spectra obtained at HP from LP + MP with accuracies of 76.39%, 81.95% and 67.34%, respectively.

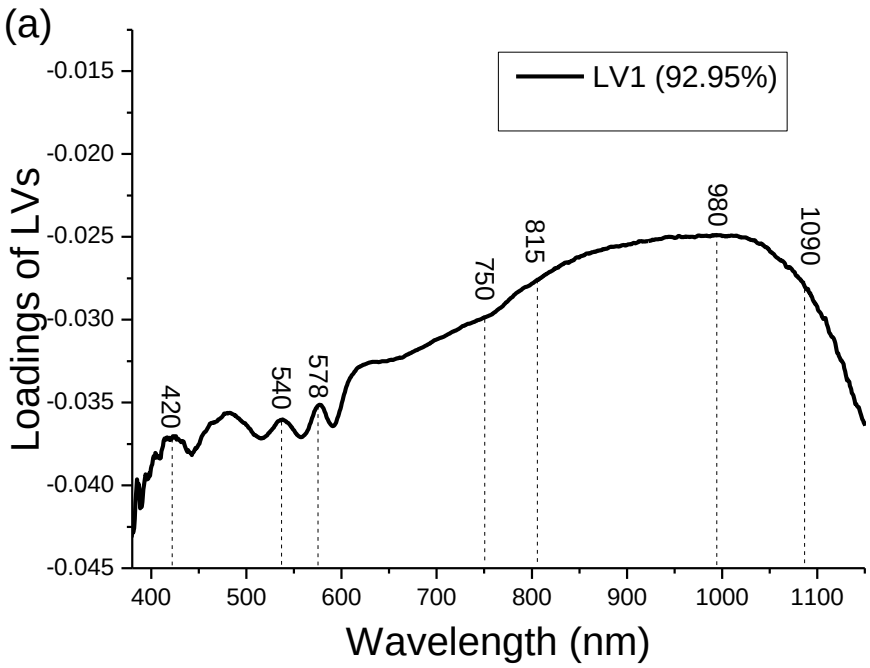
(a)
LV1 (92.95%)
Loadings of LVs
Wavelength (nm)
-0.015
-0.020
-0.025
-0.030
-0.035
-0.040
-0.045
400
500
600
700
800
900
1000
1100
420
540
578
750
815
980
1090

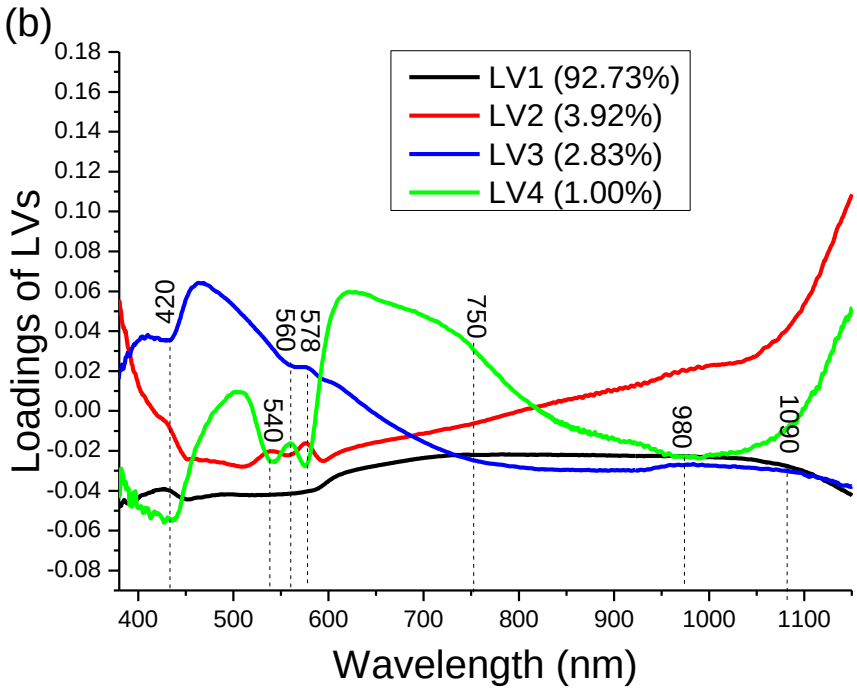
(b)
LV1 (92.73%)
LV2 (3.92%)
LV3 (2.83%)
LV4 (1.00%)
Loadings of LVs
Wavelength (nm)
0.18
0.16
0.14
0.12
0.10
0.08
0.06
0.04
0.02
0.00
-0.02
-0.04
-0.06
-0.08
400
500
600
700
800
900
1000
1100
420
540
560
578
750
980
1090

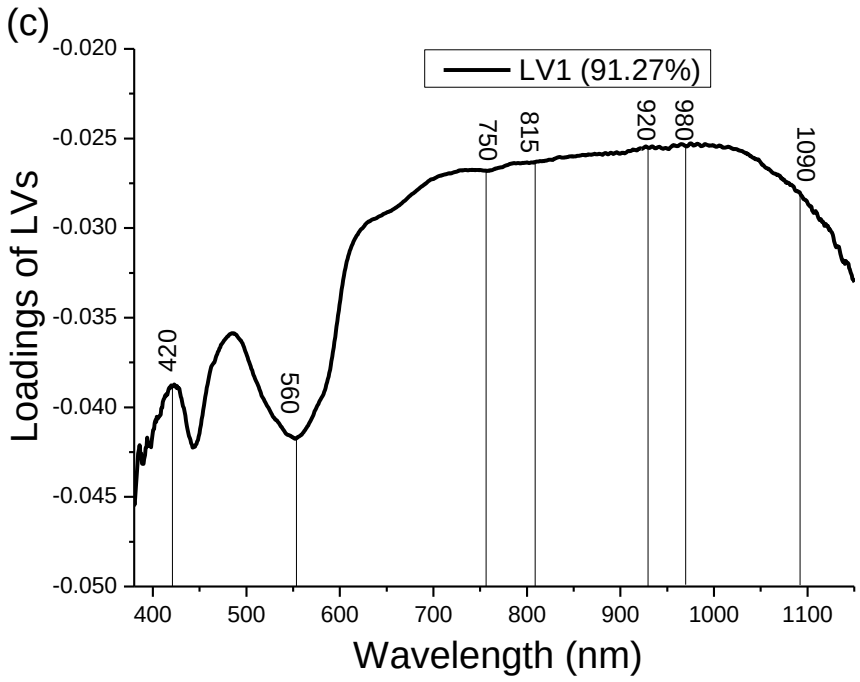

Figure 5.4 The diagnostically significant LVs calculated from the diffuse reflectance (DR) spectra of (a) fingertip (b) volar forearm and (c) palm measured at three different probe pressure levels (LP ~10 kPa, MP ~50 kPa and HP ~130 kPa)

The above results show that there is a distinct separation between LP and HP spectra at the three measurement sites. However, the variation in the accuracy for the differentiation of MP spectra among the measurement sites show the site-specific nature of the pressure induced spectral distortions.[31, 32, 105] Thus, it is highly imperative to monitor the applied probe pressure in real-time to reduce the pressure induced distortions to a great extent.

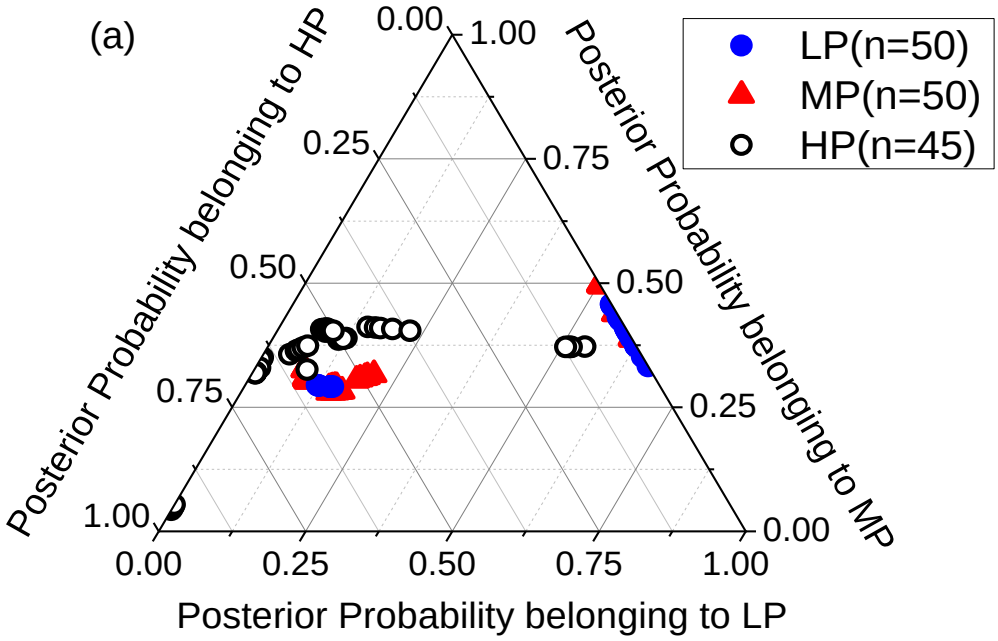
(a)
LP(n=50)
MP(n=50)
HP(n=45)
Posterior Probability belonging to HP
Posterior Probability belonging to MP
Posterior Probability belonging to LP
0.00
0.25
0.50
0.75
1.00

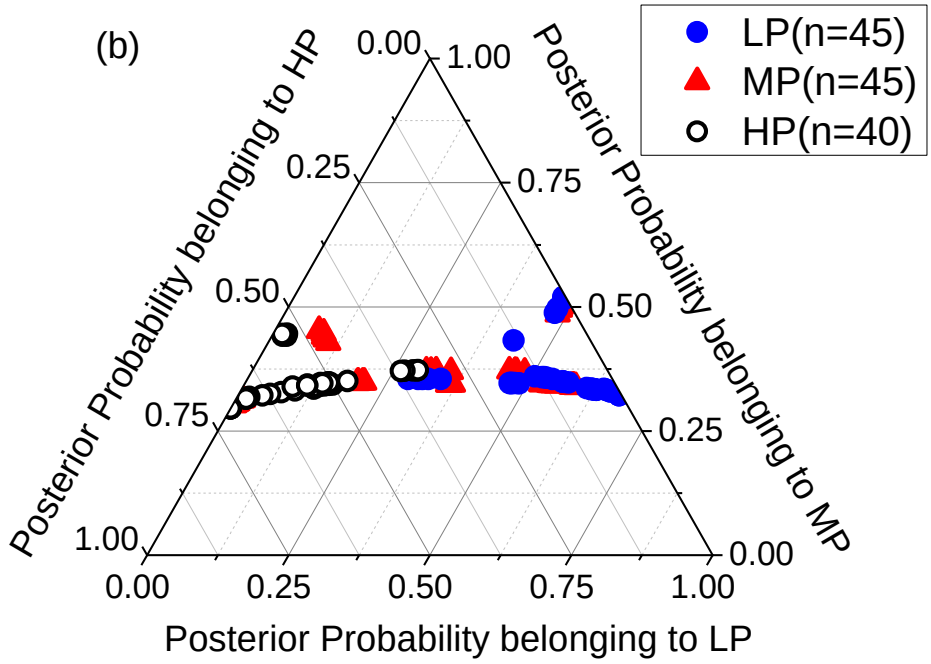
(b)
LP(n=45)
MP(n=45)
HP(n=40)
Posterior Probability belonging to HP
Posterior Probability belonging to MP
Posterior Probability belonging to LP
0.00
0.25
0.50
0.75
1.00

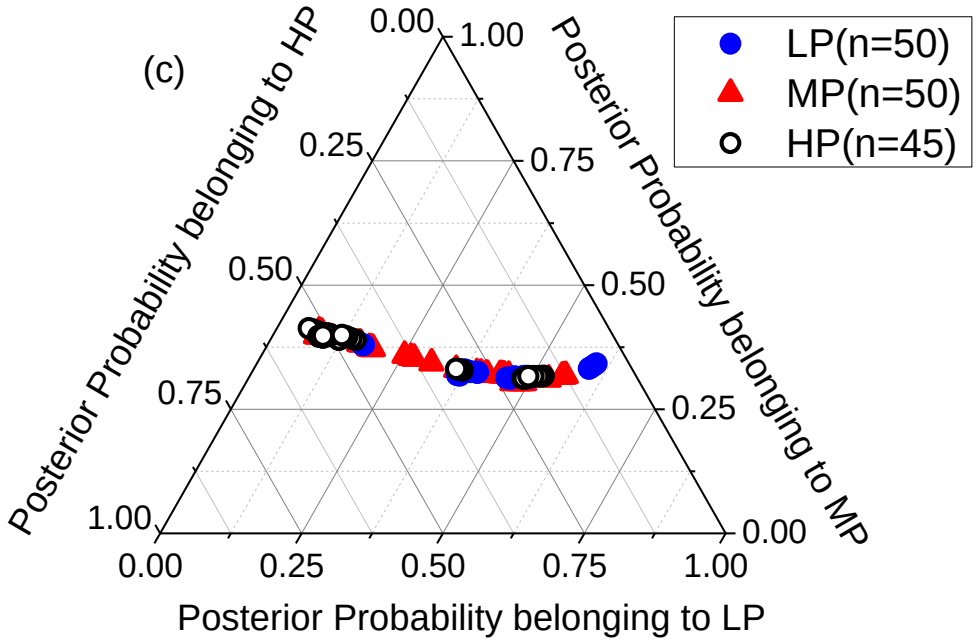

Figure 5.5 Two-dimensional ternary plot of the posterior probabilities belonging to low pressure (LP), medium pressure (MP), and high pressure (HP) categories calculated from the PLS-DA models together with leave-one patient-out, cross validation, generated from *in vivo* diffuse reflectance (DR) spectra of (a) fingertip (b) volar forearm and (c) palm

5.1.4 Discussion

The diagnostic capability of diffuse reflectance spectroscopy has been analyzed in detail by various studies.[10, 11, 36, 133] DR spectroscopy makes use of a fiber-based probe that is impressed upon the target tissue site during spectral data acquisition. The probe-tissue contact state is very essential to minimize refractive index mismatch and specular reflection which consequently results in less spectral distortions when compared to non-contact measurements.[30, 35, 36]However, it has been reported that the probe-tissue contact pressure is a confounding operator dependent variable that may distort the optical properties of underlying tissue.[29, 86] The variation in the applied probe pressure by different operators has been investigated in detail by many studies which have shown that this variation is considerably large to cause alterations in the acquired spectra and thereby

affect the diagnostic efficacy of DR spectroscopy.[84, 85, 87] These pressure induced spectral distortions can be greatly reduced if measurements are carried out at constant pressure levels. In order to achieve this, it is necessary to develop a system to monitor the applied probe pressure in real-time that will take into account the dynamic pressure changes that come into play when spectral data is acquired from deformable, soft tissue target sites.

In this study, we report the successful utilization of novel pressure sensitive fiber-optic probe [ref] for real-time quantitative monitoring of the magnitude of exerted probe-tissue contact pressure during *in vivo* skin tissue DR spectroscopy. This is necessary because the precise control of applied probe pressure is arduous in clinical scenario, particularly during endoscopic procedures to access remote internal organs and diagnostic information can be diluted significantly if the applied probe pressure is not monitored properly. Furthermore, skin tissue blanches when pressure is applied,[32] creating a challenging experimental scenario to test the developed novel pressure sensitive spectroscopy platform. The acquired high-quality *in vivo* skin tissue DR spectra (n=420) from index fingertip (n=145), volar forearm (n=130) and palm (n=145) at LP (~10 kPa), MP (~50 kPa) and HP (~130 kPa) with an integration time of 10 ms exhibited notably decreased intensity with progressive increase in applied pressure. The pressure induced variation in the reflectance signal can be observed throughout the entire spectral range from 375 to 1150 nm. The characteristic minima associated with oxy/deoxy-haemoglobin (420, 540, 560, 578 nm), fats (750, 815, 900 nm), lipids (920 nm), water (980 nm) and melanin (1090 nm) can be distinctly observed at each reference pressure level.[31, 123, 134, 135] The decrease in the reflectance intensity with applied high probe pressure may be primarily due to increased concentration of endogenous chromophores

(e.g., haemoglobin, water, fats and lipids) in the skin.[31] The rise in hemoglobin concentration with pressure is mainly due to the occlusion of blood flow under the probe tip, in agreement with the reported literatures.[106, 136] The higher concentrations of water, lipids and other endogenous chromophores with the magnitude of exerted probe pressure is associated with the compression of the tissue.[31, 32] The gradual transition of oxy-hemoglobin (540 and 570 nm) to deoxy-hemoglobin with the applied probe pressure is evident from the variation in the peak height of the characteristic oxy-hemoglobin absorption peaks. The excitation peaks of other chromophores like flavins (460 nm), porphyrins (400 nm), and lipo-pigments (435 nm) also correspond with those in the reflectance spectra and may also contribute to the pressure induced distortions in the reflectance signal.[64] Significant p-values ($p<0.05$; one-way ANOVA with Bonferroni correction at 5%) at different pressure levels for major chromophores like hemoglobin (540 and 578 nm), lipids (420 nm) and water (980 nm) further substantiate the pressure induced variations in the DR spectra.

To further analyze the spectral variations in the DR signal; multiclass PLS-DA modeling was performed on the finger, volar forearm and palm datasets. The number of principal components to be included in the model was chosen based on the minimum classification error (Figure 5.3). The corresponding loading vectors (Figure 5.4) contain the important features of the major chromophores (hemoglobin, fats, lipids and water) and they prove that the spectral variations are primarily caused by the pressure induced modifications in the concentrations of these chromophores. PLS-DA models shown in Figure 5.5 were developed to differentiate DR spectral distortions introduced by the variation in the applied probe-tissue contact pressure. It can be seen that there is a very good separation

between spectra acquired at LP vs. MP and HP; with accuracies of 82.11%, 82.40% and 76.01% for fingertip, volar forearm and palm respectively; indicating that high probe pressure has a profound effect on the reflectance spectra (i.e. The separation between LP and HP spectra can be clearly observed in Figure 5.5). On the other hand, the yielded accuracies for differentiating MP spectra were 49.48 % (fingertip), 64.90 % (volar forearm) and 52.00 % (palm). The improved differentiation of MP spectra at the forearm can be attributed to the higher concentration of melanin in the volar forearm compared to fingertip and palm.[32] Therefore, the concentration of melanin in the target tissue site affects the reflectance signal significantly; proving that the pressure induced distortions in reflectance spectra is significant and tissue site specific; in agreement with reported results.[31, 32]

Thus the developed pressure sensitive spectroscopy platform enables quantitative assessment of probe-tissue contact pressure in real-time during *in vivo* spectroscopy measurements and can be used to mitigate the probe pressure induced spectral variability in reflectance spectroscopy. The real-time pressure sensitive fiber-optic probe further automates probe handling training (e.g., ensuring proper probe-tissue contact, maintaining constant LP during spectral acquisition) for operators during spectral data acquisition.

5.1.5 Conclusion

Thus the utilization of the pressure sensitive spectroscopy platform enables quantitative assessment of probe-tissue contact pressure in real-time during *in vivo* diffuse reflectance spectroscopy. The results show that probe pressure induced variability in DR spectra is significant; substantiating the need for real-time quantitative monitoring

of applied probe pressure in order to mitigate the distortions introduced in the reflectance signal due to probe pressure variability. We hope that by characterizing the probe pressure induced DR spectral distortions, the diagnostic efficacy of DR spectroscopy can be further enhanced.

Chapter 6. Summary and Future directions

6.1 Summary

The major aim of this dissertation was the development of pressure sensitive fiber-optic probe for real-time quantitative monitoring of probe tissue contact pressure on *in vivo* optical spectroscopy techniques. Real-time monitoring of applied probe pressure would enable the mitigation of the operator-dependent confounding effect of probe pressure induced distortions introduced in the acquired spectral data by providing instantaneous feedback about the exerted probe pressure to operators during spectral data acquisition.

The developed pressure sensitive spectroscopy platform; which was first tested on *in vivo* UV/visible AF spectroscopy validated the significance of the probe-tissue contact pressure on *in vivo* UV/visible AF spectroscopy. The results showed that the applied probe pressure had a profound site-specific effect on the acquired UV/visible AF spectral data. It also emphasized the need for real-time monitoring of applied probe pressure to minimize the spectral distortions introduced in the UV/visible AF spectral profiles.

The developed pressure sensitive spectroscopic platform was then utilized to characterize the probe pressure induced variations on *in vivo* NIR AF and Raman spectroscopy which showed that subtle variations in the NIR AF and Raman spectra were introduced at increased probe pressures; indicating the inevitability of real-time monitoring of probe-tissue contact pressure during NIR AF and Raman spectroscopic procedures.

Finally, the detailed study that was carried out using the developed pressure sensitive fiber-optic spectroscopic platform to evaluate the effects of applied probe

pressure on *in vivo* DR spectroscopy. It proved that probe pressure is an important parameter that warrants careful monitoring during DR spectral data acquisition. The diffuse reflectance spectra showed a significant site-specific decrease in intensity with applied probe pressure; further demonstrating the need to monitor the probe tissue contact pressure.

The results that were obtained in this dissertation show that probe pressure is a vital operator-dependent variable that can affect the spectral data significantly. Hence, it is important to make the spectral measurements operator independent in order to improve the diagnostic efficacy of the conventional optical spectroscopy techniques. This can be achieved by the real-time monitoring of the applied probe-tissue contact pressure that can provide assistance to different operators while spectroscopic measurements are being carried out.

6.2 Future directions

The developed pressure sensitive spectroscopic platform has great potential to be put to clinical use in the future. The real-time pressure sensitive capability of the probes also serves as an in-built system feature that can provide automatic probe-handling advice to operators during spectral data acquisition.

With the recent advances in pressure sensing technology and proper miniaturization of the integrated pressure sensor coupled probes, the pressure sensitive spectroscopic platform can be employed in many future applications. Some of the applications are discussed below

i. Integration of pressure sensitive probe with endoscope for diagnosis of gastro-intestinal cancer:

Raman spectroscopy has been used recently in clinical trials for the diagnosis of gastro-intestinal (GI) cancer.[22, 28, 86, 102] For this purpose, the Raman probes are integrated with the endoscope to access the remote internal organs in the GI tract. However, the quality of the acquired spectra is operator-dependent and it has been hypothesized that the applied probe pressure plays an important role in the spectral variability of acquired spectra. Further miniaturization of the sensor coupled probe (< 2mm) is required to integrate the pressure sensitive probe with the endoscopes.

ii. Integration with keyhole surgery equipment (i.e laparoscope) for assistance during tumor removal:

The recent advances in Raman spectroscopy for disease diagnosis[137-139] have shown its huge potential in assisting surgeons during the removal of malignant tumors. The non-invasiveness and high sensitivity to detect abnormal tissues can be of vital importance in guiding surgeons during surgery for tumor removal. Pressure sensitive probes if utilized have the potential to further improve the diagnostic prediction capability of Raman probes.

iii. Other potential applications:

The developed pressure sensitive probe has the potential to be used for studying the influence of blood signal on tissue optical properties *in vivo*, characterization of various chromphores in tissues and real-time monitoring of contact state on other fiber based spectroscopic applications.

However, many challenges have to be addressed before its utilization in the aforementioned applications. With the recent advancements in the spectroscopy probe design and sophisticated sensor technologies; these challenges can be overcome in the near future.

References

1.G. Zonios, L. T. Perelman, V. M. Backman, R. Manoharan, M. Fitzmaurice, J. Van Dam, and M. S. Feld, "Diffuse reflectance spectroscopy of human adenomatous colon polyps in vivo," *Applied Optics* **38**(31), 6628-6637 (1999).

2.K. Bensalah, D. Peswani, A. Tuncel, J. D. Raman, I. Zeltser, H. Liu, and J. Cadeddu, "Optical reflectance spectroscopy to differentiate benign from malignant renal tumors at surgery," *Urology* **73**(1), 178-181 (2009).

3.U. Utzinger, M. Brewer, E. Silva, D. Gershenson, R. C. Blast Jr, M. Follen, and R. R. Richards-Kortum, "Reflectance spectroscopy for in vivo characterization of ovarian tissue," *Lasers in Surgery and Medicine* **28**(1), 56-66 (2001).

4.Y. N. Mirabal, S. K. Chang, E. N. Atkinson, A. Malpica, M. Follen, and R. R. Richards-Kortum, "Reflectance spectroscopy for in vivo detection of cervical precancer," *Journal of Biomedical Optics* **7**(4), 587-594 (2002).

5.S. K. Chang, I. Pavlova, N. M. Marin, M. Follen, and R. R. Richards-Kortum, "Fluorescence spectroscopy as a diagnostic tool for detecting cervical pre-cancer," *Gynecologic Oncology* **99**(3 Suppl 1), S61-63 (2005).

6.L. Brancaleon, A. J. Durkin, J. H. Tu, G. Menaker, J. D. Fallon, and N. Kollias, "In vivo fluorescence spectroscopy of nonmelanoma skin cancer," *Photochemistry and Photobiology* **73**(2), 178-183 (2001).

7.M. F. Mitchell, S. B. Cantor, N. Ramanujam, G. Tortolero-Luna, and R. R. Richards-Kortum, "Fluorescence spectroscopy for diagnosis of squamous intraepithelial lesions of the cervix," *Obstetrics and Gynecology* **93**(3), 462-470 (1999).

8.Z. Huang, H. Lui, D. I. McLean, M. Korbelik, and H. Zeng, "Raman spectroscopy in

combination with background near-infrared autofluorescence enhances the in vivo assessment of malignant tissues," *Photochemistry and Photobiology* **81**(5), 1219-1226 (2005).

9.C. Jiyoung, G. Sharad, P. Inho, L. Doheon, and C. Y. Jong, "Breast cancer diagnosis from fluorescence spectroscopy using Support Vector Machine," *Proceedings of SPIE* **6434**, (2007).

10.V. Zoya, S. H. Abigail, L. B. Kate, F. Maryann, S. Robert, W. Nancy, N. Jon, R. D. Ramachandra, and M. S. Feld, "Diagnosing breast cancer using diffuse reflectance spectroscopy and intrinsic fluorescence spectroscopy," *Journal of Biomedical Optics* **13**(2), 024012 (2008).

11.G. U. Alejandro, Z. Jun, D. Madeleine, H. C. V. Jeong, G. P. Victor, and V. W. Lihong, "In vivo diagnosis of melanoma and non-melanoma skin cancer using oblique incidence diffuse reflectance spectroscopy," *Cancer Research* **72**, 2738-2745 (2012).

12.A. Stirban, "Noninvasive skin fluorescence spectroscopy for diabetes screening," *Journal of diabetes science and technology* **7**(4), 1001-1004 (2013).

13.A. Suresh, N. Sujatha, V. B. Narayanamurthy, V. Seshadri, and P. Richa, "Diffuse reflectance spectroscopyformonitoringdiabetic footulcer – A pilotstudy," *Optics and Lasers in Engineering* **53**, 1-5 (2014).

14.A. Sahu, K. Dalal, S. Naglot, P. Aggarwal, and K. C. Murali, "Serum Based Diagnosis of Asthma Using Raman Spectroscopy: An Early Phase Pilot Study," *PLoS ONE* **8**(11), 78921 (2013).

15.E. J. Saude, C. D. Skappak, S. Regush, K. Cook, A. Ben-Zvi, A. Becker, R. Moqbel, B. D. Sykes, B. H. Rowe, and D. J. Adamko, "Metabolomic profiling of asthma:

diagnostic utility of urine nuclear magnetic resonance spectroscopy," *The Journal of allergy and clinical Immunology* **127**(3), 757-764 (2011).

16.I. C. Baianu, "Early Diagnosis of Alzheimer's disease by NIR Fluorescence Spectroscopy and Nuclear Medicine," *Nature Proceedings*, (2011).

17.B. H. Eugene, I. Irving, R. D. Ramachandra, S. F. Michael, J. F. Robert, A. C. McKee, L. Devayani, and N. W. Kowall, "Near Infrared Fluorescence Spectroscopy Detects Alzheimer's Disease In-vitro," *Photochemistry and Photobiology* **70**(2), 236-242 (1999).

18.C. D. Sudworth, J. K. Archer, and D. Mann, "Near infrared Raman spectroscopy for Alzheimer's disease detection," *Proc. SPIE* **5862**, TuC3 (2005).

19.W. C. Lin, S. A. Toms, M. Johnson, E. D. Jansen, and A. Mahadevan-Jansen, "In vivo brain tumor demarcation using optical spectroscopy," *Photochemistry and Photobiology* **73**(4), 396-402 (2001).

20.M. Brydegaard, N. Haj-Hosseini, K. Wårdell, and S. Andersson-Engels, "Photobleaching Insensitive Fluorescence Diagnostics in Skin and Brain Tissue," *Journal of Photonics* **3**(3), 407-421 (2011).

21.J. Richter, N. Haj-Hosseini, S. Andersson-Engels, and K. Wårdell, "Fluorescence spectroscopy measurements for resection of malignant brain tumors," *Lasers in Surgery and Medicine* **43**, 8-14 (2011).

22.M. S. Bergholt, W. Zheng, K. Y. Ho, M. Teh, K. G. Yeoh, J. B. Y. So, A. Shabbir, and Z. Huang, "Fiber-optic Raman spectroscopy probes gastric carcinogenesis in vivo at endoscopy," *Journal of Biophotonics* **6**(1), 49-59 (2013).

23.M. S. Bergholt, W. Zheng, K. Y. Ho, M. Teh, K. G. Yeoh, J. B. Y. So, A. Shabbir, and Z. Huang, "Fiberoptic confocal Raman spectroscopy for real-time in vivo diagnosis of

dysplasia in barrett's esophagus," *Gastroenterology*, (2013).

24.M. S. Bergholt, W. Zheng, K. Lin, K. Y. Ho, M. Teh, K. G. Yeoh, J. B. Yan So, and Z. Huang, "In vivo diagnosis of esophageal cancer using image-guided Raman endoscopy and biomolecular modeling," *Technology in cancer research & treatment* **10**(2), 103-112 (2011).

25.M. S. Bergholt, W. Zheng, K. Lin, K. Y. Ho, M. Teh, K. G. Yeoh, J. B. Y. So, and Z. Huang, "In vivo diagnosis of gastric cancer using raman endoscopy and ant colony optimization techniques," *International Journal of Cancer* **128**(11), 2673-2680 (2011).

26.R. O. P. Draga, M. C. M. Grimbergen, P. L. M. Vijverberg, C. F. P. van Swol, T. G. N. Jonges, J. A. Kummer, and J. L. H. R. Bosch, "In vivo bladder cancer diagnosis by high-volume Raman spectroscopy," *Analytical Chemistry* **82**(14), 5993-5999 (2010).

27.S. Duraipandian, M. S. Bergholt, W. Zheng, K. Y. Ho, M. Teh, K. G. Yeoh, J. B. Y. So, and Z. Huang, "Real-time Raman spectroscopy for in vivo, online gastric cancer diagnosis during clinical endoscopic examination," *Journal of Biomedical Optics* **17**(8), 081418 (2012).

28.Z. Huang, M. S. Bergholt, W. Zheng, K. Lin, K. Y. Ho, M. Teh, and K. G. Yeoh, "In vivo early diagnosis of gastric dysplasia using narrow-band image-guided Raman endoscopy," *Journal of Biomedical Optics* **15**(3), 037017 (2010).

29.Y. Ti, and W. C. Lin, "Effects of probe contact pressure on in vivo optical spectroscopy," *Optics Express* **16**(6), 4250-4262 (2008).

30.V. V. Sapozhnikova, R. V. Kuranov, I. Cicenaite, R. O. Esenaliev, and D. S. Prough, "Effect of blood glucose monitoring of skin pressure exerted by an optical coherent tomography probe," *Journal of Biomedical Optics* **13**(2), 021112 (2008).

31.C. Blaž, B. Miran, B. Maksimilijan, P. Franjo, and L. Boštjan, "Pressure induced near infrared spectra response as a valuable source of information for soft tissue classification," *Journal of Biomedical Optics* **18**(4), 047002 (2013).

32.L. Lim, B. Nichols, N. Rajaram, and J. W. Tunnell, "Probe pressure effects on human skin diffuse reflectance and fluorescence spectroscopy measurements," *Journal of Biomedical Optics* **16**(1), 011012 (2011).

33.S. Ruderman, J. G. Andrew, S. Valentina, D. R. Jeremy, J. F. Angela, D. J. Borko, and V. M. Backman, "Analysis of pressure, angle and temporal effects on tissue optical properties from polarization-gated spectroscopic probe measurements," *Biomedical Optics Express* **1**(2), 489-499 (2010).

34.A. Cerussi, S. Siavoshi, A. J. Durkin, C. Chen, W. Tanamai, D. Hsiang, and B. J. Tromberg, "Effect of contact force on breast tissue optical property measurements using a broadband diffuse optical spectroscopy handheld probe," *Applied Optics* **48**(21), 4270-4277 (2009).

35.E. K. Chan, B. Sorg, D. Protsenko, M. O'Neil, M. Motamedi, and A. J. Welch, "Effects of compression on soft tissue optical properties," *IEEE Journal of Selected Topics in Quantum Electronics* **2**(4), 943-950 (1996).

36.W. Chen, R. Liu, K. Xu, and R. K. Wang, "Influence of contact state on NIR diffuse reflectance spectroscopy in vivo," *Journal of Phyics: Applied Physics* **38**, 2691-2695 (2005).

37.J. A. D. Atencio, E. E. O. Guillén, S. V. Y. Montiel, M. C. Rodríguez, J. C. Ramos, J. L. Gutiérrez, and F. Martínez, "Influence of probe pressure on human skin diffuse reflectance spectroscopy measurements," *ISSN 1060-992X, Optical Memory and Neural*

Networks (Information Optics) **18**(1), 6-14 (2009).

38.S. Duraipandian, M. S. Bergholt, W. Zheng, K. Y. Ho, M. Teh, K. G. Yeoh, J. B. Yan So, and Z. Huang, "Real-time Raman spectroscopy for in vivo, online gastric cancer diagnosis during clinical endoscopic examination," *Journal of Biomedical Optics* **17**(8), 081418 (2012).

39.M. Doi, and S. Tominaga, "Spectral estimation of human skin color using the Kubelka-Munk theory," *SPIE/IS&T Electronic Imaging, SPIE* **5008**, 221-228 (2003).

40.R. R. Anderson, and J. A. Parrish, "The optics of human skin," *Journal of Investigative Dermatology* **77**(1), 13-19 (1981).

41.I. Meglinsky, and Matcher, "Modelling the sampling volume for skin blood oxygenation," *Medical and Biological Engineering & Computing* **39**, 44-49 (2001).

42.R. Flewelling, "Noninvasive optical monitoring," in *The Biomedical Engineering Handbook* J. Bronzino, Ed., pp. 1-11, IEEE Press (1981).

43.R. R. Anderson, and J. A. Parrish, "Optical Properties of Human Skin," in *The Science of Photomedicine* J. A. P. James D. Regan, Ed., pp. 147-194, Springer US (1982).

44.P. N. Kristian, Z. Lu, J. S. Jakob, S. Knut, and M. Johan, "The optics of human skin: Aspects important for human health," *The Norwegian Academy of Science and Letters*, 35-46 (2008).

45.Z. Huang, A. McWilliams, H. Lui, D. I. McLean, S. Lam, and H. Zeng, "Near-infrared Raman spectroscopy for optical diagnosis of lung cancer," *International Journal of Cancer* **107**(6), 1047-1052 (2003).

46.D. P. Lau, Z. Huang, H. Lui, C. S. Man, K. Berean, M. D. Morrison, and H. Zeng, "Raman spectroscopy for optical diagnosis in normal and cancerous tissue of the

nasopharynx—preliminary findings," *Lasers in Surgery and Medicine* **32**(3), 210-214 (2003).

47.K. Lin, D. P. Lau, and Z. Huang, "Optical diagnosis of laryngeal cancer using high wavenumber Raman spectroscopy," *Biosensors & Bioelectronics* **35**(1), 213-217 (2012).

48.C. H. Liu, B. B. Das, W. L. S. Glassman, G. C. Tang, K. M. Yoo, H. R. Zhu, D. L. Akins, S. S. Lubicz, J. Cleary, R. Prudente, E. Celmer, A. Caron, and R. R. Alfano, "Raman, fluorescence, and time-resolved light scattering as optical diagnostic techniques to separate diseased and normal biomedical media," *Journal of Photochemistry and Photobiology B: Biology* **16**(2), 187-209 (1992).

49.S. K. Teh, W. Zheng, K. Y. Ho, M. Teh, K. G. Yeoh, and Z. Huang, "Near-infrared Raman spectroscopy for optical diagnosis in the stomach: Identification of Helicobacter-pylori infection and intestinal metaplasia," *International Journal of Cancer* **126**(8), 1920-1927 (2010).

50.H. Zeng, J. Zhao, M. Short, D. I. McLean, S. Lam, A. McWilliams, and H. Lui, "Raman spectroscopy for in vivo tissue analysis and diagnosis, from instrument development to clinical applications," *Journal of Innovative Optical Health Sciences* **1**(1), 95-106 (2008).

51.G. K. Aamir Shahzad, Martin Knapp, Erwin Gaubitzer,, and M. P. a. M. Edetsberger, "Fluorescence spectroscopy An emerging excellent diagnostic tool in Medical Sciences," *Journal of Translational Medicine* **7**(99), (2009).

52.A. Shahzad, M. Knapp, M. Edetsberger, M. Puchinger, E. Gaubitzer, and G. Köhler, "Diagnostic Application of Fluorescence Spectroscopy

in Oncology Field: Hopes and Challenges," *Applied Spectroscopy Reviews* **45**(1), 92-99

(2010).

53.N. Ramanujam, "Fluorescence Spectroscopy In Vivo," in *Encyclopedia of Analytical Chemistry* R. A. Meyers, Ed., pp. 20-56 (2000).

54.J. Markley, "What is Optical Spectroscopy?," M. Wiley, Ed.

55.R. W. Frei, "Diffuse Reflectance Spectroscopy; Applications, Standards, and Calibration," *Journal Of Research* **80A**(4), 551-565 (1976).

56.C. Blaž, B. Miran, P. Franjo, and L. Boštjan, "Analysis of soft tissue near infrared spectra under dynamic pressure effects," *Optical Biopsy X, Proceedings of SPIE* **8220**, 822001-822007 (2012).

57.J. R. Lakowicz, *Principles of Fluorescence Spectroscopy*, Plenum Press (1983).

58.T. Sheng-Hao, B. Paulo, A. J. Durkin, and N. Kollias, "Chromophore concentrations, absorption and scattering properties of human skin in-vivo," *Optics Express* **17**(17), 14599-14617 (2009).

59.N. Kollias, G. Zonios, and G. N. Stamatas, "Fluorescence spectroscopy of skin," *Vibrational spectroscopy* **28**(1), 17-23 (2002).

60.Y. Li, "Separation of endogenous fluorophores in normal and cancer cells," University of Iowa (2009).

61.W. Zheng, D. P. Lau, C. Cheng, K. Chee Soo, and M. Olivo, "Optimal excitation-emission wavelengths for autofluorescence diagnosis of bladder tumors," *International Journal of Cancer* **104**, 477-481 (2003).

62.B. Banerjee, B. Miedema, and H. R. Chandrasekhar, "Emission Spectra of Colonic Tissue and Endogenous Fluorophores," *The American Journal of the Medical Sciences* **316**(3), 220-226 (1998).

63.M. Zellweger, "Fluorescence Spectroscopy of Exogenous, Exogenously-induced and Endogenous Fluorophores for the Photodetection and Photodynamic Therapy of Cancer ", Ecole Polytechnique Fédérale de Lausanne (2000).

64.A. W. Georges, M. S. Willem, and C. W. Brian, "In Vivo Fluorescence Spectroscopy and Imaging for Oncological Applications," *Photochemistry and Photobiology* **68**(5), 603-632 (1998).

65.C. Y. Wang, T. Tsai, H. C. Chen, S. C. Chang, C. Chen, and C. Chiang, "Autofluorescence spectroscopy for in vivo diagnosis of DMBA induced hamster buccal pouch precancers and cancers," *Journal of Oral Pathology Medicine* **32**, 18-24 (2003).

66.B. Lin, M. S. Bergholt, D. P. Lau, and Z. Huang, "Diagnosis of early stage nasopharyngeal carcinoma using ultraviolet autofluorescence excitation-emission matrix spectroscopy and parallel factor analysis," *Analyst* **136**(19), 3896-3903 (2011).

67.X. Shao, W. Zheng, and Z. Huang, "In vivo diagnosis of colonic precancer and cancer using near-infrared autofluorescence spectroscopy and biochemical modeling," *Journal of Biomedical Optics* **16**(6), 067005 (2011).

68.I. Bliznakova, E. Borisova, P. Troyanova, N. Momchilov, and L. Avramov, "Autofluorescence spectroscopy for noninvasive skin phototypes differentiation," *Proceedings of SPIE* **6604**, 660429 (2007).

69.A. H. Chau, J. T. Motz, J. A. Gardecki, S. Waxman, B. E. Bouma, and G. J. Tearney, "Fingerprint and high-wavenumber Raman spectroscopy in a human-swine coronary xenograftin vivo," *Optical Letters* **13**(4), 040501 (2008).

70.W. Z. Jianhua Mo, Jeffrey J. H. Low, Joseph Ng, A. Ilancheran and Zhiwei Huang "High wavenumber Raman spectroscopy for in vivo detection of cervical dysplasia,"

Analytical Chemistry **81**(21), 8908-8915 (2009).

71.S. K. Teh, W. Zheng, K. Y. Ho, M. Teh, K. G. Yeoh, and Z. Huang, "Diagnostic potential of near-infrared Raman spectroscopy in the stomach: differentiating dysplasia from normal tissue," *British Journal of Cancer* **98**(2), 457-465 (2008).

72.A. T. Tu, *Raman spectroscopy in biology: principles and applications*, Wiley New York (1982).

73.R. L. McCreery, *Chemical Analysis*, Wiley-Interscience, New York, USA (2000).

74.L. P. Choo-Smith, H. G. M. Edwards, H. P. Endtz, J. M. Kros, F. Heule, H. Barr, J. S. Robinson, H. A. Bruining, and G. J. Puppels, "Medical Applications of Raman Spectroscopy: from proof of principle to clinical implementation," *Biopolymers (biospectroscopy)* **67**, 1-9 (2002).

75.T. Lam, "A new era in affordable Raman spectroscopy," *Raman Technology for Today's Spectroscopists*, 30-37 (2004).

76.M. G. Shim, and B. C. Wilson, "Development of an in vivo Raman spectroscopic system for diagnostic applications," *Journal of Raman Spectroscopy* **28**(2-3), 131-142 (1997).

77.A. K. Bandyopadhyay, N. Dilawar, A. Vijayakumar, D. Varandani, and D. Singh, "A low cost laser-raman spectrometer," *Bulletin of Materials Science* **21**(5), 433-438 (1998).

78.J. T. Motz, M. Hunter, L. H. Galindo, J. A. Gardecki, J. R. Kramer, R. R. Dasari, and M. S. Feld, "Optical fiber probe for biomedical Raman spectroscopy," *Applied Optics* **43**(3), 542-554 (2004).

79.G. Zhang, S. G. Demos, and R. R. Alfano, "Raman spectra of biomedical samples using optical fiber probes," *Proc. SPIE* **2976**, 2-9 (1997).

80.J. C. C. Day, Bennett, R., Smith, B., Kendall, C. A., Hutchings, J., Meaden, G. M., Born, C., Yu S., Stone N., "A miniature confocal Raman probe for endoscopic use," *Physics in medicine and biology* **54**(23), 7077-7087 (2009).

81.Q. S. Han, A. P. Scott, L. J. Steven, W. C. Lee, and W. G. Kenton, "Pressure effects on soft tissues monitored by changes in tissue optical properties," *Laser-Tissue Interaction IX, Proceedings of SPIE* **3254**, 0277-0286 (1998).

82.R. Reif, M. S. Amorosino, K. W. Calabro, O. A. Amar, S. K. Singh, and I. J. Bigioa, "Analysis of changes in reflectance measurements on biological tissues subjected to different probe pressures," *Journal of Biomedical Optics* **13**(1), 010502 (2008).

83.L. L. Randeberg, B. Skallerud, N. E. I. Langlois, O. A. Haugen, and L. O. Svaasand, "The Optics of Bruising," in *Optical-Thermal Response of Laser-Irradiated Tissue* M. J. C. v. G. e. A.J. Welch, Ed., Springer Science (2011).

84.A. Nath, K. Rivoire, S. C. Chang, D. Cox, E. N. Atkinson, M. Follen, and R. R. Richards-Kortum, "Effect of probe pressure on cervical fluorescence spectroscopy measurements," *Journal of Biomedical Optics* **9**(3), 523-533 (2004).

85.A. Nath, K. Rivoire, S. C. Chang, D. Cox, E. N. Atkinson, M. Follen, and R. R. Richards-Kortum, "The effects of repeated spectroscopic pressure measurements on fluorescence intensity in the cervix," *Americal Journal of Obstetrics and Gynecology* **191**(5), 1606-1617 (2004).

86.M. G. Shim, L. M. Song, N. E. Marcon, and B. C. Wilson, "In vivo near-infrared Raman spectroscopy: demonstration of feasibility during clinical gastrointestinal endoscopy," *Photochemistry and Photobiology* **72**(1), 146-150 (2000).

87.I. J. Pence, E. Vargis, and A. Mahadevan-Jansen, "Assessing variability of in vivo

tissue Raman spectra," *Applied Spectroscopy* **67**(7), 789-800 (2013).

88.P. Lijia, C. Alex, Y. Guihua, W. Yaqun, I. Scott, A. Ranulf, S. Yi, D. Reinhold, and B. Zhenan, "An ultra-sensitive resistive pressure sensor based on hollow-sphere microstructure induced elasticity in conducting polymer film," *Nature Communications* **5**, (2014).

89.L. Wang, and Y. Li, "A review for conductive polymer piezoresistive composites and a development of a compliant pressure transducer," *IEEE Transactions on Instrumentation and Measurement* **62**(2), 495 - 502 (2013).

90.N. Stone, C. A. Kendall, J. Smith, P. Crow, and H. Barr, "Raman spectroscopy for identification of epithelial cancers," *Faraday Discussions* **126**, 141-157 (2004).

91.A. Savitzky, and M. J. E. Golay, "Smoothing and differentiation of data by simplified least squares procedures," *Analytical Chemistry* **36**(8), 1627-1639 (1964).

92.T. Bocklitz, A. Walter, K. Hartmann, P. Rösch, and J. Popp, "How to pre-process Raman spectra for reliable and stable models?," *Analytica Chimica Acta* **704**(1–2), 47-56 (2011).

93.A. Mahadevan-Jansen, and R. R. Richards-Kortum, "Raman spectroscopy for cancer detection: a review," *Proc. SPIE* **6**(1), 2722-2728 (1997).

94.B. D. Beier, and A. J. Berger, "Method for automated background subtraction from Raman spectra containing known contaminants," *Analyst* **134**(6), 1198-1202 (2009).

95.C. A. Lieber, and A. Mahadevan-Jansen, "Automated method for subtraction of fluorescence from biological Raman spectra," *Applied Spectroscopy* **57**(11), 1363-1367 (2003).

96.A. Cao, A. K. Pandya, G. K. Serhatkulu, R. E. Weber, H. Dai, J. S. Thakur, M. Naik,

R. Naik, G. W. Auner, R. Rabah, and D. C. Freeman, "A robust method for automated background subtraction of tissue fluorescence," *Journal of Raman Spectroscopy* **38**(9), 1199-1205 (2007).

97.I. Barman, C. R. Kong, G. P. Singh, and R. R. Dasari, "Effect of photobleaching on calibration model development in biological Raman spectroscopy," *Journal of Biomedical Optics* **16**(1), 011004 (2011).

98.J. Mo, W. Zheng, J. J. H. Low, J. Ng, A. Ilancheran, and Z. Huang, "High Wavenumber Raman Spectroscopy for in Vivo Detection of Cervical Dysplasia," *Analytic Chemistry* **81**, 8908-8915 (2009).

99.M. S. Bergholt, L. Kan, W. Zheng, D. P. C. Lau, and Z. Huang, "In vivo, real-time, transnasal, image-guided Raman endoscopy: defining spectral properties in the nasopharynx and larynx," *Journal of Biomedical Optics* **17**(7), 077002 (2012).

100.S. Duraipandian, W. Zheng, J. Ng, J. J. H. Low, A. Ilancheran, and Z. Huang, "Simultaneous fingerprint and high-wavenumber confocal Raman spectroscopy enhances early detection of cervical precancer in vivo," *Analytical Chemistry* **84**(14), 5913-5919 (2012).

101.M. S. Bergholt, W. Zheng, L. Kan, K. Y. Ho, M. Teh, K. G. Yeoh, J. B. Y. So, and Z. Huang, "Characterizing variability in in vivo Raman spectra of different anatomical locations in the upper gastrointestinal tract toward cancer detection," *Journal of Biomedical Optics* **16**(3), (2011).

102.M. S. Bergholt, W. Zheng, L. Kan, K. Y. Ho, M. Teh, K. G. Yeoh, J. B. Y. So, and Z. Huang, "Combining near-infrared-excited autofluorescence and Raman spectroscopy improves in vivo diagnosis of gastric cancer," *Biosensors & Bioelectronics* **26**(10), 4104-

4110 (2011).

103.M. S. Bergholt, W. Zheng, L. Kan, K. Y. Ho, M. Teh, K. G. Yeoh, J. B. Y. So, and Z. Huang, "Raman endoscopy for in vivo differentiation between benign and malignant ulcers in the stomach," *Analyst* **135**(12), 3162-3168 (2010).

104.H. Abdi, "Partial Least Square Regression," in *Encyclopedia of Measurement and Statistics* H. Abdi, Ed., Thousand Oaks (CA): Sage. (2007).

105.J. A. Westerhuis, H. C. J. Hoefsloot, S. Smit, D. J. Vis, A. K. Smilde, E. J. J. van Velzen, J. P. M. van Duijnhoven, and F. A. van Dorsten, "Assessment of PLSDA cross validation," *Metabolomics* **4**(1), 81–89 (2008).

106.N. Kollias, S. Inseok, and R. B. Paulo, "Interpreting diffuse reflectance for in vivo skin reactions in terms of chromophores," *Journal of Biophotonics* **3**(2), 15-24 (2010).

107.W. Rayens, and M. Barker, "Partial least squares for discrimination," *Journal of Chemometrics* **17**, 166-173 (2003).

108.R. Rifkin, and A. Klautau, "In defense of one-vs-all classification," *Journal of Machine Learning Research* **5**, 101-141 (2004).

109.Y. P. Sinichkin, S. R. Utz, A. H. Mavliutov, and H. A. Pilipenko, "In vivo fluorescence spectroscopy of the human skin : experiments and models," *Journal of Biomedical Optics* **3**(2), 201-211 (1998).

110.B. R. Masters, P. T. C. So, and E. Gratton, "Multiphoton excitation fluorescence microscopy and spectroscopy of in vivo human skin," *Biophysical Journal* **72**(6), 2405-2412 (1997).

111.F. H. Mustafa, and M. S. Jaafar, "Comparison of wavelength-dependent penetration depths of lasers in different types of skin in photodynamic therapy," *Indian Journal of*

Physics **87**(3), 203-209 (2013).

112.E. A. Pozzi, L. R. Schwall, R. Jimenez, and J. M. Weber, "Pressure-induced changes in the fluorescence behavior of red fluorescent proteins," *The Journal of Physical Chemistry B* **116**(34), 10311 - 10316 (2012).

113.P. Constantine, K. Matthew, W. Lisa, P. John, and A. Mahadevan-Jansen, "Near-infrared autofluorescence for the detection of parathyroid glands," *Journal of Biomedical Optics* **16**(6), 067012 (2011).

114.M. S. Bergholt, W. Zheng, K. Lin, K. Y. Ho, M. Teh, K. G. Yeoh, J. B. Yan So, and Z. Huang, "Combining near-infrared-excited autofluorescence and Raman spectroscopy improves in vivo diagnosis of gastric cancer," *Biosensors & Bioelectronics* **26**(10), 4104-4110 (2011).

115.J. Mo, W. Zheng, J. J. H. Low, J. Ng, A. Ilancheran, and Z. Huang, "Near-infrared autofluorescence spectroscopy for in vivo diagnosis of cervical precancer," *Proeedings of SPIE* **6853**, 685317 (2008).

116.X. Shao, W. Zheng, and Z. Huang, "Polarized near-infrared autofluorescence imaging combined with near-infrared diffuse reflectance imaging for improving colonic cancer detection," *Optics Express* **18**(23), 133094 (2010).

117.Z. Huang, S. K. Teh, W. Zheng, J. Mo, K. Lin, X. Shao, K. Y. Ho, M. Teh, and K. G. Yeoh, "Integrated Raman spectroscopy and trimodal wide-field imaging techniques for real-time in vivo tissue Raman measurements at endoscopy," *Optics Letters* **34**(6), 758-760 (2009).

118.X. Shao, W. Zheng, and Z. Huang, "Near-infrared autofluorescence imaging for colonic cancer detection," *Proceedings of SPIE* **7634**, 76340B (2009).

119.X. Han, H. Lui, D. I. McLean, and H. Zeng, "Near-infrared autofluorescence imaging of cutaneous melanins and human skin in vivo," *Journal of Biomedical Optics* **14**(2), 024017 (2009).

120.C. N. Keilhauer, and F. C. Delori, "Near-infrared autofluorescence imaging of the fundus: visualization of ocular melanin," *Investigative Opthalmology and Visual Science* **47**(8), 3556-3564 (2006).

121.S. G. Demos, R. Bold, R. V. White, and R. Ramsamooj, "Investigation of near-infrared autofluorescence imaging for the detection of breast cancer," *IEEE Journal of Quantum Electronics* **11**(4), 791-798 (2005).

122.E. Ibtissam, A. Jessica, T. Melissa, L. I. Bennett, T. Thomas, L. Min, X. Hao, and J. W. Gerald, "Using a portable terahertz spectrometer to measure the optical properties of in vivo human skin," *Journal of Biomedical Optics* **18**(12), 120503 (2013).

123.J. M. Murkin, and M. Arango, "Near-infrared spectroscopy as an index of brain and tissue oxygenation," *British Journal of Anaesthesia* **103**, 3-13 (2009).

124.S. Duraipandian, W. Zheng, J. Ng, J. J. H. Low, A. Ilancheran, and Z. Huang, "Near-infrared-excited confocal Raman spectroscopy advances in vivo detection of cervical precancer," *Journal of Biomedical Optics* **18**(6), 067007 (2013).

125.A. S. Haka, Z. Volynskaya, J. A. Gardecki, J. Nazemi, R. Shenk, N. Wang, R. R. Dasari, M. Fitzmaurice, and M. S. Feld, "Diagnosing breast cancer using Raman spectroscopy: prospective analysis," *Journal of Biomedical Optics* **14**(5), 054023 (2009).

126.U. Utzinger, D. L. Heintzelman, A. Mahadevan-Jansen, A. Malpica, M. Follen, and R. R. Richards-Kortum, "Near-infrared Raman spectroscopy for in vivo detection of cervical precancers," *Applied Spectroscopy* **55**(8), 955-959 (2001).

127.M. Short, S. Lam, A. McWilliams, J. Zhao, H. Lui, and H. Zeng, "Development and preliminary results of an endoscopic Raman probe for potential in vivo diagnosis of lung cancers," *Optics Letters* **33**(7), 711-713 (2008).

128.Z. Huang, H. Zeng, I. Hamzavi, D. I. McLean, and H. Lui, "Rapid near-infrared Raman spectroscopy system for real-time in vivo skin measurements," *Optics Letters* **26**(22), 1782-1784 (2001).

129.P. T. T. Wong, and K. Heremans, "Pressure effects on the Raman spectra of proteins: pressure-induced changes in the conformation of lysozyme in aqueous solutions," *Chemical Physics Letters* **118**(1), 101-104 (1985).

130.P. T. T. Wong, R. K. Wong, and M. F. K. Fung, "Pressure-tuning FT-IR study of human cervical tissues," *Applied Spectroscopy* **47**(7), 1058-1063 (1993).

131.Y. Taniguchi, H. E. Stanley, and H. Ludwig, "Biological systems under extreme conditions: structure and function," in Springer (2002).

132.L. Chenxi, J. Jingying, and X. Kexin, "The Variation of Water in human tissue under certain compression: studied under diffuse reflectance spectroscopy," *Journal of Innovative Optical Health Sciences* **6**(1), 1350005 (2013).

133.S. Inseok, L. Yang, R. B. Paulo, and N. Kollias, "Assessing human skin with diffuse reflectance spectroscopy and colorimetry," *Photonics Therapeutics and Diagnostics VIII, Proceedings of SPIE* **8207**, 82070P82071-82075 (2012).

134.R. L. P. van Veen, and H. J. C. M. Sterenborg, "Determination of VIS- NIR absorption coefficients of mammalian fat, with time- and spatially resolved diffuse reflectance and tramsmission spectroscopy," *Optical Society of America*, (2000).

135.C. Qian, G. Z. Natalia, T. W. Steven, J. A. Walter, and Y. B. Mikhail, "Multispectral

imaging in the extended near-infrared window based on endogenous chromophores," *Journal of Biomedical Optics* **18**(10), 101318 (2013).

136.N. S. Georgios, and N. Kollias, "Blood stasis contributions to the perception of skin pigmentation," *Journal of Biomedical Optics* **9**(2), 315-322 (2004).

137.J. W. Spliethoff, D. J. Evers, H. M. Klomp, J. W. van Sandick, M. W. Wouters, R. Nachabe, G. W. Lucassen, B. H. Hendriks, J. Wesseling, and T. J. Ruers, "Improved identification of peripheral lung tumors by using diffuse reflectance and fluorescence spectroscopy," *Lung Cancer* **80**(2), 165-171 (2013).

138.X. S, X. Yizhuang, W. Jinguang, Z. Yuanfu, and S. Kelin, "Detection of lung cancer tissue by attenuated total reflection–Fourier transform infrared spectroscopy—a pilot study of 60 samples," *Journal of Surgical Research* **179**(1), 33-38 (2013).

139.M. Young-Kun, T. Yamamoto, E. Kohda, T. Ito, and H. Hiro-o, "1064 nm near-infrared multichannel Raman spectroscopy of fresh human lung tissues," *Journal of Raman Spectroscopy* **36**, 73-76 (2005).